Chem Soc Rev

REVIEW ARTICLE

View Article Online
View Journal | View Issue

Cite this: *Chem. Soc. Rev.*, 2022, **51**, 1415

Received 20th December 2021

DOI: 10.1039/d1cs01168e

rsc.li/chem-soc-rev

Direct decarboxylative Giese reactions

David M. Kitcatt,[a] Simon Nicolle[b] and Ai-Lan Lee *[a]

The quest to find milder and more sustainable methods to generate highly reactive, carbon-centred intermediates has led to a resurgence of interest in radical chemistry. In particular, carboxylic acids are seen as attractive radical precursors due their availability, low cost, diversity, and sustainability. Moreover, the corresponding nucleophilic carbon-radical can be easily accessed through a favourable radical decarboxylation process, extruding CO_2 as a traceless by-product. This review summarizes the recent progress on using carboxylic acids directly as convenient radical precursors for the formation of carbon–carbon bonds *via* the 1,4-radical conjugate addition (Giese) reaction.

1. Introduction

The past few decades have seen a flourishing of innovative radical chemistries to overcome unique synthetic challenges. Chemists have realised the old perception that radicals are overly reactive and uncontrollable was ill-conceived,[1] and many research groups have played their part in the development of novel and elegant synthetic transformations for the construction of complex organic motifs. Radical chemistry provides access to valuable products using simple radical precursors (RPs), achieving good chemo- and regioselectivity without the need for harsh reaction conditions and protecting groups.[1]

Within radical chemistry, a concentrated area of research has focused upon developing new synthetic methodologies to form carbon–carbon bonds *via* addition to alkenes. Traditional methods involved organometallic, two-electron, conjugate addition reactions onto electron-deficient olefins (Michael acceptors), but these organometallic reagents were often toxic, difficult to prepare and/or unstable, thus limiting their applicability.[2] Recent decades have witnessed the extensive utility of Giese-type[3] reactions involving additions of radical intermediates onto versatile Michael acceptors, allowing scope expansion to secondary, tertiary, or heteroatom-stabilised substrates as suitable coupling partners.

[a] *Institute of Chemical Sciences, School of Engineering and Physical Sciences, Heriot-Watt University, Edinburgh, EH14 4AS, UK. E-mail: a.lee@hw.ac.uk*
[b] *GlaxoSmithKline, Gunnels Wood Rd, Stevenage SG1 2NY, UK*

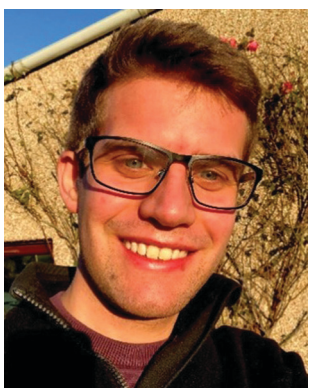

David M. Kitcatt

David M. Kitcatt received his MChem (Hons) at the University of Bath in 2020, during which he also completed his year in industry at the Francis Crick Institute. Since then, he is currently pursuing his doctoral studies at Heriot-Watt University under the supervision of Dr Ai-Lan Lee (HWU) and Dr Simon Nicolle (GSK), funded by an EPSRC/GSK industrial CASE Award. His research interests focus on the development of mild radical decarboxylation methodologies to achieve synthetically useful chemical transformations.

Simon Nicolle

Simon Nicolle obtained his PhD in Organic Chemistry from Nottingham University (2016) where he worked on the development of new methodologies for the preparation of diazo compounds and exploring new processes featuring reactive metallocarbene intermediates, under the supervision of Prof. Chris Moody and Prof. Chris Hayes. He started his industrial career in 2016 by joining the Fibrosis Discovery Unit at GlaxoSmithKline (GSK), Stevenage, as a postdoctoral researcher and later as a medicinal chemist. Beyond the contribution to the research of new therapeutics, his role also involves the application of modern methodologies to accelerate drug discovery.

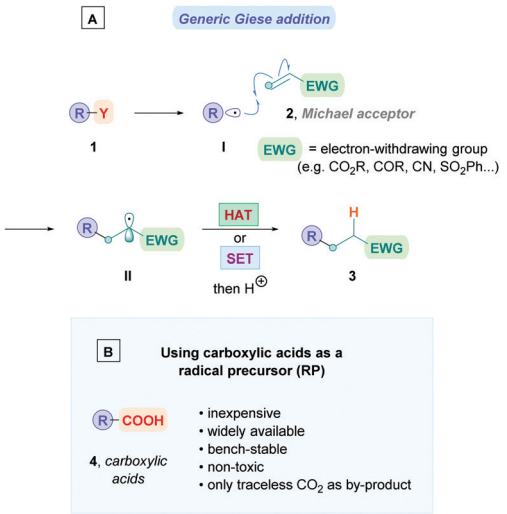

Scheme 1 (A) Classic mechanism for the radical Giese reaction. (B) The advantages of using carboxylic acids as radical precursors.

The Giese reaction[3] comprises the generation of a nucleophilic carbon-centred radical **I** from a radical precursor **1**, which adds to a π-bond in conjugation with an electron-withdrawing group (EWG) (*e.g.*, **2**) through a regioselective 1,4-addition pathway, establishing a new carbon–carbon bond[4] and producing an electrophilic radical intermediate **II** which is subsequently either trapped by a hydrogen atom-transfer (HAT) process to form a second σ-bond giving the Giese adduct **3**, or alternatively, **II** could undergo single electron transfer (SET) followed by protonation to form **3** (Scheme 1A). Nucleophilic carbon-centred radicals **I** proceed to add to electron-deficient olefins at rates on the order of 10^6 M^{-1} s^{-1}.[3b,5] Conveniently, this rate is faster than that of the common counter-productive reactions, including atom-transfer reactions with sensitive functional groups such as alcohols and amines, as well as carbonyl additions, which are on the order of 10^2 M^{-1} s^{-1}.[6] This difference in rates underscores the chemoselective advantage of radical conjugate additions, which can proceed in the presence of unprotected functional groups.[7]

Ai-Lan Lee

Ai-Lan obtained her MSci (Hons) (2000) and PhD (2004) from University of Cambridge, working under the supervision of Prof. Steven V. Ley. She was subsequently awarded a Lindemann Trust Fellowship (2004–2005) to work at Boston College with Prof. Amir Hoveyda. In 2006, Ai-Lan was appointed as a fixed-term Lecturer at the University of Edinburgh, carrying out research with Prof. David Leigh. She started as a Lecturer at Heriot-Watt University in 2007 and is currently Associate Professor and Reader. Her research interests include decarboxylative radical reactions and development of new gold-, palladium- and photoredox-catalysed reactions.

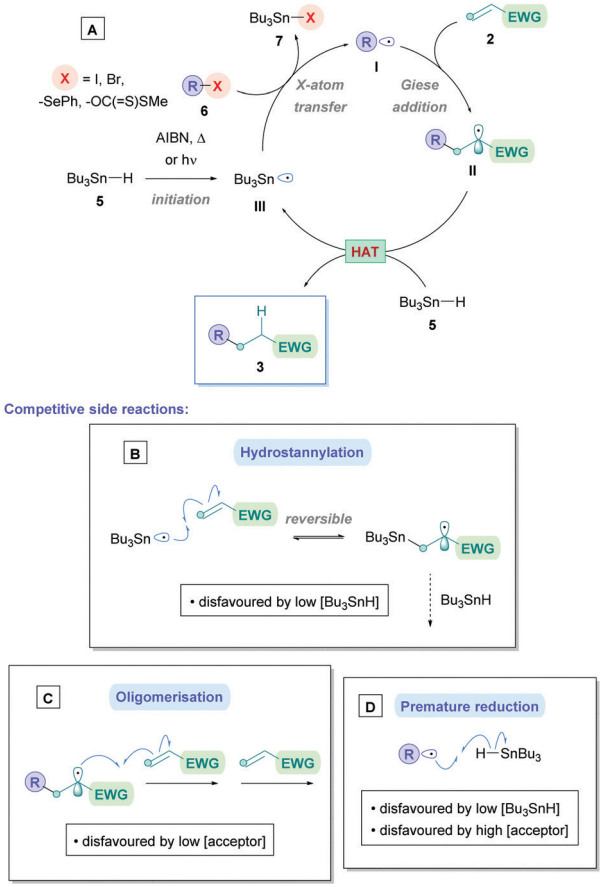

Scheme 2 (A) Traditional Giese reaction mechanism using tin hydride reagent.[7] Competitive reactions include (B) hydrostannylation of acceptor, (C) oligomerisation of acceptor, and (D) premature reduction of alkyl radical.

Traditionally, Giese reactions depended upon toxic tin hydride reagents (*e.g.*, **5** in Scheme 2A) with alkyl halides or selenides as radical precursors (**6**), together with an initiation source in the form of light, heat or a radical initiator (*e.g.*, AIBN) (Scheme 2A).[3] Upon initiation, a tin radical (**III**) is generated which undergoes X-atom transfer with the radical precursor **6** to produce the alkyl radical **I**. Subsequent conjugate addition onto Michael acceptor **2** and HAT with another equivalent of tin hydride **5** furnishes the Giese adduct **3**. These reactions suffered from competitive side-reactions, most noticeably where the tin radical can add to the Michael acceptor (hydrostannylation) (Scheme 2B), oligomerisation of the Michael acceptor (Scheme 2C), or premature H-abstraction of the generated alkyl radical (Scheme 2D), though these limitations can be suppressed by employing appropriate reaction conditions. The restricted scope of possible radical precursors has further added to the limitations due to availability and costs. To circumvent these issues, there has been growing endeavours towards innovative methodologies that are environmentally benign and utilise more sustainable radical precursors.

It is worth noting that the Giese reaction can be interrupted, whereby radical **II** has been exploited to participate in other pathways allowing the final HAT process to be bypassed.[8] These examples will not be discussed as they are beyond the scope of this review.

Within this context, carboxylic acids have become a versatile radical precursor over recent decades owing to their non-toxicity, low costs, bench-stability, and wide availability from renewable biomass sources.[9] Exhibiting extensive structural diversity, carboxylic acids can be found in amino acids, fatty acids, and sugar acids, making them ideal substrates for synthesising high-value compounds such as pharmaceuticals. Moreover, the desired radicals are generated by a radical decarboxylation mechanism with the extruded CO_2 as the traceless by-product, providing an entropic driving force for radical formation. It is unsurprising, therefore, that carboxylic acids have found widespread exploitation for decarboxylative Giese reactions.

Radical decarboxylation reactions have been known for a long time, with the likes of Kolbe,[10] Hunsdiecker,[11] and Barton[12] being amongst the earliest pioneers, yet their protocols suffered from narrow substrate scope and quite forcing conditions such as high temperatures and ultraviolet (UV) irradiation. It is only within the last 30 years that more benign decarboxylation methods have been developed that can accommodate a broader range of substrates.

Decarboxylative Giese reactions (DGRs) can proceed using either the indirect method or the direct method. The indirect method involves pre-activation of the carboxylic acid to a redox-active ester designed to induce facile decarboxylation. Historically, the Barton decarboxylation[13] (Scheme 3A) was the popular protocol, but the affiliated Barton esters (**8**) were often unstable and require toxic reducing agents. More modern advancements have given rise to new redox-active esters, the most popular being *N*-(acyloxy)phthalimide (NHPI) esters (**9**)[14] which are more stable and undergo facile reductive single-electron transfer (SET) with visible light, or inexpensive transition metal catalysis with nickel or iron catalysts (Scheme 3B).[9a,15] Perhaps the most notable example of using NHPI esters was elegantly demonstrated by the Baran group, providing a convenient means to access Giese products using nickel catalysis (Scheme 3B).[15e] Their protocol bypassed several shortcomings of conventional Barton's chemistry, providing a cheap and operational simple method for a broad scope of substrates. Further experimentation uncovered that indirect DGR could be achieved *via* a one-pot strategy.[15e] Despite the commendable progress, the indirect method has the disadvantage of producing undesirable by-products which must be separated from the product, on top of the extra step(s) needed for acid pre-functionalisation. Conversely, the direct method simply involves decarboxylation of the unactivated acid (**4**) through oxidative electron transfer (Scheme 3C), thus minimising waste and negating pre-functionalisation. For these reasons, the direct method is the more attractive approach and will be the subject of this review.

There are two potential main pathways associated with which the direct method can proceed. The carboxylic acid **4** could be subjected to hydrogen atom abstraction (HAT), which generates the carboxyl radical **V**, followed by subsequent decarboxylation to alkyl radical **I** (Scheme 4A), though this pathway is rarely used owing to costly energetic requirements to homolytically cleave the strong O–H bond (468.6 ± 12.6 kJ mol^{-1} for acetic acid).[16] Alternatively, a more common approach is deprotonation of the carboxylic acid **4** with a base to form the corresponding carboxylate **IV** (Scheme 4B), which is then oxidised through SET to **V** ($E^{red}_{1/2}$ = +1.25 to +1.31 V *vs.* the saturated calomel electrode (SCE))[17] followed by subsequent decarboxylation to **I**.

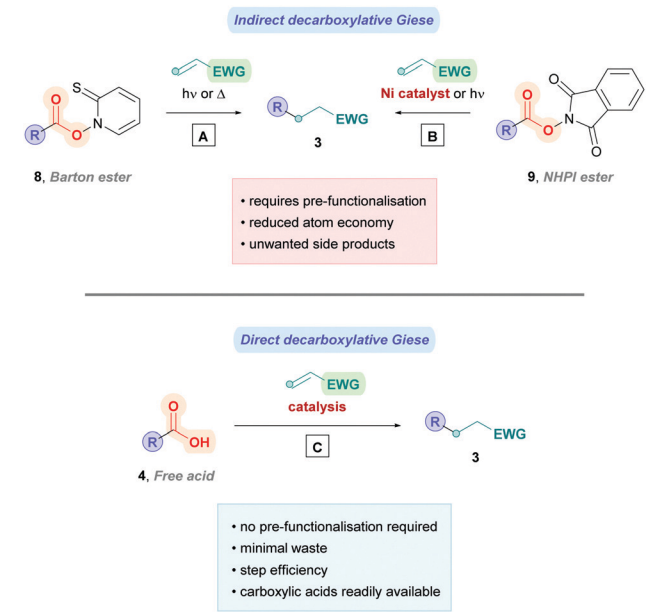

Scheme 3 Differences between (A and B) indirect and (C) direct decarboxylative Giese reactions.

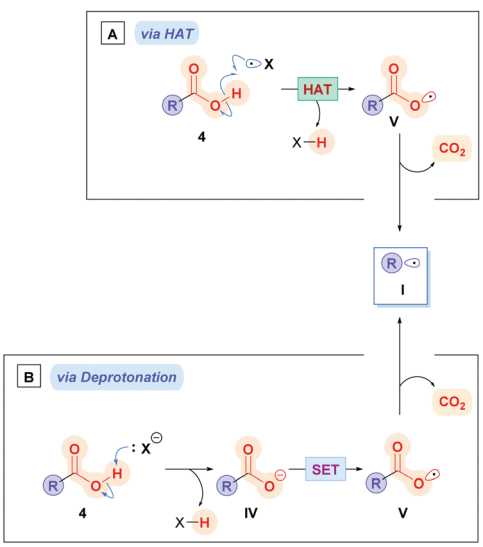

Scheme 4 Two modes of radical decarboxylation: (A) *via* HAT or (B) *via* deprotonation.

While a number of reviews[3b,7,18] have been published on the Giese reaction, it should be noted that the last general review on radical conjugate additions was published in 2005 by Srikanth and Castle.[18,19] An updated review is apt due to extensive progress made in this field in recent years. Indeed, a review on photomediated Giese reactions was very recently published by Kanegusuku and Roisen during the preparation of this review, covering selected high impact examples of photomediated Giese reactions from various radical precursors using homogenous catalysis.[7] Our review is distinct and complementary as it will focus more comprehensively on the development and latest applications of direct decarboxylative Giese additions over the last few decades, which will not be limited to photomediated reactions. Carboxylic acids radical precursors covered in this review will also include α-oxo acids, oxamic acids and oxalic acid monoesters. Discussions will first begin with photocatalysis, showing applications of homogenous (involving transition metal and organocatalysts, and synergistic dual catalysis) and heterogenous photocatalysis. Examples mediated by silver catalysis under Kochi conditions will be discussed next, followed by discussions on the application of organic electrochemistry to this transformation. This review will also seek to highlight the successes and limitations of the different examples, as well as identifying areas where further progress would be beneficial.

2. Photocatalysis

Currently, the most popular method to achieve direct DGRs is through visible-light photoredox catalysis. The advent of visible-light photosensitisers (or photocatalysts) to act as electron-transfer 'reagents' have provided the means to generate highly reactive intermediates under mild conditions, beneficially serving a plethora of valuable transformation.[20] Photocatalytic DGRs typically proceed *via* a reductive quenching pathway, and the various proposed mechanistic details can be summarised by the catalytic cycle shown in Scheme 5. Visible-light photoexcitation of the photocatalyst (**PC**) generates an oxidising species (***PC$_{ox}$**) to initiate decarboxylation. As discussed previously, the carboxylic acid (**4**) is usually deprotonated to the more easily oxidised carboxylate (**IV**) ($E_{1/2}^{red}$ = +1.25 to +1.31 V *vs.* the saturated calomel electrode (SCE))[17] before decarboxylation, thus the presence of stoichiometric base is commonplace. If no base is present, then the acid would be more difficult to oxidise ($E_{1/2}^{red}$ = +2.51 V *vs.* SCE for 2-phenylacetic acid).[21] Oxidative single electron transfer (SET) between ***PC$_{ox}$** and the carboxylate **IV** generates the reducing species (**PC$_{red}$**) and the corresponding carboxyl radical. Facile decarboxylation subsequently affords the carbon-centred radical **I** which undergoes conjugate addition with a Michael acceptor **2**. The resulting secondary radical intermediate **II** is reduced to the carbanion species **VI** *via* SET with **PC$_{red}$**, which regenerates **PC** to close the cycle. Subsequent protonation of the carbanion affords the desired Giese product **3**.

The use of iridium-based photocatalysts in DGRs will initially be discussed, followed by photocatalytic systems involving titania (TiO_2) and iron, before progressing to the more extensively exploited organo-based photocatalysts. Since the majority of the photocatalysed examples covered follow the pathway of Scheme 5, mechanistic explanations will be kept to a minimum. Processes that deviate from this mechanism, however, will be highlighted.

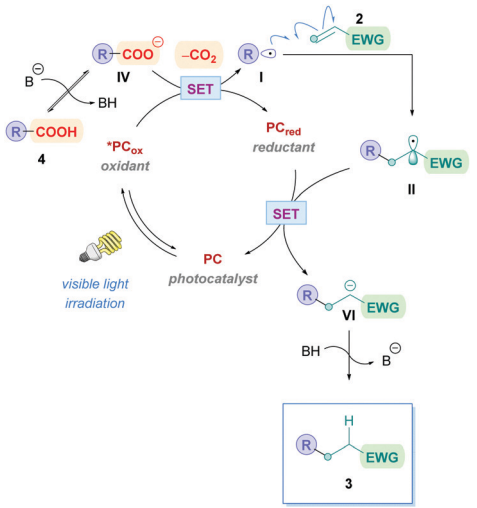

Scheme 5 General mechanism for direct decarboxylative Giese additions *via* photocatalysis. Mechanisms are consistent with a reductive quenching pathway.

2.1 Transition metal-based photoredox catalysis

2.1.1 Iridium-based photocatalysis. Metallaphotoredox catalysts, particularly complexes containing iridium and ruthenium centres, have been in frequent use for a myriad of photocatalytic transformations and novel bond formations.[20a,22] These complexes are typically comprised of a polypyridyl scaffold to allow for light absorption in the visible region of the electromagnetic spectrum. Upon light absorption the photocatalyst is photoexcited, giving rise to a long-lived excited species which can subsequently engage in bimolecular electron transfer processes in competition with deactivation pathways. Depending on the desired chemical transformation, these photocatalysts in their excited state can serve to act as potent reducing or oxidising agents.[20a,22]

By far the most prevalent photocatalysts used for direct DGRs have been iridium-based, with some of the most common photoactive complexes shown in Scheme 6A. To facilitate direct DGR, these Ir-PCs proceed *via* Ir(III)/Ir(II) catalytic cycle (Scheme 6B) – referring to the mechanism depicted in Scheme 5 as a template, **PC$_{ox}$** would correspond to ***Ir^{III}** and **PC$_{red}$** would correspond to the **Ir^{II}** complex.

The first example of iridium-based photocatalysis for direct DGR was reported in 2013 by Miyake, Nishibayashi and coworkers, who looked into the conjugate addition of arylacetic acids bearing amino groups at the *para*-position (Scheme 7).[23] Using 1.1 equiv. of Michael acceptor, Giese addition was achieved using **[Ir-1][BF$_4$]** as the chosen iridium photocatalyst in the presence of 14 W white LED illumination, affording

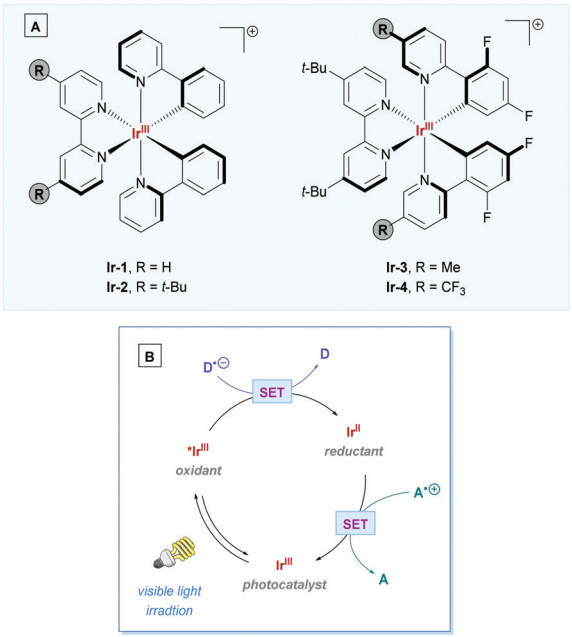

Scheme 6 (A) Commonly employed Ir(III) photocatalysts: $[Ir(ppy)_2(bpy)]^+$ (**Ir-1**); $[Ir(ppy)_2(dtbbpy)]^+$ (**Ir-2**); $[Ir(dF(Me)ppy)_2(dtbbpy)]^+$ (**Ir-3**); and $[Ir(dF(CF_3)ppy)_2(dtbbpy)]^+$ (**Ir-4**). (B) General Ir(III) photocatalytic cycle following the reductive quenching pathway of Scheme 5. Details are omitted to highlight the change in oxidation states of the iridium centre. D = electron donator, A = electron acceptor.

benzylated adducts (**12**) containing tertiary, secondary and primary amino groups from low to high yields (16–98%). During optimisation, they reported no homocoupling of the benzyl radicals, indicating the benefits of employing photocatalysis to add benzyl radicals across olefins. The transformation was reported with a reaction time of 18 h, under a mild temperature of 25 °C. This protocol was only limited to *para*-substituted anilines because, interestingly, when testing the benzylation of phenylacetic acids bearing a morpholino group at the *para*-, *meta*- and *ortho*-positions (**12h–j**), a high yield (96%) was obtained for **12h** but no yields were observed for **12i and j**. Stern–Volmer studies with **12i** suggested that oxidation of **12i** did occur but with no decarboxylation. Based on other studies,[24] it was postulated that the radical character (or spin population) of the carbon atom at the β-position with respect to the carboxyl group of the oxidised **12j** was not sufficient to induce efficient decarboxylation. In contrast, oxidation of **12j** was scarce probably due to intramolecular hydrogen bonding between the amino group and the carboxylic acid that inhibits oxidative SET.[25]

The MacMillan group later made significant improvements to light-assisted DGRs by providing a more generalised protocol for a wide variety of cyclic and acyclic carboxylic acid substrates (Scheme 8).[26] In the presence of stoichiometric inorganic base (organic bases gave poorer results), photocatalyst **[Ir-4][PF$_6$]** was irradiated with a 26 W fluorescent light bulb at room

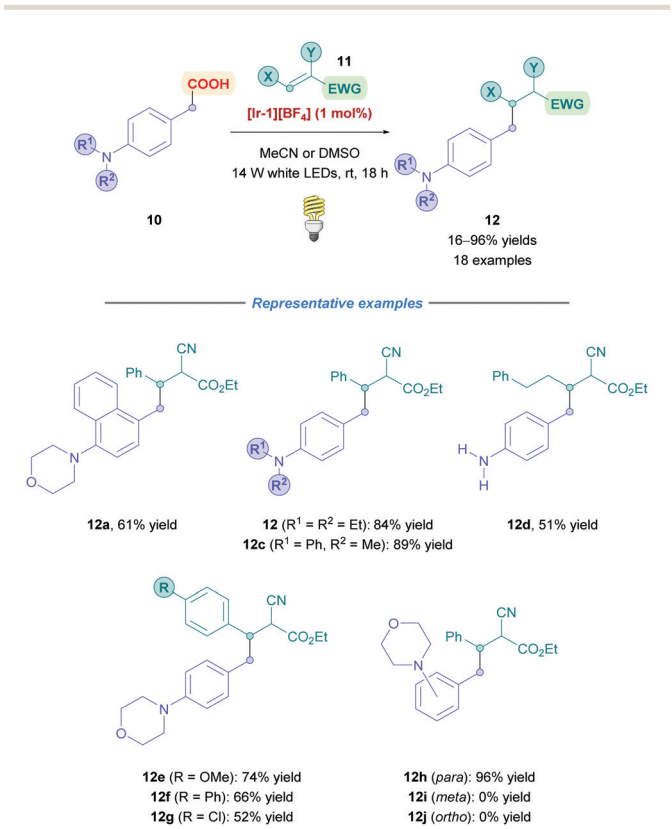

Scheme 7 Ir-Catalysed direct DGR of arylacetic acids.

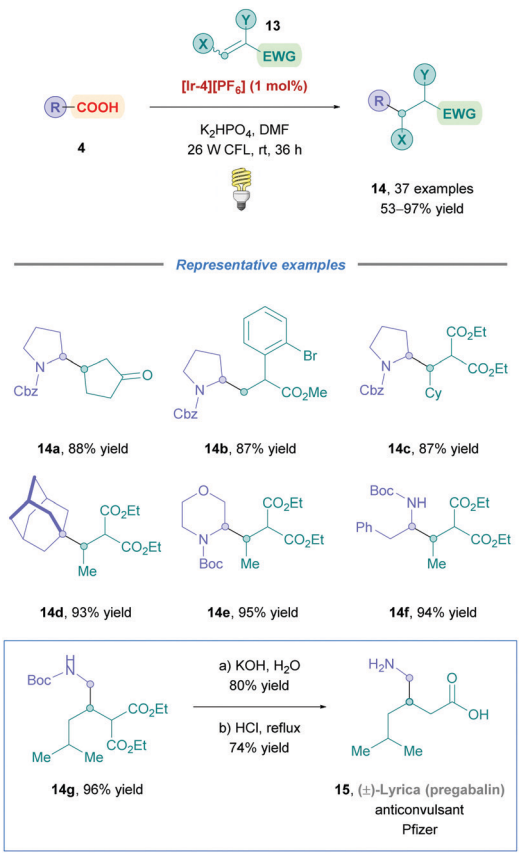

Scheme 8 MacMillan's general Ir-catalysed direct DGR protocol.

temperature to access conjugate adducts (**14**) using hydrocarbon-substituted (**14d**), α-oxy, and α-amino (**14a–c, e–f**) carboxylic acids as starting materials with moderate to excellent yields (53–97%) across the board. The reaction conditions were also compatible with a broad range of Michael acceptors including olefins bearing ketones (**14a**), aryl bromides (**14b**), aldehydes, esters (**14b and c**) and carboxylic acids. Furthermore, the electronic nature of aromatic systems at the α-position of the olefin (**14b**) had little impact on the reaction efficiency. The group further demonstrated the applicability of this protocol by providing a three-step racemic synthesis of the anticonvulsant drug pregabalin (**15**, commercialised by Pfizer under the trade name Lyrica).

These seminal works later helped inspire other research groups to exploit Ir-based photoredox catalysis on a range of different carboxylic acid (Section 2.1.1.1) and Michael acceptor substrates (Section 2.1.1.2).

2.1.1.1 Exploration of carboxylic acid substrates. Fu and co-workers successfully applied Ir photoredox catalysis to develop a new type of acyl conjugate addition using α-keto acids (**16**) as nucleophiles (Scheme 9).[27] Due to their thermal-instability,[28] Michael acceptors are rendered incompatible for the harsh conditions often seen in transition-metal-catalysed decarboxylation coupling reactions.[29] However, the characteristic mild conditions of Ir photoredox catalysis provided an alternative means to access these acyl conjugate products (**17**). Employing $[Ir(dF(CF_3)ppy)_2(phen)][PF_6]$ (**[Ir-5][PF$_6$]**) as the PC, Fu assessed a variety of 2-oxo-2-(hetero)arylacetic acids with a series of Michael acceptors bearing nitriles (**17a**), sulfones (**17b**), esters (**17d**), ketones (**17c, e–h**), amides, and aldehydes, accomplishing moderate to excellent yields (45–94%). Phenylacetic acids with both EWGs and EDGs, including halogens, were shown to be well tolerated, with lower yields observed for those with electron-withdrawing substituents, presumably due to corresponding lower nucleophilicity (**17e** *vs.* **17f**). Moderate yields were reported for 2-heteroaryl-substituted glyoxylic acids (*e.g.*, **17h**). Substituents on both the α- and β-positions of the Michael acceptor were well tolerated, including the useful CF_3 group at the β-position (**17d**). Some acceptors, such as simple acrylic acid, were unsuccessful as substrates, possibly due to competitive reductive quenching with the 2-oxocarboxylate. Michael acceptors that give rise to tertiary and benzylic radicals (*cf.* radical **II** in Scheme 5) were also incompatible, due to their lower oxidation potentials being insufficient to re-oxidise the corresponding **Ir(II)** species (*cf.* Scheme 6B).

α-Keto acids have also been used to achieve Giese alkylations. Upon decarboxylation of radical **VII** (Scheme 10A), the resulting acyl radical **VIII** can undergo further decarbonylation to give the corresponding alkyl radical **IX**, whilst extruding traceless CO in the process. The propensity for the acyl radical to decarbonylate is dependent upon the stability of the resulting alkyl radical. Consequently, decarbonylations that give more stable tertiary radicals are favoured, while primary and secondary α-keto acids tend to give their acylated Giese adducts. This trend can be seen in the work by Xu and co-workers, where they reported the photocatalytic decarboxylation/decarbonylation

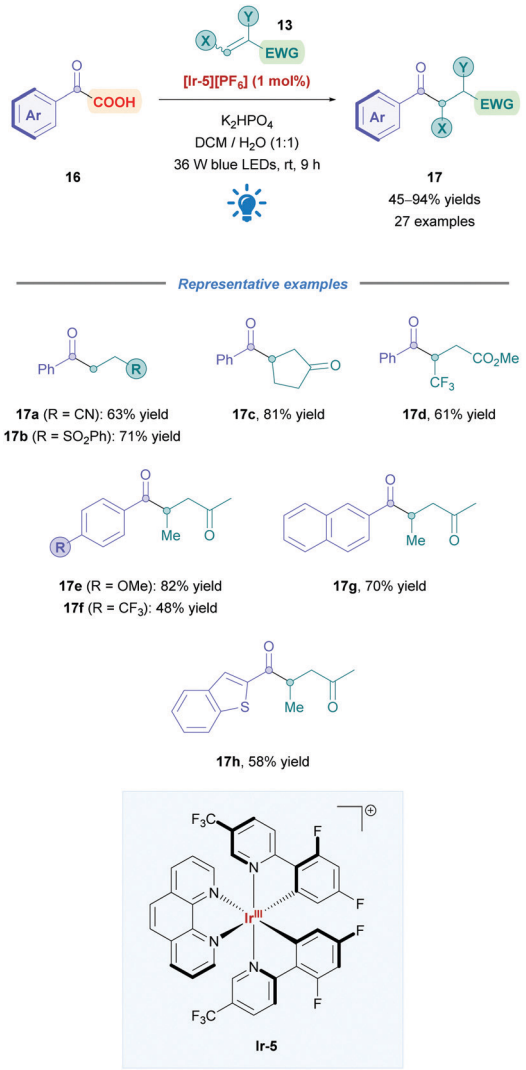

Scheme 9 Fu's Ir-catalysed direct DGR of α-oxocarboxylic acids.

of α-keto acids (**18**) using **[Ir-4][PF$_6$]**, achieving Giese alkylation of tertiary radicals in excellent yields (**20**, 75–97%) and acylation when using secondary and primary α-keto acids.[30] In a similar fashion, oxalic acid monoesters can also be used as radical precursors (Scheme 10B). Upon initial decarboxylation of **X** to give radical **XI**, a second decarbonylation event can occur to give the desired alkyl radical **IX**. Using photocatalysis (with **[Ir-4][PF$_6$]**), MacMillan and co-workers employed caesium oxalates (**21**) as activated alcohols to conjugate alkyl radicals to electron-deficient olefins (**19**) with moderate to excellent yields of **20** (54–99%).[31] Because of the same trends reasoned above, this protocol is most efficient to install tertiary alkyl radical, though two examples of secondary oxalates were reported. Overman and co-workers have also used caesium oxalates to engage in selective 1,6-conjugate additions,[32] which has successfully been employed for the synthesis of the diterpenoid *trans*-clerodane.[33]

Rueping and co-workers expanded the utility of amino acid derived α-amino radicals for both primary and secondary amines (Scheme 11).[34] Employing PC **[Ir-2][PF$_6$]**, *N*-aryl glycine

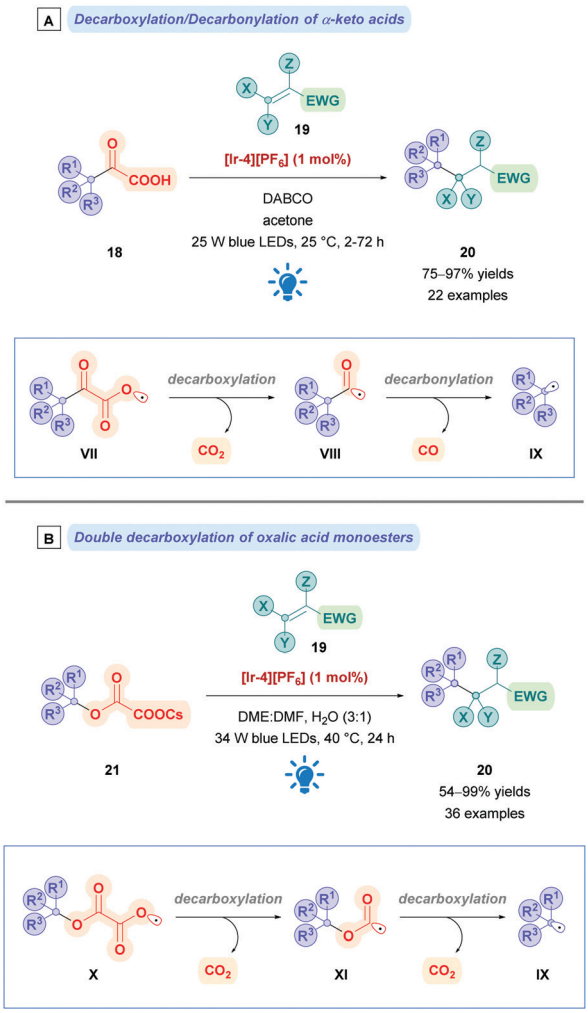

Scheme 10 Photocatalysed Giese alkylations using (A) α-keto acids and (B) oxalates.

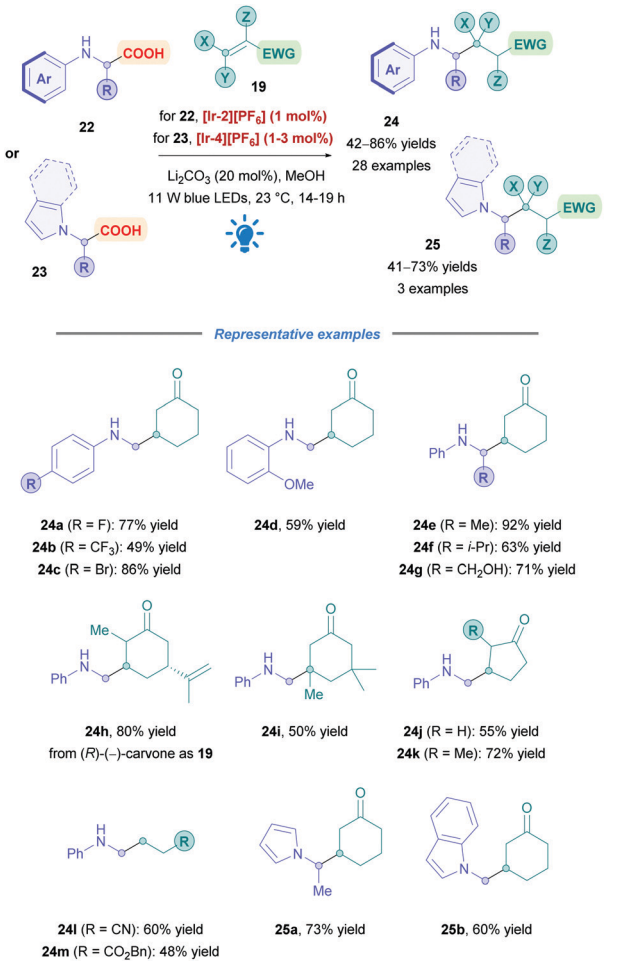

Scheme 11 Rueping's Ir-catalysed direct DGR of *N*-aryl-α-amino and N-heterocycles.

derivatives (**24a–d, h–m**) were of primary focus, but other amino acids such as *N*-phenyl alanine (**24e**), valine (**24f**), and serine (**24g**) were also investigated, overall achieving moderate to good yields (42–86%). Halogenated aryl rings were tolerated (**24a–c**), and poor reactivity was observed with EDGs in the *para* position; yields were improved when these groups occupied the *ortho* position (**24d**). Accessing a quaternary centre (**24i**) was also successful in appreciable yields. The group also attempted to further the scope by applying the reaction conditions to amino acids bearing *N*-unsaturated heterocycles (**23**). Though using PC **[Ir-2][PF$_6$]** did not give the desired transformation, switching to the more oxidising **[Ir-4][PF$_6$]** furnished the conjugate products (*e.g.*, **25a–b**) in good yields (60% and 73% yields respectively). The group's methodology has the added benefit of using catalytic amounts of basic Li_2CO_3, which was shown to be essential for successful coupling. The reaction time was also noticeably shorter (9 h) compared to most photocatalytic reactions, however, the presence of an inert Ar atmosphere was a necessity.

The most popular and effective Ir photocatalyst for DGRs is **[Ir-4][PF$_6$]**, but it is expensive and requires additional ligand synthesis step(s) for its preparation.[35] To overcome these limitations, Cozzi and co-workers employed an alternative Ir complex **[Ir-6][BF$_6$]** which possesses phenyl tetrazole ligands. This catalyst has the advantage of being more easily prepared, and the efficiency is comparable to photocatalyst **[Ir-4][PF$_6$]**.[36] They applied catalyst **[Ir-6][BF$_6$]** to the DGR of dithiane radical precursors (**26**), acting as a potential surrogate for a methyl ($CH_3^\bullet$) radical (Scheme 12).[37] Due to their inherent instability, the generation of primary radicals, especially methyl radicals, *via* decarboxylation continues to be a challenge within photocatalysis. Dithianes also act as useful functional handles for the installation of carbonyl-bearing groups (**27k** into **28**) and alkylation (**27k** into **29**). The reaction has a broad substrate scope with excellent yields (up to 93%) for a variety of Michael acceptors (*e.g.*, unsaturated esters, amides, and aldehydes) (**27a–g**), as well as 2-substituted dithiane-2-carboxylic acids (**27h–j**). Due to the lower reduction potential of its photoexcited state ($^*E_{1/2}^{III/II}$ = +0.4 V *vs.* ferrocene/ferrocenium couple), catalyst **[Ir-6][BF$_6$]** has a greater selectivity for the oxidation of α-functionalised acids than catalyst **[Ir-4][PF$_6$]**. Scale-up from 0.2 mmol to 2.4 mmol was also successful without any issues.

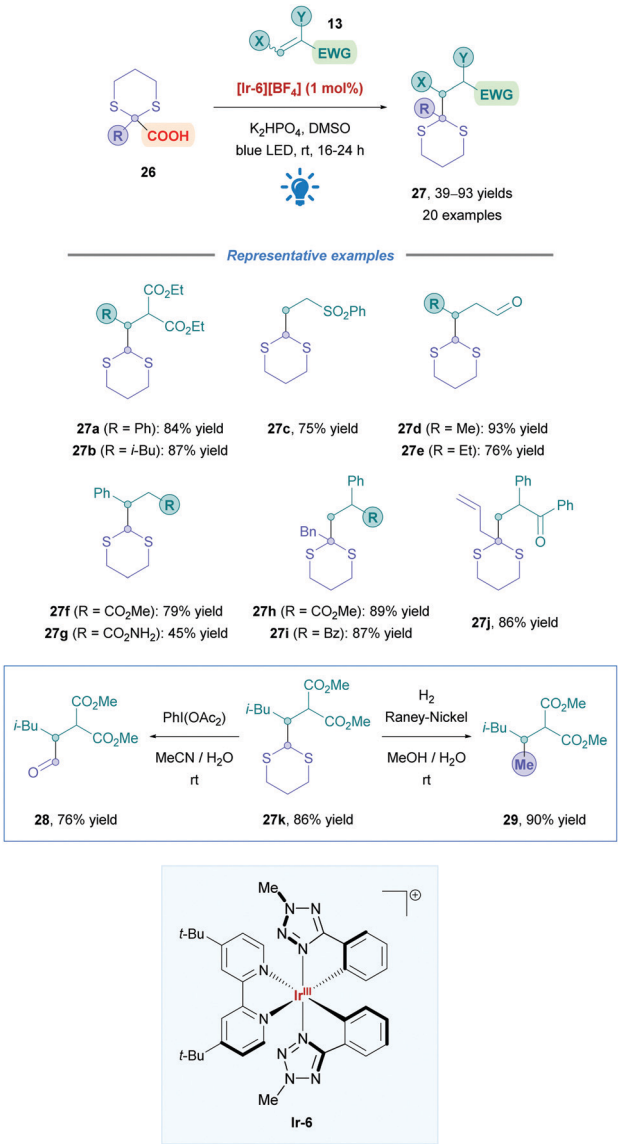

Scheme 12 Ir-Catalysed direct DGR of dithiane.

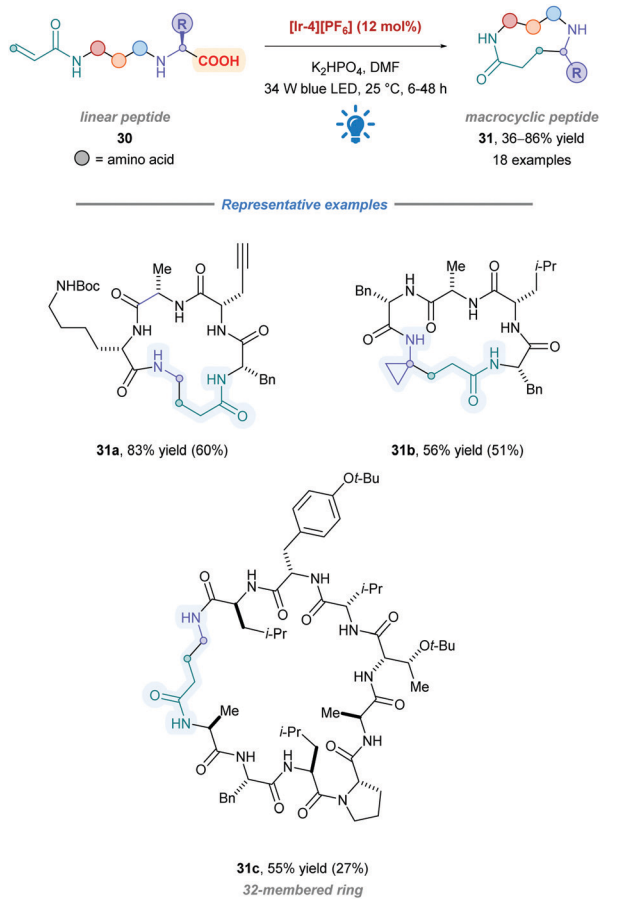

Scheme 13 Ir-Catalysed direct DGR for peptide macrocyclization. Yield of isolated product obtained by preparative HPLC in parentheses.

Following their seminal 2014 work,[26] the MacMillan group applied their previous protocol to access macrocyclic peptides (**31**) (Scheme 13).[38] They sought to utilize the C-terminal carboxylate to generate an α-amino radical, which subsequently undergoes intramolecular conjugate addition with a pendant Michael acceptor in the form of an acrylamide. High catalytic loadings (12 mol% of **[Ir-4][PF$_6$]**) accommodated the high dilution necessary to diminish oligomerisation pathways. Peptide lengths ranging from 3 to 15 amino acids (**31a–c**) with many functional side chains were all shown to be successfully cyclised with reasonable yields. Owing to their lower pK_a and oxidation potential, high selectivity was observed for decarboxylation of the α-amino acid C-terminal residue in preference to any side-chain carboxylic acids ($E_{1/2}^{red}$ = +1.2 V *vs.* SCE for Boc-Gly-CO_2K).[38] In many of the cases, purification of the cyclic peptides, unfortunately, resulted in significantly reduced yields when compared to crude yields.

Very recently, Ruf and co-workers expanded upon the work of MacMillan and co-workers to show successful C-terminal derivatisation of small peptide substrates.[39] They used a more extensive array of Michael acceptors including α,β-unsaturated ketones, as well as less electrophilic olefins such as cinnamic acid ester and vinyl-substituted (hetero)aromatic motifs.

Xu and co-workers sought to introduce a formyl group across Michael acceptors using glyoxylic acid derivatives (**32**) as synthetic equivalents.[40] Upon Giese addition of the glyoxylic acid derivative **32** simple treatment with acid furnishes the desired aldehyde (Scheme 14). The group paid particular attention to Michael acceptors that are generally less effective substrates for transition-metal-catalysed hydroformylation using CO and H_2 as syngas.[41] A broad scope of Michael acceptors showed moderate to excellent yields (35–95%), including α,β-unsaturated esters (**33a–b**), amides (**33d**), aldehydes, ketones, and nitriles. It is worth mentioning also that vinylpyridine and α-aryl styrene were successful substrates (*e.g.* **33c**). Good functional group tolerance was observed such as with aryl chlorides, aryl fluorides and boronic esters. Giese addition onto styrene, or styrenes possessing EWGs, proved to be fruitless, possibly due to oligomerisation, or an energy transfer event between the Ir PC and styrene. In addition to glyoxylic acid diethylacetals as the primary substrate, cyclic acetals 4,4,5,5-tetramethyl-1,3-dioxolane-2-carboxylic acid

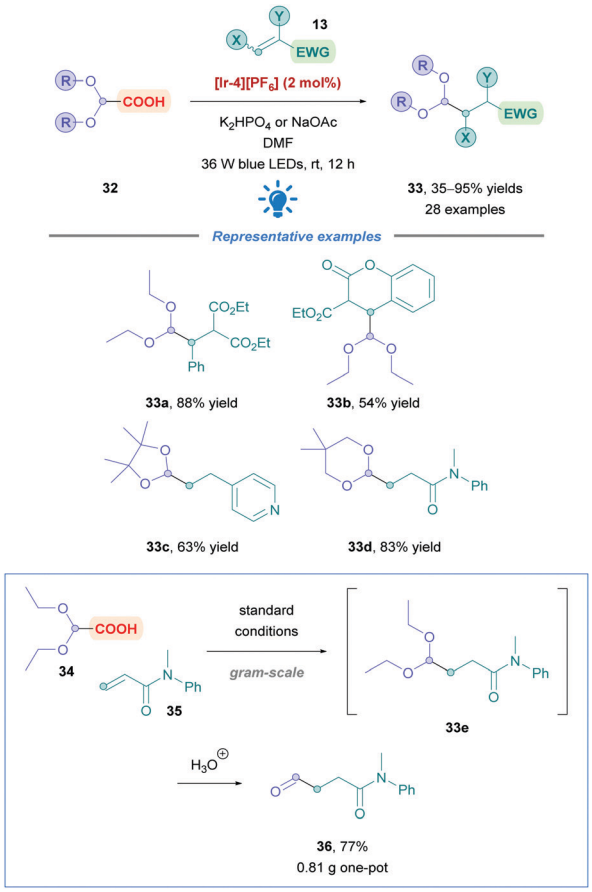

Scheme 14 Ir-Catalysed direct DGR of glyoxylic acids.

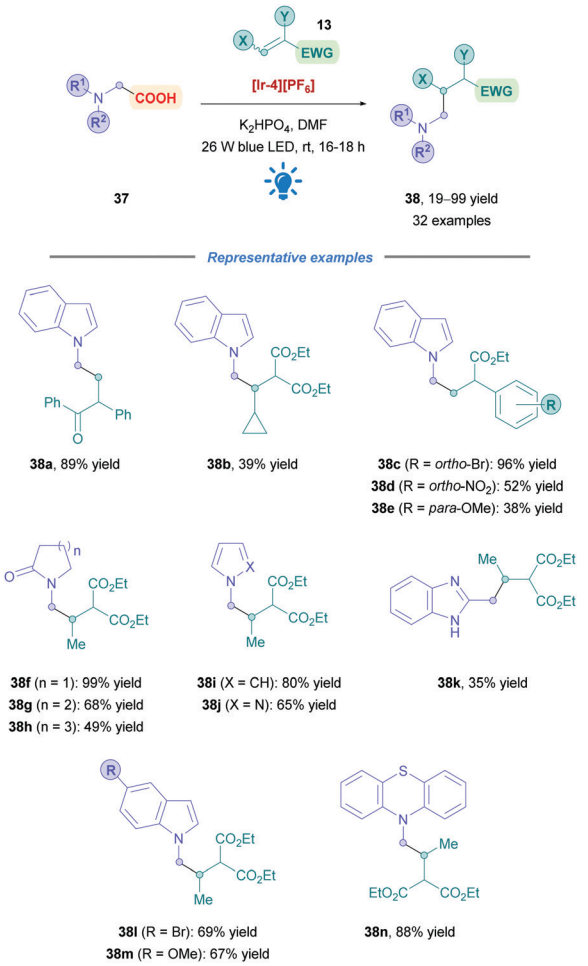

Scheme 15 Ir-Catalysed direct DGR of α-amino acids.

and 5,5-dimethyl-1,3-dioxane-2-carboxylic acid underwent efficient Giese addition (**33c and d**, respectively). The value of this protocol was demonstrated through the gram-scale, one-pot synthesis of aldehyde **36**, among others, achieving yields comparable to that of the small-scale reactions.

The next advancement was driven by the fact that *N*-substituted heterocycles are important scaffolds for the pharmaceutical industry. Seeking to expand access to this motif, AstraZeneca reported the DGR of *N*-methyl radicals, using *N*-substituted acetic acids (**37**) as easily accessible radical precursors (Scheme 15).[42] They employed **[Ir-4][PF$_6$]** to install weakly nucleophilic heterocyclic *N*-substituted acetic acids with low to excellent yields (19–99%), with substrates including indoles (**38a–e, l and m**), indazoles, imidazoles, benzimidazoles (**38k**), pyrroles (**38i**), and pyrazoles (**38j**). Efficient Giese addition was observed for olefins bearing halogens, EWGs and EDGs with good to excellent yields (**38c–e, l and m**). Moreover, cyclic amides of different ring sizes (**38f–h**) and fused phenyl substituted cyclic amides showed smooth DGR. Giese addition appeared not to be significantly hindered when increasing the steric bulk on the olefin. Indeed, it was shown that unsubstituted maleates and acrylates underwent limited conjugate addition. Prolonged irradiation of up to 16–18 h was required for all substrates, possibly due to the weak nucleophilicity of the generated *N*-methyl radicals.

MacMillan's original protocol[26] has also been applied by the Fujimoto group to the formal synthesis of L-ossamine (**42**), a deoxyaminosugar motif found in the polyketide natural product ossamycin (Scheme 16).[43] Using Ir complex **[Ir-4][PF$_6$]** as the PC, light-promoted DGR of the protected D-threonine onto methyl acrylate was performed in flow with a residence time of 4 h to give conjugate addition product **41** in 80% yield and moderate diastereoselectivity (62 : 38 d.r.).

2.1.1.2 Further studies on other Michael acceptor substrates. In addition to exploring the possible carboxylic acid substrates that could be used, some work has been carried out to identify Michael acceptors that offer unique functional handles. For example, Tian and co-workers used α-aryl vinylphosphonates (**43**) to generate valuable α-aryl alkylphosphonates (**44**) with moderate to excellent yields (50–99%) (Scheme 17A).[44] α-Aryl phosphonates have stirred an interest within medicinal chemistry because of their attractive biological properties.[44,45] Furthermore, vinylphosphonates are less prone to undergo oligomerisation in comparison to their conjugated carbonyl counterparts. The group reported a broad substrate scope using Ir PC **[Ir-4][PF$_6$]**, with good efficiency and functional group tolerance (**44a–f** and **48a–e**). Addition of benzyl radicals was

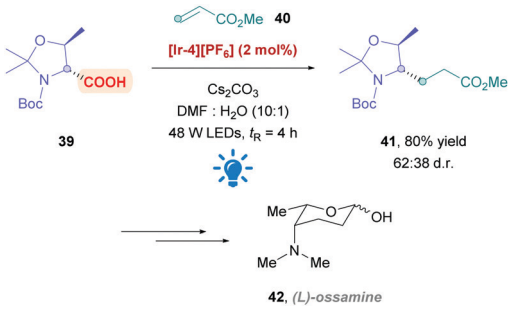

Scheme 16 Use Ir-catalysed direct DGR for the total synthesis of L-ossamine.

shown to be limited, but using potassium benzyltrifluoroborate as a radical precursor, instead of phenylacetic acid, significantly improved yields. Hydroformylation, similarly to the work of Xu,[40] could be achieved through sequential Giese addition using glyoxylic acid acetal, followed by $LiBF_4$-mediated hydrolysis, affording a variety of diethyl (1-aryl-3-oxopropyl)phosphonates (**45**) (Scheme 17B). They also showcased the utility of their protocol by providing a synthesis of the fosmidomycin derivative **49**. Competitive decarboxylative alkylation experiments gave evidence that unsaturated carbonyls are better radical acceptors than vinylphosphonates.

The Aggarwal group described a novel DGR of amino acid derivatives onto vinyl boronic esters (**50**), accessing a myriad of boronic esters (Scheme 18) (**51**).[46] The proposed mechanism surprisingly involved a unique reductive SET of an α-boryl radical by the reduced-state $\mathbf{PC_{red}}$, which was further supported by deuterium-labelling studies and DFT (density functional theory) calculations. Various cyclic and acyclic amino acids proceeded with good yields (**51a–i**). Catalyst **[Ir-2][PF$_6$]** was most effective for amino acids possessing tertiary N-protected amines (Conditions A). However, amino acids bearing free NH groups required minor modifications to the reaction conditions, changing the PC to **[Ir-4][PF$_6$]** and solvent to DMA (Conditions B). Various vinyl boronic ester derivatives were examined, obtaining products with moderate to good yields (**51a–e**, 53–87%). Unfortunately, α-styrenyl boronic esters was rendered incompatible because of the rapid protodeboronation under the reaction conditions. The group further investigated the substrate scope by applying the protocol to simple alkyl carboxylic acids (**51j–l**). Again, reaction conditions were further tuned by employing the more reducing PC **[Ir-3][PF$_6$]** (Condition C). Natural product or marketed drug carboxylic acids (*e.g.*, **51j–k**) underwent Giese addition with moderate yields (40–63%), demonstrating the potential for application to late-stage functionalisations.

Identifying new peptide-based drug candidates remains of interest within the pharmaceutical industry.[47] Peptides solely consisting of natural amino acids tend to have poor pharmacokinetic properties primarily due to their low membrane permeability and metabolic instability.[47] Thus, much effort has focused on the synthesis and installation of unnatural amino acids (UAAs) to overcome some of these limitations.

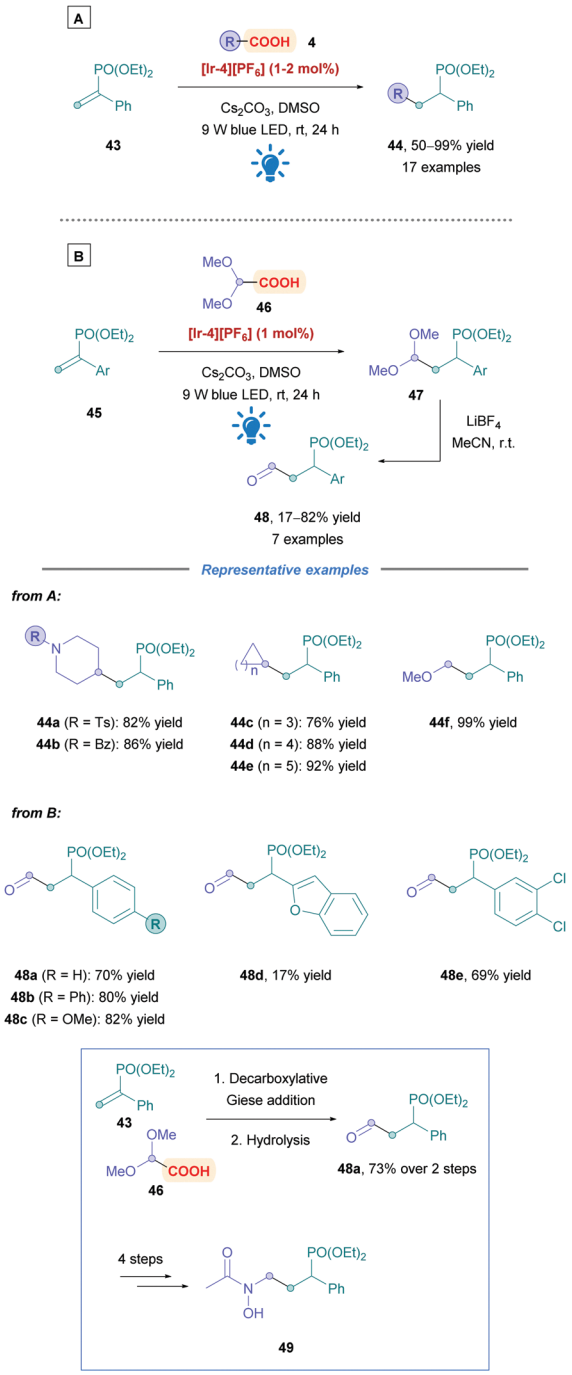

Scheme 17 Ir-Catalysed direct DGR onto vinylphosphonates with (A) alkyl acids and (B) glyoxylic acids.

Recently, Gómez-Suárez and co-workers developed a convenient preparation of diverse range of UAAs through direct DGR onto chiral dehydroalanine derivative (Dha, **52**)[48] (Scheme 19).[49] This versatile Michael acceptor can be accessibly synthesised in a 3-step procedure from benzyl cysteine on multigram scales.[49] Employing **[Ir-4][PF$_6$]** as the PC, a whole host of acid substrates where tested to give either acylated or alkylated *syn* oxazolidinones (**53**) with excellent diastereoselectivity (d.r. $>20:1$). Broad substrate scope with high functional group

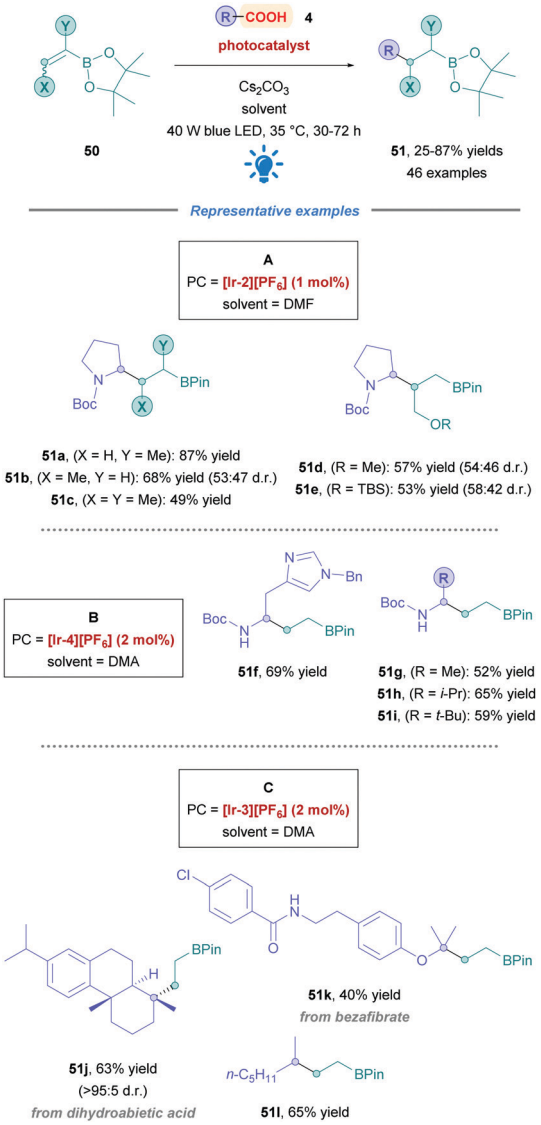

Scheme 18 Ir-Catalysed direct DGR onto vinyl boronic esters (A) cyclic and (B) acyclic amino acids, and (C) alkyl carboxylic acids.

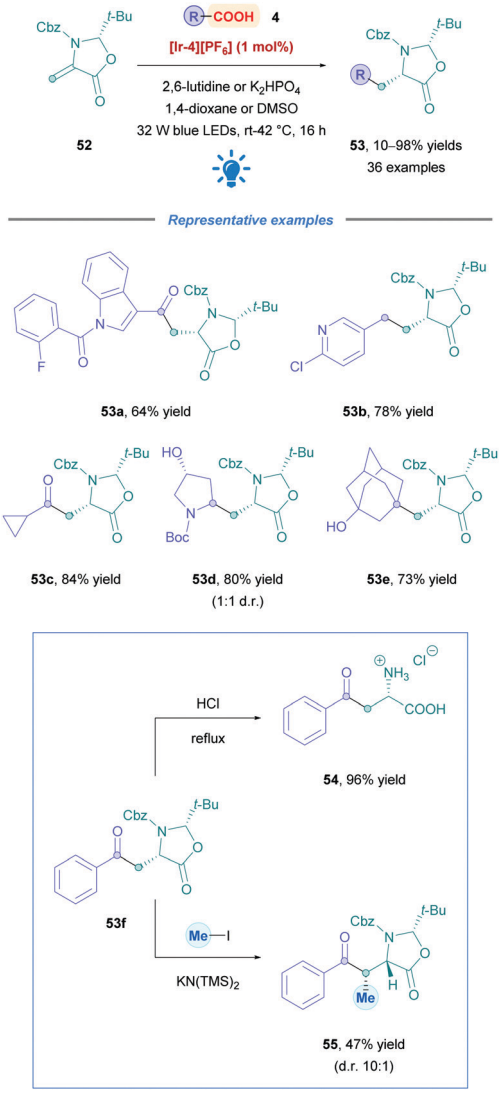

Scheme 19 Diastereoselective Ir-catalysed direct DGR onto Dha.

tolerance was observed for aliphatic α-keto acids (**53a and c**), as well as primary, secondary and tertiary aliphatic acids (**53b, d, and e**). Low to excellent yields were obtained throughout (10–98%). Having accessed the oxazolidinone core, and treatment with acid gives rise to the desired (L)-amino acid (*e.g.*, **54**). Subsequent N-Fmoc protection then renders the UAA suitable for solid phase peptide synthesis. Alternatively, further enolate-assisted alkylation methodologies could be employed to further increase complexity and stereochemical information, such as the formation of **55**.

During their total synthesis of (+)-fastigiatine **59**, the Rychnovsky group employed a MacMillan-type protocol[26] to install the protected glycine derivative **57** onto the bicyclic α,β-unsaturated ketone **56** to afford the Giese product **58** (Scheme 20).[50] Using PC **[Ir-4][PF$_6$]**, they achieved a very good yield of **59** (87%) with the desired diastereomer favoured by a 1 : 5.2 ratio. Interestingly, a previous approach using aminomethyl cuprate addition resulted in poorer diastereoselectivity.

2.1.2 Iron-based photocatalysis. Due to their long-lived excited states (microseconds), stable metal–ligand bonds, strong absorbance in the visible region, and high reduction and oxidation potentials, iridium- and ruthenium-based PCs have gained prominence in the field of photoredox chemistry.[51] Yet the cost and scarcity of these precious metals has motivated chemists to develop photoredox active complexes using cheap, earth-abundant 3d transition-metals such as iron.[52] However, iron complexes are severely limited in their photocatalytic applicability: in addition to lower oxidation and reduction potentials, and weaker metal–ligand bonds, their photoexcited states are ultra-short (pico- to nanosecond range) for electron transfer reactions, due to rapid excited-state deactivation. The metal-centred excited state energies can be raised using strong donor ligands such as *N*-heterocyclic carbenes (NHCs) as demonstrated by the Wärnmark group, who synthesised a Fe(III) complex with an extended charge-transfer excited state lifetime (2 ns).[53]

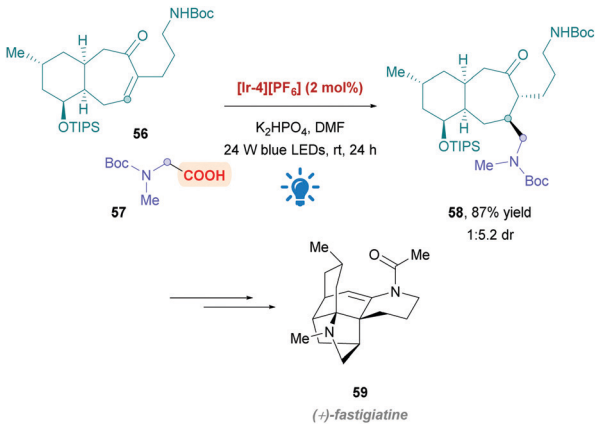

Scheme 20 Use Ir-catalysed direct DGR for the total synthesis of (+)-fastigiatine.

Another intriguing mode for Fe-based photocatalysis is through intramolecular charge-transfer, whereby the organic substrate is directly bound to the metal centre. This approach negates the need for long-lived transition states and takes advantage of photo-labile metal–ligand bonds. In 1953, Parker and co-workers reported the photolysis of ferrioxalate which gave rise to decarboxylation,[54] and the decades proceeding has seen extensive mechanistic studies of this process.[55] A recent review by Reiser and co-workers discusses some of the latest advances in visible-light induced homolysis of earth-abundant organometallic complexes.[56] Recently, Jin and co-workers took advantage of the photoredox-active nature of Fe(III) carboxylates to achieve direct DGR onto vinylidene cyanide derivatives (**60**). Fe(III) carboxylates were generated from catalytic amounts of Fe_2SO_4, and gave low to excellent yields (17–99%) of the corresponding Giese adducts (**61**).[57] They postulated a mechanism (Scheme 21) whereby the carboxylic acid **4** initially coordinates to the Fe(III) species **L-Fe^{III}**, forming the Fe(III)–carboxylate complex **XIV**. Visible-light irradiation (427 nm) promotes excitation of **XIV**, triggering an intramolecular ligand-to-metal-charge-transfer (LMCT) event which induces decarboxylation to generate the alkyl radical **I** and the reduced Fe(II) complex **L-Fe^{II}**. Radical addition of **I** onto Michael acceptor **60** generates radical intermediate **XII**, which engages in SET with **L-Fe^{II}** to form the anion **XIII** whilst the Fe(II) is re-oxidised to Fe(III) (**L-Fe^{III}**) to close the catalytic cycle. Final protonation of **XIII** furnishes the desired Giese adduct **61**. The entire process benefits from being redox neutral, avoiding the use of any additional oxidant.

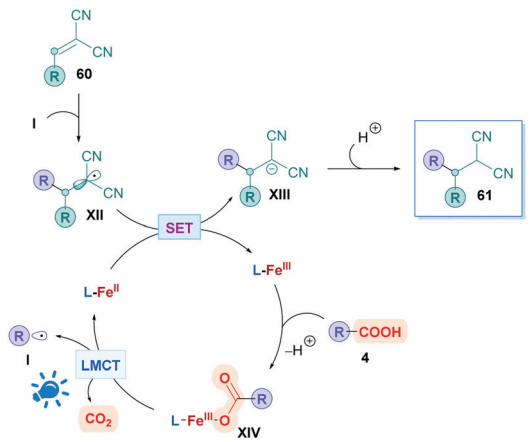

Scheme 21 Proposed mechanism for Fe-catalysed direct DGR.

Reaction optimisation studies unveiled that the di-(2-picolyl)-amine **62** served as the best ligand, and no additional base was required for acid deprotonation (Scheme 22). The Michael acceptor scope was primarily restricted to 2-benzylidenemalononitrile derivatives **60**, with aryl motifs bearing electron-withdrawing and -donating groups showing to be well tolerated (*e.g.*, **61a–c**). 2-Alkylidenemalononitrile (**61d**) and malonate-type Michael acceptors (**61e**) could also be employed with synthetically useful yields (69%). Regarding the acid scope, a wide variety of different acid types could be employed. Stabilised radical precursors including α-oxy (**61f**), -amino (**61g**), and benzyl acids (**61h and i**)

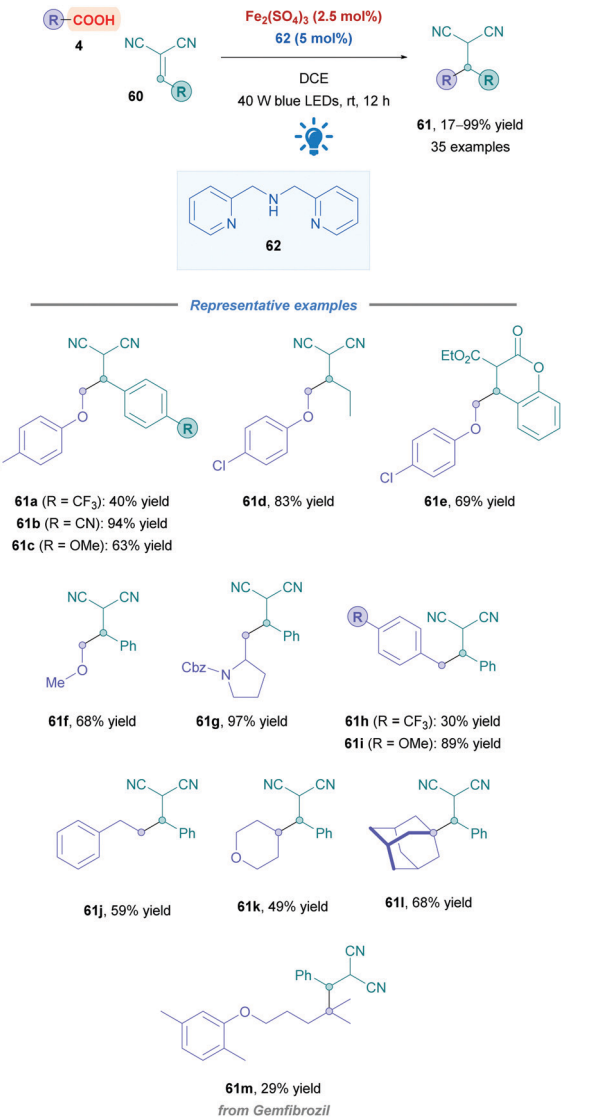

Scheme 22 Fe-Catalysed direct DGR.

gave generally good overall yields (30–97%) of their corresponding adducts. Acids that form unstabilised primary (**61j**), secondary (**61k**), and tertiary (**61l–m**) radicals also gave low to good yields (29–68%).

Although photocatalysis using 3d transition metals does not yet recapitulate the transformations accessible using heavier transition metals, important advances are continuously made in this exciting research area. One possible development in this field would be to establish a broader substrate scope for direct DGRs.

2.1.3 Tungsten-based photocatalysis. Another competent metal-based photocatalyst that has gained wide attraction is the decatungstate anion, routinely employed as the tetrabutylammonium salt (**TBADT**: tetrabutylammonium decatungstate, $(n\text{-Bu}_4\text{N})_4[W_{10}O_{32}]$) (Scheme 23A).[58] As well as being efficient in HAT and oxidation reactions, TBADT has been shown to be a convenient and robust photocatalyst that can be readily synthesised.[59] As a member of the large family called polyoxometalates (POMs),[60] reduction of the anion gives rise to mixed-valence polyanions known as heteropoly blues, characterised by the extra electrons at the metal centres. This colour change to blue provides a convenient means for reaction monitoring.

The mechanism of action for TBADT is depicted in Scheme 23B. Irradiation of $[W_{10}O_{32}]^{4-}$ with light (324 nm)[61] initially forms the singlet excited state $^*[W_{10}O_{32}]^{4-}$ (S_1). Due to its short lifetime, in the order of a few tens of picoseconds, it does not interact with organic substrates and rapidly decays to the relaxed, more reactive excited state. This excited state is an unknown species and is frequently labelled as **wO**.[58a,61] **wO** is formed with a quantum yield (Φ_{wO}) of around 0.5–0.6.[62] The organic substrate can then interact with **wO** through oxidative SET, although, depending on the redox properties of the substrate, a HAT process is also possible.

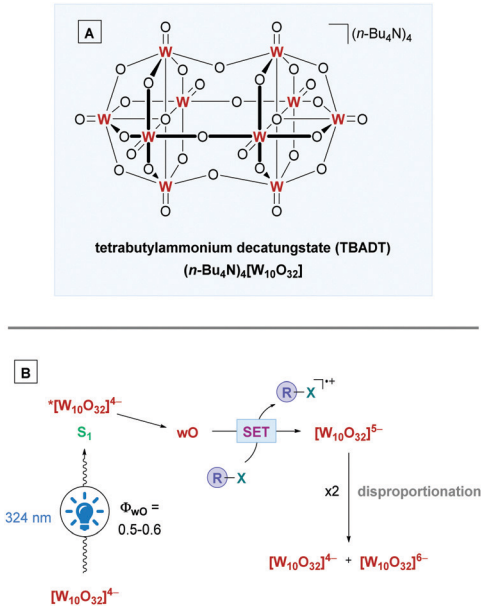

Scheme 23 (A) Structure of TBADT. (B) Proposed mechanism for oxidation using TBADT.

The reduction potential of **wO**, $E(\mathbf{wO}/[W_{10}O_{32}]^{5-})$ has been estimated to range from +2.26 to +2.61V *vs.* SCE,[63] with a new study predicting a potential of +2.44 V *vs.* SCE.[64] Reduction of **wO** gives the $[W_{10}O_{32}]^{5-}$ anion, which disproportionates over a longer time scale to the reduced form $[W_{10}O_{32}]^{6-}$ and the oxidised form $[W_{10}O_{32}]^{4-}$. All the above decatungstate species mentioned, except for $[W_{10}O_{32}]^{4-}$, give rise to the blue colouration.

Because of its high oxidation potential, Ravelli and co-workers sought to exploit **TBADT** for the direct DGR of benzyl radicals from aryl acetic acids.[21] In contrast to secondary, tertiary, and α-heteroatom radicals, benzyl radicals exhibit a lack of reactivity towards electron-deficient olefins and have a tendency to dimerise.[65] To overcome these issues, the group envisaged that the deactivated catalyst $[W_{10}O_{32}]^{5-}$ could serve to activate simple olefins through reduction, regenerating the photocatalyst $[W_{10}O_{32}]^{4-}$ and affording the corresponding radical anion of the olefin. This activated olefin would then act as a more efficient radical trap for the benzyl radical. The reduction potential of the reduced photocatalyst ($[W_{10}O_{32}]^{5-}$) is estimated to be within the range of −0.9 and −1.4 V *vs.* SCE,[21,66] whilst the formal reduction potentials ($E^{0\prime}$) of simple olefins, *e.g.*, maleic anhydride, maleimides, fumarates, and fumaronitrile, are within the range −1.09 and −1.47 V *vs.* SCE,[63b] thus the $[W_{10}O_{32}]^{5-}$ species can be sufficiently reducing for these olefins.

Reaction optimisation using phenylacetic acid and fumaronitrile with **TBADT** (4 mol%) in aq. MeCN solution, under UV radiation (310 nm), revealed that $NaHCO_3$, $NaClO_4$, and biphenyl were essential additives for an efficient Giese addition (83% optimised yield). The $NaHCO_3$ served as a base to deprotonate the acid to the more reducible carboxylate, and the combination $NaClO_4$/biphenyl is postulated to facilitate the electron transfer process.[63b,67]

The optimised conditions showed moderate to excellent yields for a variety of arylacetic acids (**63**) with Michael acceptors (**19**) (Scheme 24). Phenylacetic acids bearing the electron-donating methoxy group in the *ortho*- and *para*-positions were well tolerated (**64c**, 70% and **64a**, 81%), and the electron-withdrawing *meta*-methoxy derivative unsurprisingly gave the lowest yield (**64b**, 54%), presumably due to lower radical nucleophilicity.[68] Aryl moieties bearing deactivating groups in the form of halogens (**64d–e**) were similarly well tolerated but gave lower yields (44–56%). Good yields were also obtained for thiopheneacetic acid (**64m**, 52%) and *N*-Boc-protected aminophenylacetic acid (**64f**, 79%,) – the unprotected aminophenylacetic acid was insoluble under the reaction conditions. Interestingly, selective decarboxylation was observed when using (3,4-methylenedioxy)phenylacetic acid (giving **64l**), despite the presence of the methylene hydrogen atoms which can be subjected to HAT by **TBADT**.[69] 2-Phenylpropionic and mandelic acid derivatives also proved to be successful substrates, however, mandelic acid itself was unsuccessful, giving rise to benzaldehyde instead. Other Michael acceptors including *N*-phenyl maleimide and benzylidenemalononitirile could also serve as efficient radical traps for benzyl radicals. Dimethyl fumarate (giving **64j**) required an excess of acid and biphenyl to

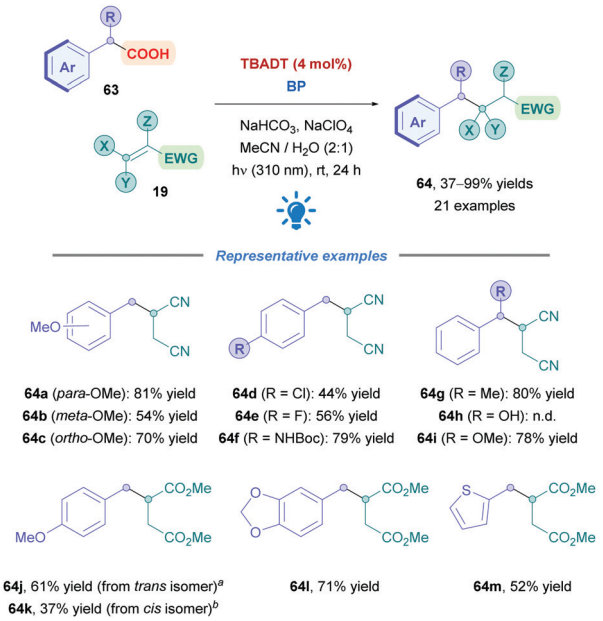

Scheme 24 TBADT-catalysed direct DGR of benzylcarboxylic acids.

be omitted to improve yields, and its *cis* isomer dimethyl maleate (giving **64k**) proved to be sluggish due to its higher reduction potential (−1.65 V *vs.* SCE).[63b]

The proposed mechanism is presented in Scheme 25, where, firstly, photoexcitation of $[W_{10}O_{32}]^{4-}$ populates the highly oxidising **wO** state. **wO** could undergo oxidative SET with carboxylate **XV** to the corresponding carboxyl radical **XVI**. This process, however, is slow as evidenced by low yields obtained

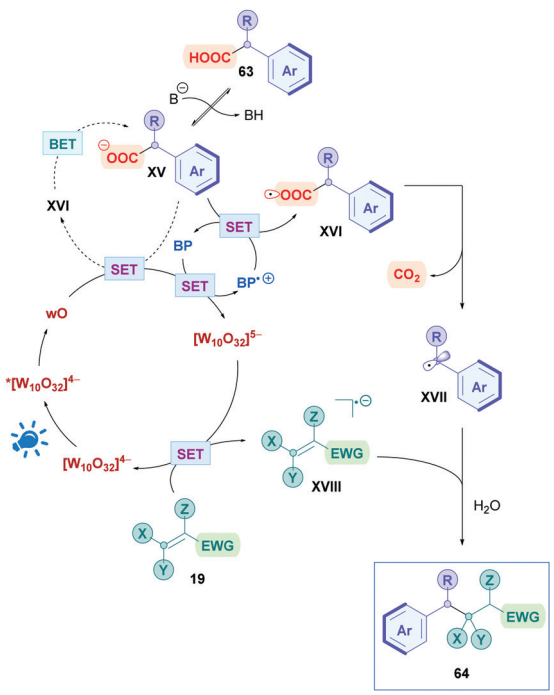

Scheme 25 Proposed mechanism for TBADT-catalysed direct DGR of benzylcarboxylic acids.

from when performing the reaction without biphenyl. Two possible explanations could account for this behaviour. There may be electrostatic repulsion effects between **wO** and **XV** since they are both negatively charged. Alternatively, back-electron transfer (BET) may be involved that prevents decarboxylation. This slow reactivity is bypassed by the presence of biphenyl (**BP**), which is readily oxidised by **wO** ($E^{red}_{1/2}$(**BP**$^{\bullet+}$/**BP**) = +1.95 V *vs.* SCE)[70] to the long lived radical cation **BP**$^{\bullet+}$ together with $[W_{10}O_{32}]^{5-}$. As well as being positively charged to overcome the electrostatic repulsions, **BP**$^{\bullet+}$ can oxidise **XV** to trigger decarboxylation, giving the benzyl radical **XVII** and the regenerated **BP**. Meanwhile, the $[W_{10}O_{32}]^{5-}$ species can oxidise the olefin **19** to its activated radical anion **XVIII** whilst closing the catalytic cycle by reforming $[W_{10}O_{32}]^{4-}$. Subsequent conjugate addition of **XVII** with **XVIII**, followed by protonation (either from the aqueous solvent or protonated base), affords the final product **64**.

2.2 Organophotocatalysis

Despite the impressive utility of Ir-based photocatalysis, unsurprisingly, the major drawback for these catalysts is the scarcity of the metals used, leading to high financial costs and sustainability issues. Consequently, the field of organophotocatalysis has greatly expanded in recent years to find cheaper alternatives. In addition to lower costs, organic PCs are more sustainable and offer a myriad of modular scaffolds with characteristic and tunable physiochemical properties.[71] Organo-PCs tend to achieve higher oxidation powers than their TM-PC counterparts, allowing access to thermodynamically challenging chemical transformations.[71a]

It is of no surprise that organophotoredox catalysis has found application within the realm of direct DGRs. This section will discuss some of the different families of organo-PCs that has been employed, again identifying any significant advantages and limitations for each system.

2.2.1 Arenes coupled with dicyanoarenes as photocatalysts. One of the first use of organo-photosensitisers for direct DGRs was reported by Yoshimi, Hatanaka and co-workers in 2009.[72] They utilized a photochemical system using an arene as a PC, together with a dicyanoarene (DCA) as a redox mediator. Both species are neutral, stable, and inexpensive organic molecules. The proposed mechanism using this catalytic system is shown in Scheme 26A. Upon irradiation of UV light, photoexcitation of the arene **Ar** gives rise to the excited species ***Ar**. Subsequent reductive SET to **DCA** generates the key oxidant **Ar**$^{\bullet+}$ and reductant **DCA**$^{\bullet-}$. Oxidant **Ar**$^{\bullet+}$ facilitates base-promoted decarboxylation of carboxylate **IV** to generate radical **I**, as well as the regeneration of PC **Ar**. Conjugate addition of **I** with the Michael acceptor **2** gives the stabilised radical **II**. The key reductant **DCA**$^{\bullet-}$ is quenched through BET with **II** to regenerate **DCA**, and the resulting anion **VI** is subsequently protonated to afford the desired Giese adduct **3**. It is worth noting that DCA could also play a minor role as a photooxidant ($^{*}E^{red}_{1/2}$ = +2.2 V *vs.* SCE for **1,3-DCB**).[73] The amount of **Ar** and **DCA** required is dependent upon the BET efficiency. Some of the examples discussed in this section will showcase protocols

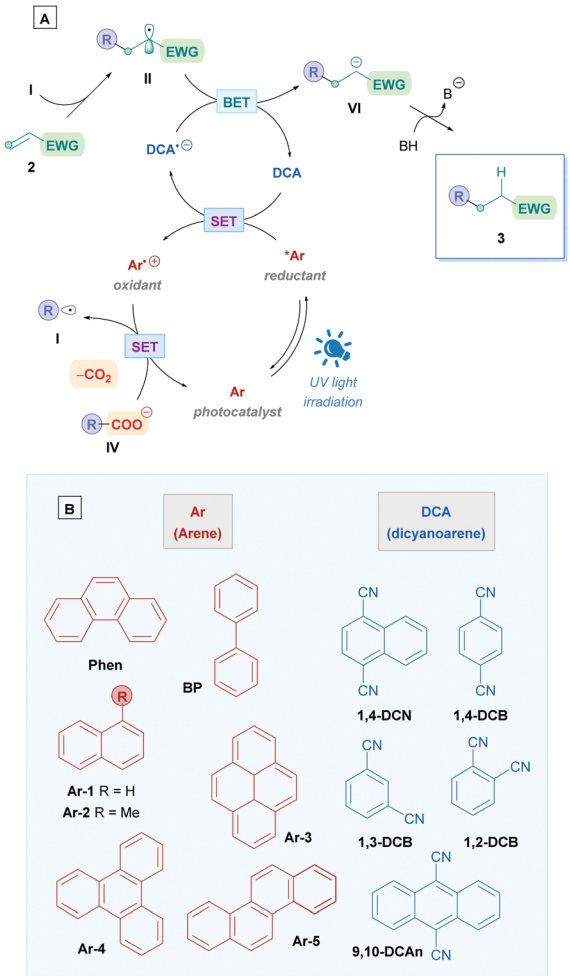

Scheme 26 (A) Proposed mechanism for the direct DGR of carboxylic acids using Ar/DCA-coupled photoelectron transfer. (B) Some commonly employed arenes and dicyanoarenes for photocatalysis. DCN = dicyanonaphthalene, DCB = dicyanobenzene, DCAn = dicyanoanthracene.

requiring stoichiometric amounts of **Ar** and **DCA** and thus not strictly catalytic, but, for the purposes of this review, these systems will still be considered catalytic.

Yoshimi, Hatanaka and co-workers applied this catalytic process to promote Giese addition for a variety of different chemical substrates, which is summarised in Scheme 31. In their seminal work, they used phenanthrene (**Phen**) as the PC and 1,4-dicyanobenzene (**1,4-DCB**) as the co-catalyst to install N-protected amino acids onto simple Michael acceptors to generate *N*-Boc-γ-amino acids (Scheme 31A).[72a] Only one equivalent of olefin **2** was required to obtain moderate to excellent yields (36–88%) without the need of a base. In addition to single amino acids, N-protected dipeptides and tripeptides (**66**) were also successful substrates (Scheme 28A). Interestingly, acrylic acid also participated smoothly as a radical acceptor, suggesting that the difference between pK_a of the starting α-amino acid and the γ-amino acid product is sufficiently large to prevent further decarboxylation, which would otherwise diminish the yield of **66**. The group also carried out an assessment of this decarboxylative coupling for primary, secondary and tertiary carboxylic acids with acrylonitrile.[72d] Employing catalytic amounts of **Phen** and 1,4-dicyanonaphthalene (**1,4-DCN**) as catalytic partners, they achieved moderate yields (33–66%) for the respective Giese adducts. Long reaction times (18 h) were required due to the relatively higher pK_a of the starting carboxylic acid, however, the time could be decreased with the addition of base such as tetra-*n*-butyl ammonium hydroxide. Sodium hydroxide was avoided due to the insolubility of the carboxylate sodium salts in acetonitrile. DMF can be used as a solvent to overcome this, but only with chrysene (**Ar-5**) and **1,4-DCB** as catalysis partners. Moreover, they also showed that **1,4-DCN** could be used as a solo catalyst to install *N*-Boc-amino acids onto acrylonitrile.[72c] However, the high oxidation potential of **1,4-DCN** (1 equiv.) renders amino acids possessing aromatic rings incompatible, and longer reaction times or a more powerful light source (UV) were required. The proposed mechanism is depicted in Scheme 27, which is comparable to most of the mechanisms already shown in this review.

Further studies to assess the influence of amino acid side chains for tripeptide systems were later conducted.[72e] Amino acids possessing electron rich substituents such as phenol and indole impeded the efficiency of the Giese addition, possibly due to these moieties quenching the photogenerated Phen radical cation (**Ar**$^{\bullet+}$). However, yields can be improved by appropriately installing a Boc protecting group onto these moieties. In contrast, the central amino acids possessing alkyl, phenyl, thioether, hydroxy and amide-containing side chains where all able to participate efficiently.

Installation of α-amino acids and peptides (**65**), along with a small collection of aliphatic carboxylic acids, onto *N*-acryloyl amino acid esters and peptides (**67**) was also successful using the photocatalytic combination of **Phen** and **1,3-DCB** (Scheme 28A), synthesising *N*-alkylcarbonyl peptides (**68**).[72f] Lower yields (25–58%) were observed due to the slower addition of the alkyl radicals onto the less electron-deficient *N*-acryloyl moiety. As a further consequence of the slower radical addition, unwanted photosubstitution processes meant that **1,4-DCB**

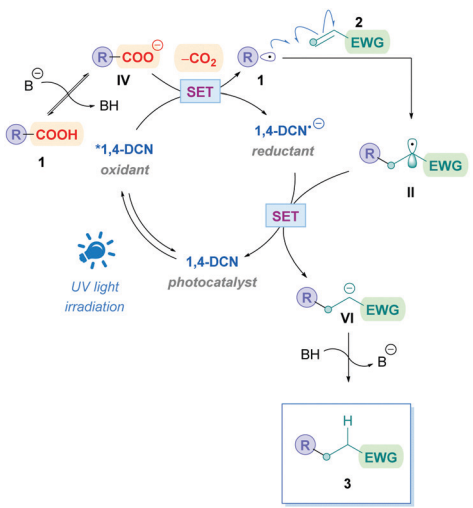

Scheme 27 Proposed mechanism for DCN-catalysed direct DGR.

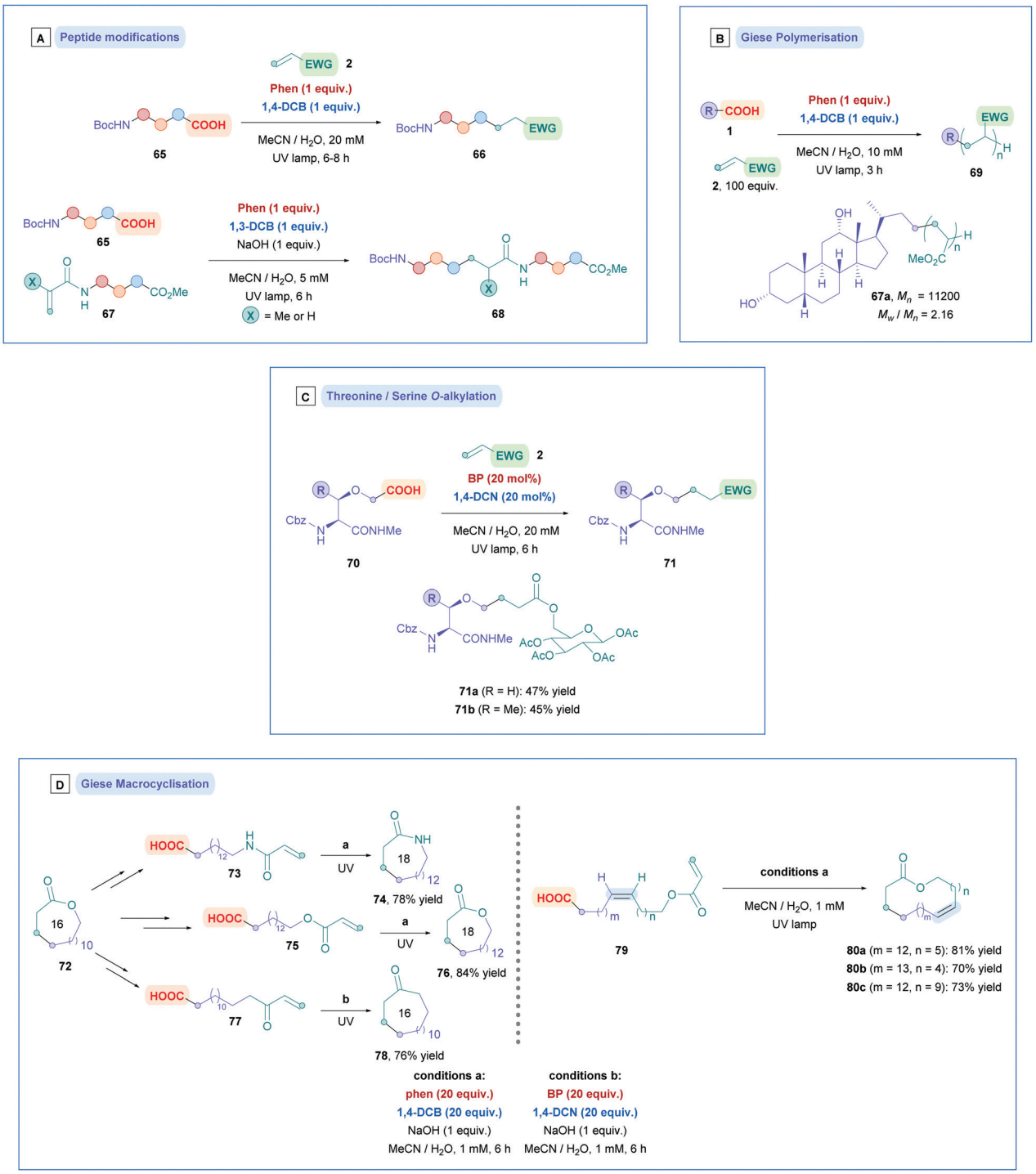

Scheme 28 (A) Ar/DCA-catalysed direct DGR of amino acids and peptides. (B) Ar/DCA-catalysed direct decarboxylative Giese polymerisation. (C) Ar/DCA-catalysed direct DGR of threonine and serine derivatives. (D) Ar/DCA-catalysed direct DGR for macrocyclisation.

could not be used, whereby formation of by-product alkylcyanobenzene *via* decyanation was apparent.

Recently, *N*-acryloyl amino acids and peptides have seen implementation in the sequential inter- and intramolecular radical cascade reactions involving the aromatic rings of tyrosine and phenylalanine derivatives (Scheme 29A).[72k] Preliminary studies using *O*-Boc protected tyrosine (**81**) with **Phen** and **1,3-DCB** revealed that three products could be obtained (**82–84**). This can be rationalised using the proposed mechanism in Scheme 29B. Photoinduced decarboxylation generates the α-amino radical which can undergo Giese addition to the acrylamide partner **2**, forming intermediate **XIX**. Radical **XIX** could either be reduced by BET with **1,3-DCB**$^{-\bullet}$ to the corresponding anion **XX**, followed by protonation to give the

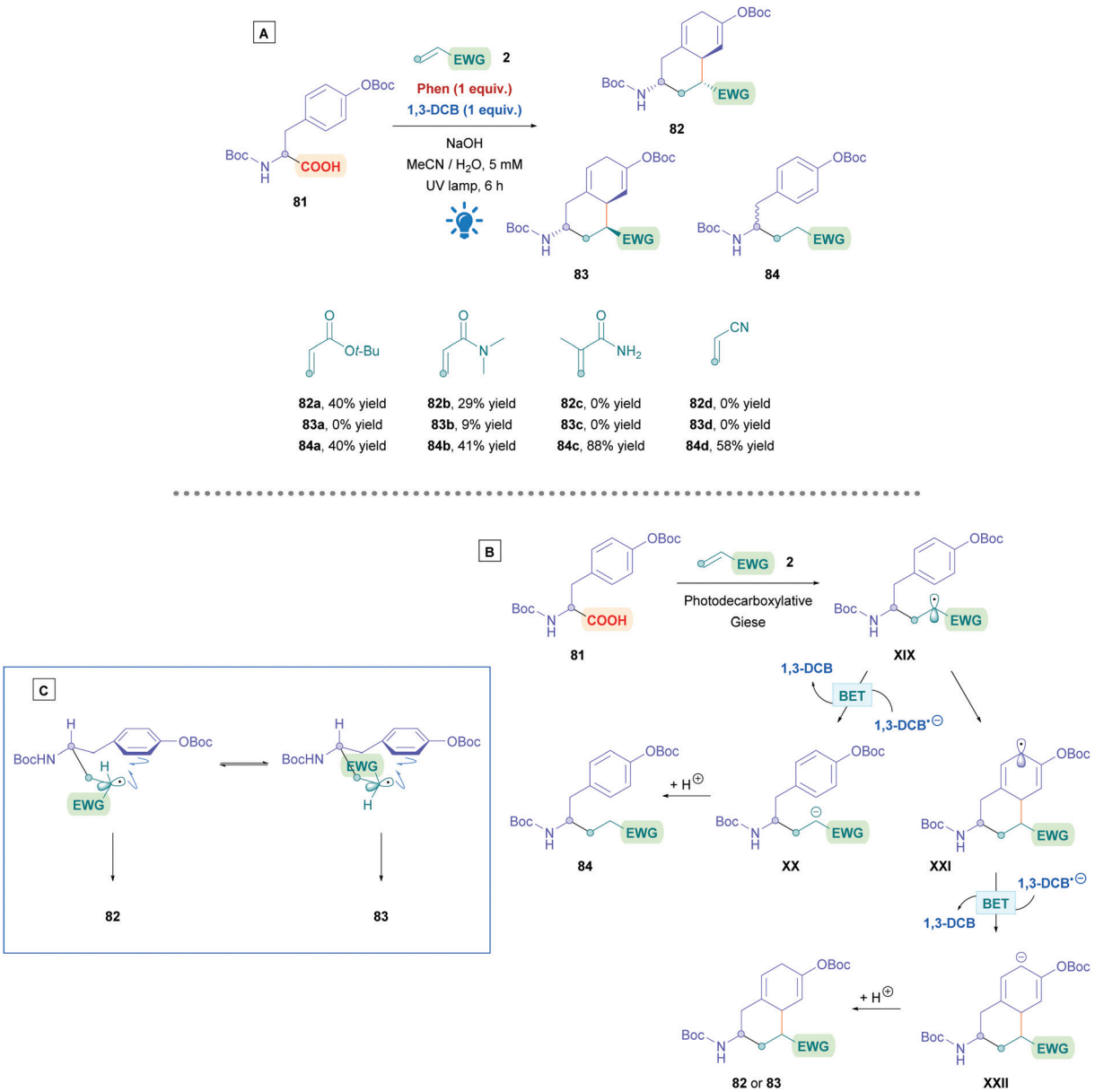

Scheme 29 (A) Ar/DCA-catalysed direct DGR of *O*-Boc protected tyrosine. (B) Proposed mechanism for the Ar/DCA-catalysed direct DGR of *O*-Boc protected tyrosine. (C) Proposed rationale for sterochemistry.

uncyclized Giese adduct **84**. Alternatively, radical cyclisation onto the benzene ring gives radical **XXI** and the same sequential process of reduction and protonation would then afford the cyclised product **82** or **83**. Interestingly, even though the negative charge in **XXII** can in theory be delocalised around the 6-membered ring, protonation of **XXII** does not seem to occur at the alternative sites to give more stable conjugated diene isomeric products, presumably for the same kinetic control reason as in the Birch reduction.[74] The relative abundance of each observed product was dependent upon the electron-donating abilities of benzene ring in **81**, steric hindrance of olefin **2**, and the electrophilicity of radical **XIX**. The rate of radical cyclisation is increased by having a more electron-rich benzene ring and a less sterically demanding Michael acceptor. Using Michael acceptors such as styrene and acrylonitrile increases the electrophilicity of radical **XIX**, allowing for more efficient reductive BET to prematurely terminate radical cyclisation and favourably giving **84**. In addition, acid substrates that do not bear an *N*-Boc group failed to undergo cyclisation, indicating the necessity of the *N*-Boc group to promote cyclisation. The stereochemistry of **82** and **83** was rationalised by using the two 6-membered transition states (Scheme 29C), where the *N*-Boc protected amino group occupies the equatorial position. Dipeptides containing C-terminal tyrosine were also subjected to the reaction conditions, forming ring-constrained peptides. The yields in these cases were diminished, presumably due to low solubility of the resulting peptides in the medium.

Radical polymerisation using this coupled photochemical system has also been explored (Scheme 28B). Yoshimi employed complex carboxylic acids to function as radical initiators which were incorporated as the polymer chain ends.[72g] Such acids included sugars, steroids, and peptides, thus adding unique complexity to polymer chains under mild conditions (*e.g.*, **67a**). Excellent conversions were observed throughout for the different acid substrates when using **Phen** and **1,4-DCB** as catalysis partners. Sequential radical polymerisation of two or more different Michael acceptor monomers could also be attained. Good participation was observed for more sterically hindered Michael acceptors such as ethyl acrylate and *t*-butyl acrylate, with greater conversion for increasing sterics. A drawback of this protocol was the lack control of the molecular weight distributions, resulting in high polydispersities (M_w/M_n) being observed throughout (2.16–3.87), where M_w is the weight-average molecular weight, and M_n is the number-average molecular weight. The M_n value was shown to be dependent on the concentration of **Phen** and **1,4-DCB** and types of electron acceptors. Using **1,4-DCN** instead of **1,4-DCB** resulted in more efficient BET which led to increased efficiency for chain termination.

Yoshimi also developed a strategic protocol for the *O*-alkylation of serine and threonine from serinyl and threoninyl acetic acids (**70**) (Scheme 28C).[72i] The synthesis of **70** involved a two-step procedure, firstly involving alkylation with α-bromo *t*-butyl acetate, followed by deprotection of the *t*-butyl group to expose the free carboxylic acid. No epimerisation of the stereogenic centre was observed during the synthesis. Dual-catalytic system involving biphenyl (**BP**) and 1,4-dicyanonaphthalene (**1,4-DCN**) were found to provide the highest yields of **71** (44–66%) compared to other catalytic systems. The use of NaOH was avoided to prevent base-promoted epimerisation and hydrolysis. The Michael acceptors used were predominantly acrylate- and acrylamide-protected amino acids and carbohydrates (*e.g.*, **71a and b**), giving their respective Giese adducts with moderate yields (up to 66%) without racemisation.

Furthermore, this photocatalytic system has been shown to induce intramolecular decarboxylative Giese cyclisation, generating macrocyclic lactones, lactams, and ketones ranging from 16- to 21-membered rings with excellent yields throughout (76–84%) (Scheme 28D left).[72a,b] The 16-membered lactone **72** was first transformed into a linear carboxylic acid possessing either a tethered acrylate amide (**73**), acrylate ester (**75**), or α,β-unsaturated ketone (**77**). Under high dilution conditions, photoinduced Giese cyclisation with **Phen** and **1,4-DCB**, **73** and **75** gave their corresponding ring-expanded, 18-membered lactam (**74**) and lactone (**76**), respectively, with excellent yields (Conditions A). Lower loadings of the catalysis partners required prolonged reaction times, thus 20 equiv. of **Phen** and **1,4-DCB** were used to complete cyclisation within 6 h. Photoinduced Giese cyclisation of **77** gave the corresponding macrocyclic ketone (**78**) of the same ring size (16-membered) as the original lactone **72**. In this case, the slower radical cyclisation onto the less electron-deficient olefin required a combination of **BP** and **1,4-DCN** as catalysis partners, since the radical anion derived from **BP** is longer lived than for **Phen**, allowing for more efficient BET of the α-carbonyl radical intermediate (Conditions B). To highlight the applicability of these methodologies, the same transformations that were applied to **72** could also be applied to **76** to generated 20-membered lactams and lactones, as well as 18-membered ketones.

Later developments introduced the synthesis for larger macrocyclic lactones (Scheme 28D right).[72j] Light-promoted decarboxylative Giese cyclisation of (*Z*)-alkene **79** afforded 25- (**80a**), 27- (**80b**), and 29-membered (**80c**) (*Z*)-selective lactones, and efficient hydrogenation afforded their corresponding saturated lactones. Precursor **79** could be easily prepared using a combination of Wittig chemistry and a more efficient installation of acryloyl groups, compared to their previous report.[72b]

Amino acids are frequently used for radical decarboxylation processes. However, generation of the α-amino radicals scrambles the stereochemistry, often giving products as racemates. The process can be rendered stereoselective through the use of chiral ligands, an example of which was demonstrated by the MacMillan group using synergistic Ir photoredox and chiral Ni catalysis.[75] Another tactic to control the stereochemistry of the process involves memory of chirality (MOC),[76] which can make use of the inherent chirality of the substrate rather than of another chiral source. Yoshimi used this strategy to provide a novel, stereospecific intermolecular Giese addition of N-protected proline derivatives to acrylonitrile (Scheme 30).[77] Choosing *N*-(2-phenyl)benzoyl-L-proline (**85**) as the acid substrate, with a catalytic system comprising of **Phen** and **1,4-DCB**, reaction with acrylonitrile (**86**) gave the corresponding Giese adduct **87** with excellent yields (85%) but little of the stereochemistry was retained (48% ee). In addition, formation of corresponding spirodihydroisoquinolinone **88** was observed as a side-product, resulting from *ipso*-radical cyclisation.[78] Stereospecificity, however, was dramatically improved when introducing ways to tightly control the biphenyl amide conformation. Using cyclic substrates **89** containing a *gem*-methyl substituent, which is derived from *N*-(2-phenyl)benzoyl-L-threonine methyl ester, the authors achieved >79% enantiomeric excess of Giese product **90**. Employing higher concentrations of acrylamide diminished the amount of **90**, whereas bulky Michael acceptors, *e.g.*, methyl acrylates, *t*-butyl acrylates and *N*-*t*-butyl acrylamide, tended to increase formation of their corresponding derivatives of **90**.

The stereoselectivity of the reaction is dictated by the axial chirality of the acid substrate about the CO (carbonyl)-C (phenyl) bond in the ground state (Scheme 31A). Acid substrate **85** can adopt two conformers of **open-85** and **closed-85**, with the closed state facilitating enantioselectivity by preventing bottom-side insertion of the olefin due to steric hindrance. Molecular orbital calculations (using HF/3-21G basis set) revealed that **open-85** is favoured over **closed-85** with a stabilisation energy of 5.0 kcal mol^{-1}. Introducing a dimethyl unit, such as **89** (Scheme 31B), inverted the energy difference towards **closed-89** (−0.6 kcal mol^{-1}), thus favouring enantioselectivity.

Very recently, Yoshimi successfully initiated direct photoinduced decarboxylation of benzoic acids (**93**), resulting in the formation of aryl radicals and their subsequent conjugate

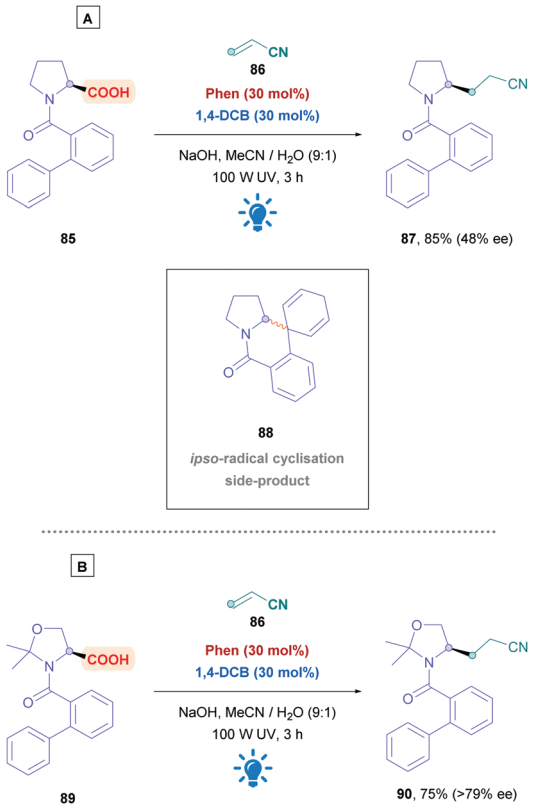

Scheme 30 Diastereoselective Ar/DCA-catalysed direct DGR using memory of chirality (MOC) on acid substrates (A) **85** and (B) **89**.

addition onto Michael acceptors (Scheme 32).[72l] This was achieved using **BP** and **DCN** (Method A), with slight heating to promote CO_2 extrusion. Alternatively, **BP** and **DCA** could be used together under visible blue light irradiation (Method B). However, lower yields were observed using Method B due to the lower solubility of **DCA** in aqueous MeCN solution. Benzoic acids possessing alkyl groups and halogens proceeded well with low to moderate yields (16–69%) (**94a–h**). Benzoic acids with appropriately protected phenolic hydroxy groups were also successful substrates, and electron-rich aryls, such as those bearing methoxy groups, did not give their corresponding adducts **94**. Decreased yields were observed for aryl with *para*-substituted EWGs (**94e**) due to the weaker nucleophilicity of the aryl radicals. Acrylonitrile was the acceptor of choice for this process, yet other acceptors included *t*-butyl acrylate, acrylamide (**93f**), and phenyl vinyl sulphone (**93h**). Higher concentrations of Michael acceptor (100 mM, 5 equiv.) were necessary to overcome competitive phenyl radical H-abstraction from MeCN. However, the high acceptor concentration also introduced the increased propensity for polymerisation, thus high concentrations of photocatalysts were required to counteract this phenomenon.

A recent application of this reagent system developed by Yoshimi was demonstrated by Inoue and co-workers for the synthesis of talatisamine precursor compound **96** (Scheme 33).[79] The group was seeking to find a more efficient means to construct the complex ABCE-ring scaffold of **96** through an intramolecular

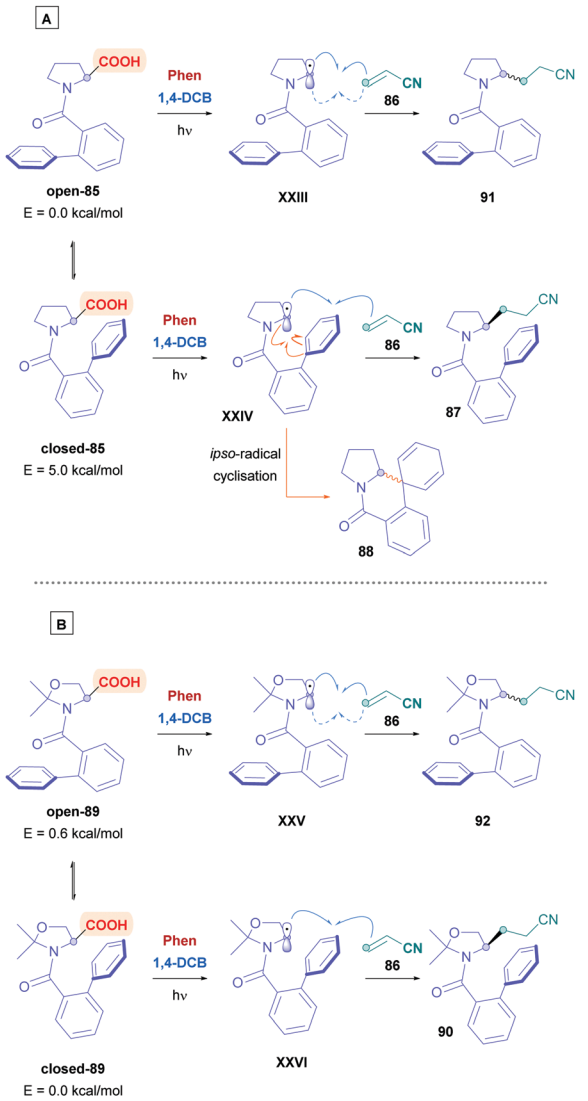

Scheme 31 Proposed mechanism to rationalised stereochemistry for acid substrates (A) **85** and (B) **89**.

decarboxylative Giese-type process. Intermediate **96** has the potential to be used toward the synthesis of C_{19}-diterpenoid alkaloid talatisamine (**97**) and other derivatives. The more common iridium or acridinium photocatalysts gave complex mixtures, but a combination of **Phen** and **1,4-DCB** induced the stereospecific, decarboxylative 7-*endo* radical cyclisation product **96**, albeit with low yields (20%).

An unfortunate drawback for these dual catalytic systems covered in this section is the need for UV light irradiation, which ultimately diminishes the substrate scope. However, many organophotoredox catalysts that can be activated by visible light have been developed, and this will be the subject for the next section.

2.2.2 Carbazolyldicyanobenzene photocatalysts. The modification of cyanoarenes have been extensively studied to tune their photocatalytic properties.[71a,c] From these studies, carbazolyldicyanobenzene (CDCB) derivatives (such as 1,2,3,5-tetrakis-(carbazol-9-yl)-4,6-dicyanobenzene (**4CzIPN**, Fig. 1)) have emerged

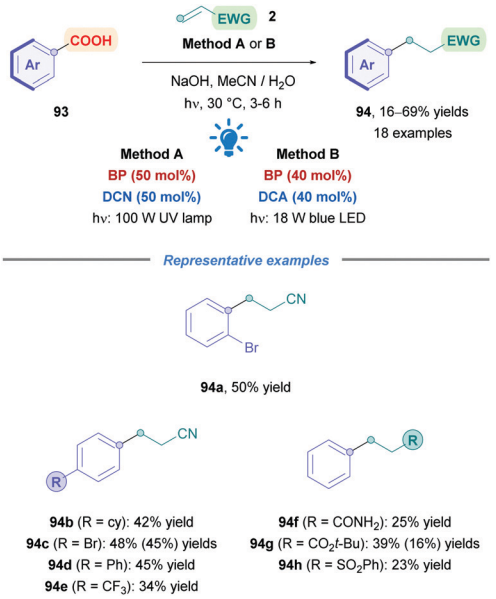

Scheme 32 Ar/DCA-catalysed direct DGR of aryl carboxylic acids. Yields in parentheses correspond to the reactions by Method B.

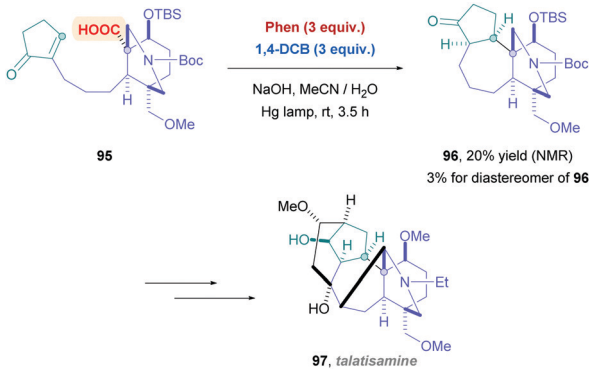

Scheme 33 Ar/DCA-catalysed direct DGR for the total synthesis of talatisamine.

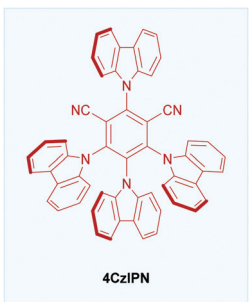

Fig. 1 Structure of 1,2,3,5-tetrakis(carbazol-9-yl)-4,6-dicyanobenzene (**4CzIPN**).

as attractive PCs. The phenyl core acts as an electron acceptor, whilst the carbazole units act as tunable electron donor moieties. Their electron-poor scaffolds give rise to high singlet energies and thus, greater oxidation potentials.[71c] In addition, large dihedral angles (about 60°) limits torsional flexibility, which in turn reduces nonradiative decay.[71b,c] These PCs can also be readily prepared through nucleophilic aromatic substitution methodologies.

Alongside the previously described work of Gómez-Suárez,[49] Schubert and Zhang also inserted radicals onto dehydroalanine derivative (Dha) derivative **52**, but using **4CzIPN** as the PC rather than the Ir-based [**Ir-4**][PF_6] used in Gómez-Suárez's work (Scheme 34A).[80] Although the investigation into the carboxylic acid scope was not as extensive, a good range of functional groups were well tolerated, including the presence of a pyridine such as in **53g**. Cyclic and acyclic primary, secondary and tertiary carboxylic acids (**53h–l**) all proceeded to give their corresponding Giese adducts with moderate to excellent yields (46–90%) with excellent diastereoselectivity (>20 : 1 d.r.). The acid substrates tested were those containing functional groups of pharmaceutical interest, including polyethylene glycol (PEG) derivatives, and fluorinated substrates. Long irradiation times were required (up to 60 h) to ensure complete consumption of Dha derivative **52**. The researchers also applied the reaction conditions to the functionalisation of peptides containing a

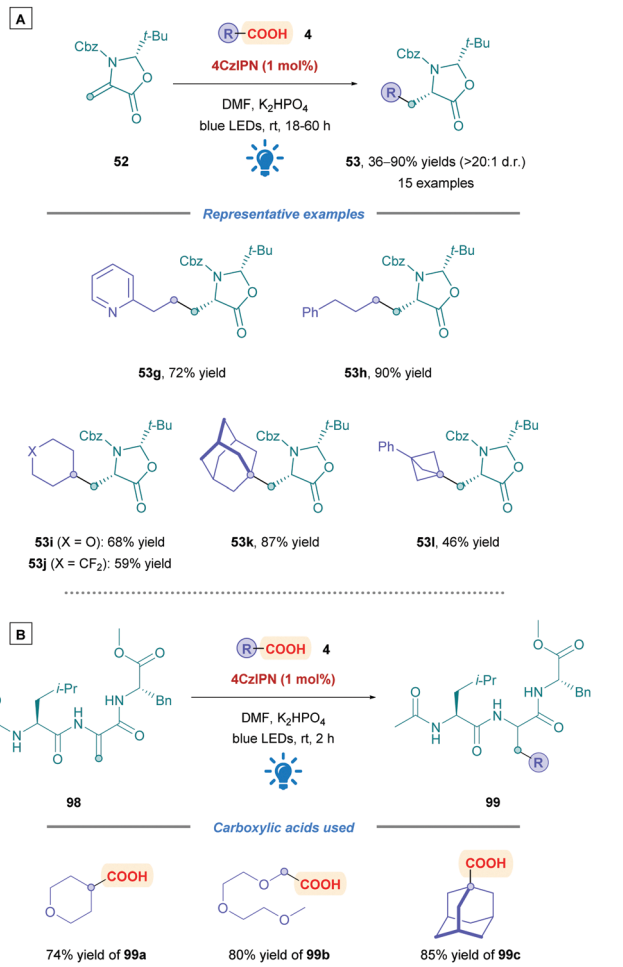

Scheme 34 4CzIPN-catalysed direct DGR onto Dha derivatives for (A) individual amino acids and (B) peptides.

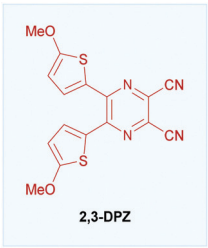

Fig. 2 Structre of 2,3-dicyanopyrazine (**2,3-DPZ**).

Dha residue (**98**) (Scheme 34B). An example each for primary, secondary, and tertiary carboxylic acids (**99a–c**) afforded the desired products with excellent yields (74–85%). The influence of the functionalisation process on the peptide physicochemical properties was illustrated by the incorporation of a PEG_2 unit (using **99b**) to enhance solubility, or the addition of the adamantyl group (using **99c**) to increase lipophilicity. Interestingly, 2 h of irradiation was sufficient to access the functionalise peptides **99**.

2.2.3 Dicyanopyrazine as photocatalysts. Related to the CDCB PCs are the dicyanopyrazines (DPZ) PCs. Particular attention has been paid to 2,3-DPZs (such as **2,3-DPZ**, Fig. 2), which are characterised by a donor–π–acceptor system allowing for modular structural modifications.[71c,81]

One of the major challenges regarding all types of Giese additions is achieving stereocontrol of the resulting Giese adduct outside of cases where substrate-controlled stereospecific radical addition is possible (such as cases presented in Scheme 30). To achieve this, Jiang and co-workers employed **2,3-DPZ** as the oxidative PC to initiate addition of radicals derived from *N*-aryl glycine derivatives **101** onto 2-vinylpyridine/quinoline derivatives **100** (Scheme 35).[82] In the presence of catalytic amounts of chiral 1,1′-spirobiindane-7,7′-diol (SPINOL)-based phosphoric acid **102**. Good to excellent yields (51–97%) of 3-(2-pyridine/quinoline)-3-substituted amines **103** were obtained with high enantioselectivities. A variety of EWGs and EDGs (**103a–f**) on the *N*-aryl and arylvinyl groups were generally well tolerated. A noticeable exception was observed for the *N*-aryl bearing the strongly electron donating methoxy group, where the reaction temperature was raised to 0 °C to compensate for the seemingly slower reaction rates. Functional group variation on the pyridine moiety was also well tolerated (**103g and h**), regardless of the substitution pattern. The low reaction temperatures indicate the highly facile nature of this protocol and are presumably also important for high enantioselectivities, though it does introduce some limitations with regards to practicality.

The proposed mechanism (Scheme 36) for this process is unique in that the photoinduced ***DPZ** ($E_{1/2}^{red}$ = +0.91 V *vs.* SCE)[83] is insufficient to oxidise carboxylates *via* a SET process. Instead, ***DPZ** oxidises the *N*-aryl amine to an aminium radical cation **XXVII**, which was further verified by Stern–Volmer analysis. A cascade reaction then proceeds involving a deprotonation, HAT, and decarboxylation to generate α-amino radical **XXVIII**. Conjugate addition of **XXIX** then proceeds onto olefin **104**,

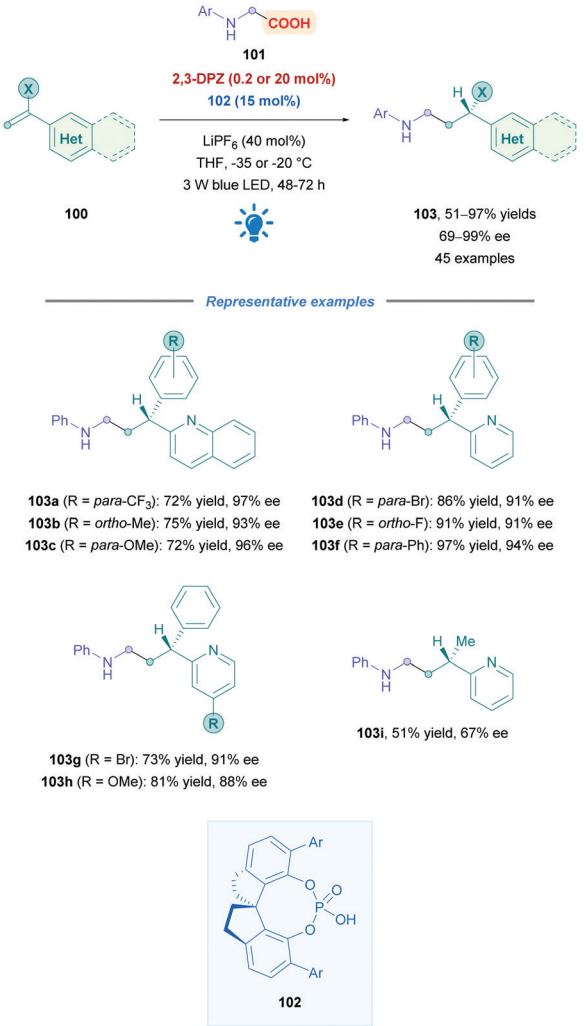

Scheme 35 Enantionselective DPZ-catalysed direct DGR of *N*-aryl-α-amino acids onto vinyl pyridine/quinoline derivatives.

which is activated by **102** *via* H-bonding, giving rise to intermediate radical **XXX**. The additive $LiPF_6$ increases the acidity of **102** and thus improves the overall yield and enantioselectivity. Upon reductive SET of the complex containing **XXX** and **102** to the corresponding pro-chiral anion, the all-important enantioselective protonation furnishes the desired chiral Giese adduct **105**. While the work constitutes excellent progress for enantioselective direct DGRs, it should be noted that because the decarboxylation is initiated *via* the oxidation of *N*-aryl amine and not the carboxyl anion, using **2,3-DPZ** as a photocatalyst severely limits the substrate scope. Indeed, the *N*-aryl group is essential and *N*-Boc protected amino acids do not undergo decarboxylation in the presence of **2,3-DPZ**.

2.2.4 Flavins as photocatalysts. Flavin catalysis is another branch of organophotoredox catalysis that has received much attention. A popular PC of this ilk includes riboflavin (vitamin B_2) and its derivatives, which are easily accessible from biological sources and tunable. Riboflavin and its derivatives possess several advantages compared to other organo-PCs: among others, they have a maximum absorption in the blue

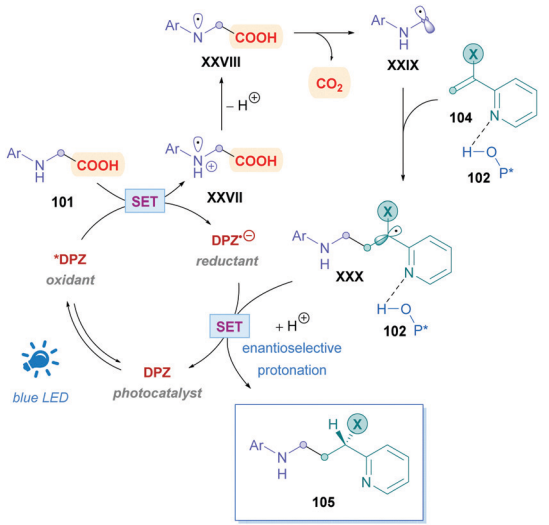

Scheme 36 Proposed mechanism for the enantionselective DPZ-catalysed direct DGR of *N*-aryl-α-amino acids onto vinyl pyridine/quinoline derivatives.

region of the visible light spectrum with high molar absorption coefficients.[84] Unique energy transfer and SET modes when activated upon irradiation also adds to the synthetic utility of these catalysts, enabling access to broad redox capabilities.[84]

Flavin catalysis has recently seen application in direct DGRs. The Macmillan group utilised flavin catalysis in their pioneering work on the site- and chemoselective bioconjugation of Michael acceptors onto C-termini of native peptides (Scheme 37).[85] The group exploited the discrepancy in oxidation potentials between internal and C-terminal carboxylates, allowing for exclusive C-terminal functionalisation. It was recognised that carboxylate-containing residues such as internal Glu and Asp would be resistant to oxidative decarboxylation due to the formation of an unstabilised carbon-centred radical ($E_{1/2}^{red}$ = +1.25 V *vs.* SCE),[86] yet formation of a stabilised α-amino radical would allow preferential C-terminal decarboxylation ($E_{1/2}^{red}$ = ∼+0.95 V *vs.* SCE).[87]

Using biological substrates required aqueous buffer, high dilution, and mild temperatures, thus a water-compatible PC was necessary to achieve the desired functionalisation. Attempts to use more commonly used PCs such as Ir- and Ru-based catalysts, and organic dyes proved to be unfruitful. The group thus turned their attention to flavin catalysis, as they are known to facilitate acetate decarboxylation *via* a two-electron pathway in aqueous media.[88] A survey of flavin catalysts and reaction conditions gave rise to the methodology presented in Scheme 37, which further unveiled that riboflavin tetrabutyrate (**FL-1**) and lumiflavin (**FL-2**) were the most effective PCs.

Functional group tolerance was assessed by employing peptides possessing amino acid residues commonly found on protein surfaces. Moderate to good yields (31–66%) were obtained for a variety of native peptides of increasing complexity (such as **107a**), demonstrating overall broad functional group tolerance (yields of >25% is sufficient to render the protocol a productive bioconjugation method). Importantly, exclusive *C*-terminal functionalisation was observed in all cases, including

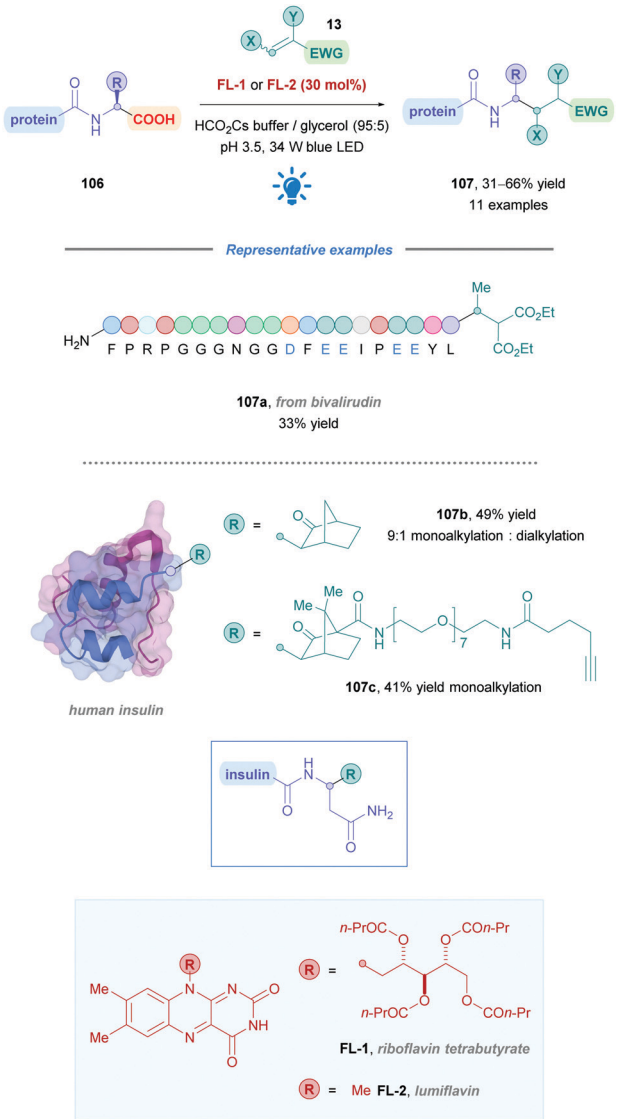

Scheme 37 Flavin-catalysed direct DGR of peptides (pdb: 3I40 for insulin structure shown).[89]

Glu- and Asp-bearing peptides where no side-chain decarboxylation was detected. The authors found that a low pH of 3.5 was critical to ensure protonation of Lys and His residues, as these were hypothesised to engage in deleterious oxidation reactions at higher pH.

Tyr residues were also subject to unwanted side-oxidation when PC **FL-1** was employed. This could be somewhat improved by using the less oxidising lumiflavin (**FL-2**) as an alternative catalyst (Scheme 37).

The functionalisation of human insulin through this protocol is a particularly neat illustration for the potential of this bioconjugation method. Insulin is composed of two parent peptide chains (each with a potentially reactive C-terminus) that are linked by two redox-sensitive disulfide bridges, as well as containing four Tyr residues. A 49% yield of a predominantly (9 : 1) A-chain mono-alkylated insulin was nevertheless obtained (**107b**), with no detectable impact on disulphide bridges or other

amino acid residues. An alkyne-substituted tag was also installed by this method (**107c**), allowing for further elaboration of the conjugated protein (Scheme 37).

Although no other examples of direct DGRs using flavin catalysis is known, this study underscores the potential for flavin catalysis and warrants further investigation.

2.2.5 Thioxanthones as photocatalysts. Thioxanthone (**TX**) is a unique aromatic ketone with interesting photochemical properties (Fig. 3). Unlike other aromatic ketone photocatalysts, **TX** has high singlet and triplet state energies, and relatively long triplet lifetimes [estimated τ_0 = 77 μs, one hundred times longer that benzophenone (τ_0 = 0.7 μs)],[90] and has the potential to participate in dual catalysis with metal complexes.[91] The conformation of **TX** is not static; it undergoes interconversion from a planar to a non-planar conformation (known as the "butterfly motion").[91,92] Each conformation possesses a discrete absorption band in the UV-Vis spectrum. These various physical chemical properties allow **TX** to mediate reaction *via* HAT, SET and triplet energy transfer (ENT). For more details, a full discussion on the photophysical properties of **TX** has been provided in a recent review by Kokotos and co-workers.[91]

Li and co-workers recently employed the TX derivative 2-chloro-thioxanthane-9-one (**Cl-TX**) as a photocatalyst for the direct DGR of aryl α-keto acids **16** onto mainly acrylate derivatives **13** (Scheme 38), achieving moderate to excellent yields (42–73%).[93] Acid substrates (**16**) bearing electron-donating (**17i–j**), and -withdrawing (**17k**) groups were well tolerated, and acrylates of different ester moieties and substitution patterns (*e.g.*, **17l–n**) reacted smoothly. α,β-Unsaturated ketones also proceeded well (**17o–q**). During optimisation studies, it was found that **TX** gave lower yields, possible due to its lower excited-state redox potential ($E^{red}_{1/2}$(TX*/TX$^{\bullet-}$) = +1.34 V *vs.* SCE in DMF)[94] than **Cl-TX** ($E^{red}_{1/2}$(Cl-TX*/Cl-TX$^{\bullet-}$) = +1.468 *vs.* SCE in DMF).[93] The mechanism of the reaction is predicted to proceed *via* the pathway analogous to that depicted in Scheme 5.

2.2.6 Pyrimidopteridine *N*-oxides as photocatalysts. Inspiration from flavin catalysis has led to the development of the structurally related pyrimidopteridine *N*-oxides (PPTNO).[95] Possessing high excited-state reduction potentials ($^*E^{red}_{1/2} \approx$ +2.32 V)[95b] and good stability, these PCs have been investigated by Pospech and co-workers for use in direct DGRs (Scheme 39).[96] They employed catalyst tetrapropyl-pyrimidopteridine *N*-oxide (**PrPPTNO**), developing conditions that require low PC loadings, substoichiometric amounts of base, short reaction times, and low light intensity. Despite the potential steric hindrance, the reaction conditions proved most effective with secondary

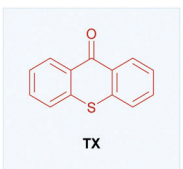

Fig. 3 Structure of thioxanthone (**TX**).

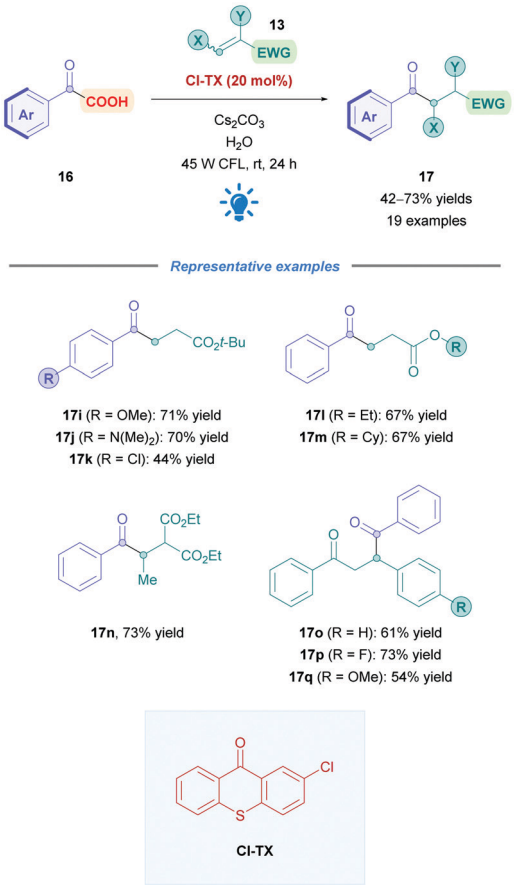

Scheme 38 Thioxanthone-catalysed direct DGR of α-keto acids.

and tertiary alkyl carboxylic acid substrates, achieving low to excellent yields (17–92%) with good functional group tolerance. Reactivity was, however, impeded for primary acids, with lower yields observed. This neatly follows the expected pattern of radical stability (1° < 2° < 3°). Substrates bearing unprotected hydroxy groups were successful (such as **14h**), yet some non-proteinogenic α-amino acids gave poorer yields. Benzylic acids failed to convert to the desired DGR product and gave the corresponding hydrodecarboxylation product instead. A variety of Michael acceptors were well tolerated, including vinyl sulfones, acrylonitriles, acrylaldehydes, and 5- to 6-membered α,β-unsaturated ketones (**14m–q**). The group also conducted a series of derivatisation reactions on the Giese adducts to showcase the applicability of their protocol, such as the conversion of Giese adduct **14d** to trisubstituted barbiturate **108** in moderate yields (33%).

The proposed reaction mechanism follows the same pathway as that of the general mechanism shown in Scheme 5. However, it should be highlighted that **PrPPTNO** serves as a pre-catalyst, whereby a deoxygenation step generates the active PC **PrPPT** (Scheme 40). Indeed, initial catalytic screening revealed that **PrPPT** was just as effective as its *N*-oxide analogue **PrPPTNO**.

2.2.7 Acridinium photocatalysts. Higher oxidative and reducing power can be attained by using ionic PCs rather than

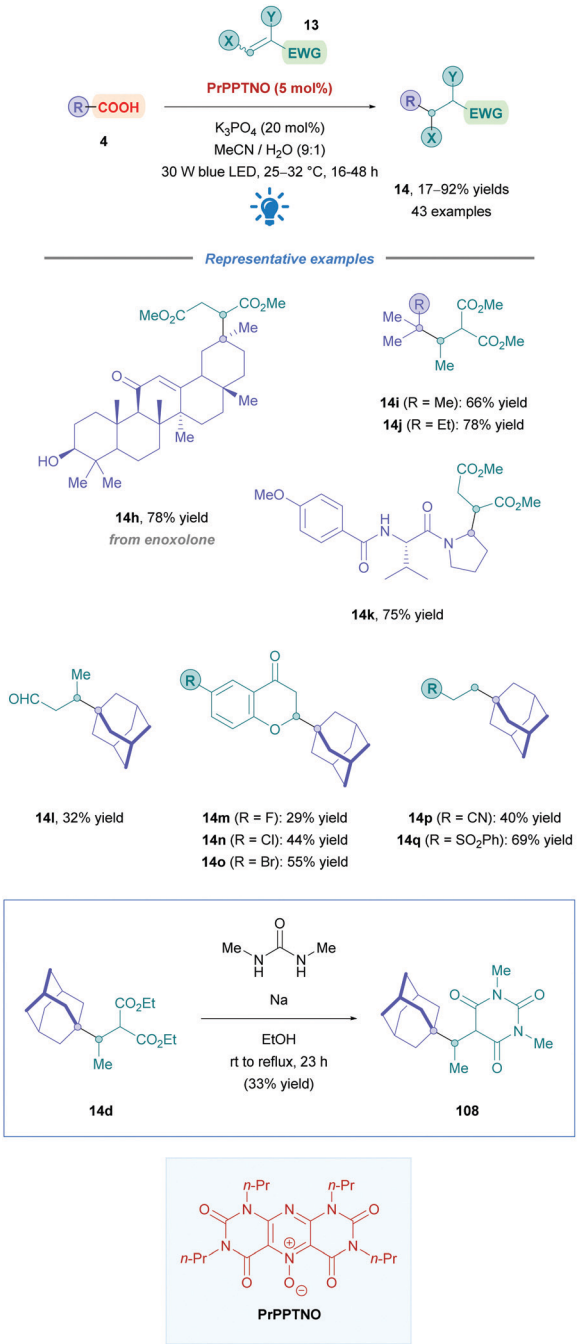

Scheme 39 PrPPTNO-catalysed direct DGR.

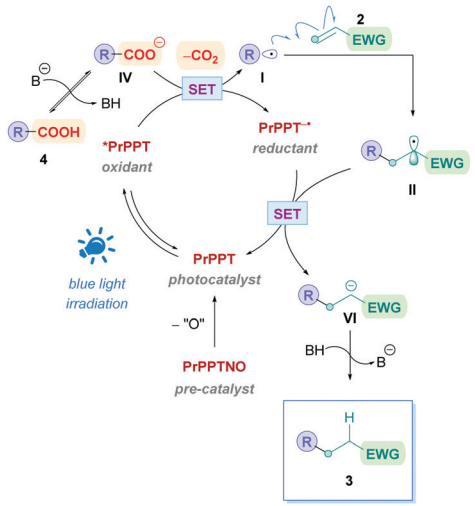

Scheme 40 Proposed mechanism of PrPPTNO-catalysed direct DGR.

neutral ones. Cationic PCs can exhibit more favourable electron-transfer kinetics between the electron donor and the PC excited state than commonly used metal-based PCs.[71c,97] The most widely studied PCs in this class are the acridinium catalysts, characterised by the photoexcited state's high oxidative power ($*E_{1/2}^{red}$ = up to 2.32 V *vs.* SCE)[98] and long lifetimes (τ = 30 ns),[99] good solubility in a range of organic solvents, and high selectivity in the presence of electron-rich species.

The first use of an acridinium PC for direct DGRs was reported by Koike, Akita and co-workers,[100] where they employed the acridinium catalyst 9-mesitylene-10-methylacridinium perchlorate ([Acr-Mes]ClO_4, Fukuzumi catalyst, **Acr-1**). However, only four carboxylic acid substrates (**4**) were examined using the same Michael acceptor, diminished yields were obtained for secondary acids, and an oxygen-free environment was necessary. Inspired by this work, Gonzalez-Gomez and Ramirez sought to improve the reaction conditions and further expand the scope (Scheme 41).[101] Minor modifications to the reaction conditions, including increased blue light irradiation and no protective atmosphere, gave improved yields within shorter reaction times. A change of solvent from MeOH to an MeCN/H_2O mixture, together with an increase in reaction concentration, enabled secondary acids to undergo DGRs with moderate to excellent yields (*e.g.*, **14v**, 78%). These improved conditions were then applied to tertiary acids (**14l** and **14q–s**), α-amino, α-oxy and aryl α-keto acids (**14t–u**) with good overall yields (54–78%). Interestingly, the group was able for the first time to report the DGR of aliphatic α-keto acids with moderate yields (**14u**, 54%).

Acids that were unsuccessful included α-hydroxy acids, electron-poor phenoxyacetic acids, simple primary aliphatic acids and phenyl acetic acids. With regards to the Michael acceptors, more sterically demanding Michael acceptor substrates proved futile, and acceptors substituted at the α-position by a single ester group also failed to react, possibly because the corresponding α-acyl radical was unable to re-oxidise the [Acr-Mes]• species to recycle the catalyst. In addition, β-phenyl-substituted acceptors were unsuccessful likely due to the competitive formation of the more stable benzylic radical, which is also unable to recycle the catalyst.

Wang and co-workers also employed Fukuzumi's catalyst to prepare enantioenriched α-deuterated α-amino acids.[102] Preparation of isotopically enriched biological compounds are highly valuable within the life sciences, as they provide a powerful tool for the elucidation of enzymatic mechanisms,[103] biosynthetic pathways,[95a,104] and structural information within peptides and proteins.[102,105] Incorporation of deuterium can also enhance metabolic stability for peptide-based therapeutics.

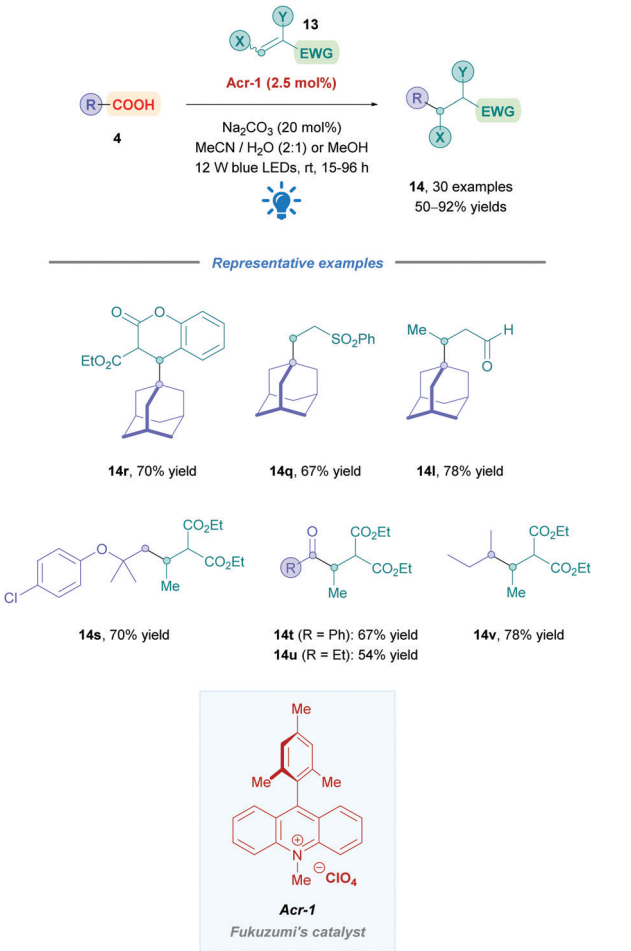

Scheme 41 Acr-catalysed direct DGR.

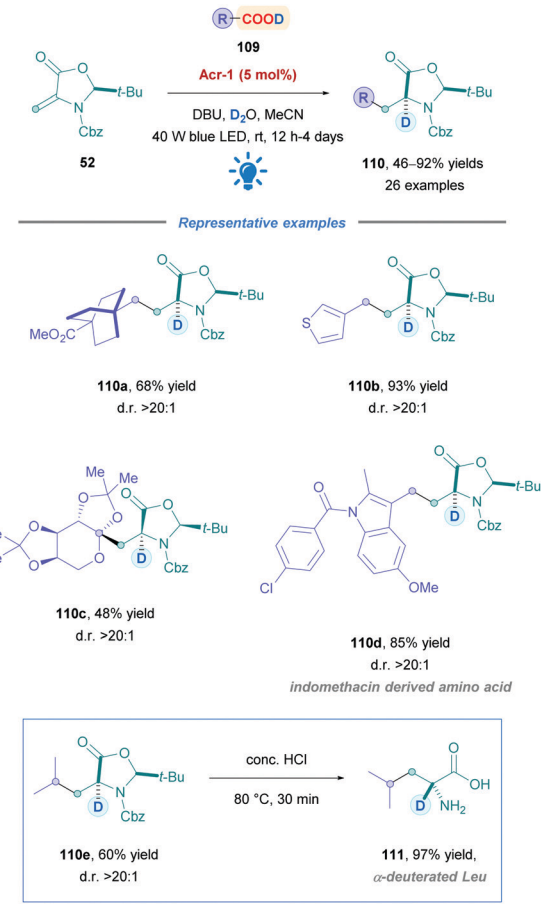

Scheme 42 Acr-Catalysed direct DGR onto Dha.

Similar to the works of Gómez-Suárez (Scheme 19),[49] Schubert (Scheme 34),[80] and their respective co-workers, the Wang group also employed Dha derivative **52** to synthesise a diverse range of deuterated non-canonical amino acids (**110**) (Scheme 42).[102] Using PC **Acr-1**, moderate to excellent yields (46–92%) were observed for primary, secondary, and tertiary acids with broad functional group tolerance. They also included sugar-derived carboxylic acids (**110c**), as well as late-stage functionalisations of carboxylic acid-containing pharmaceuticals (**110d**). Across the board, over 90% D-incorporation and diastereomeric ratios $>20:1$ were obtained. Some substrates required the use of the less oxidising carbazolyldicyanobenzene PC **4CzIPN** instead of **Acr-1**. It is interesting to note that during their optimisation using a glycosyl radical precursor, the group did not achieve product formation using **4CzIPN**. However, Schubert[80] reported the highest yields using **4CzIPN** during their optimisation using the same acceptor, but with a primary carboxylic acid radical precursor. These results illustrate the necessity to tailor the choice of the PC to the system considered, as well as the cross-applicability of PCs that enable the expansion of a given reaction's scope. Following Giese addition, the resulting adducts could be transformed to the corresponding α-deuterated α-amino acids by reacting with concentrated HCl, as showcased through the acid hydrolysis of **110e** to α-deuterated Leu **111**.

Another methodology to prepare unnatural amino acids was reported by Shah and co-workers at Merck, whereby they performed DGRs onto dehydroalanine derivative **112** to generate β-alkyl α-amino acids (Scheme 43).[106] A high-throughput experimentation screen of PCs unveiled that catalyst **Acr-2** was the most effective. The reaction conditions were chosen to be compatible with parallel library synthesis and purification, allowing for a rapid assessment of the substrate scope. Dehydroalanine derivatives **112** were bis-Boc protected, as mono-Boc substrates were found to be not sufficiently reactive. Two reaction set-ups focusing either on library synthesis throughput (Method A, parallel two steps synthesis) or on enhanced process scalability (Method B, single steps with intermediate purification) were developed using different photoreactors. Low to excellent yields of **113** (4–90%) were observed for a wide range of acids bearing functionalities such as nitriles, alkynes, aryl halides or heteroaromatics (**113a**). α-Difluoro acids gave diminished yields, possibly due to the less nucleophilic nature of the corresponding radicals, however, the difluoro moiety is tolerated in other positions (**113b**). A variety of saturated 6-membered cyclic systems were also compatible (**113c**), giving excellent yields of Giese adducts; however, some limitations were observed for 4- and

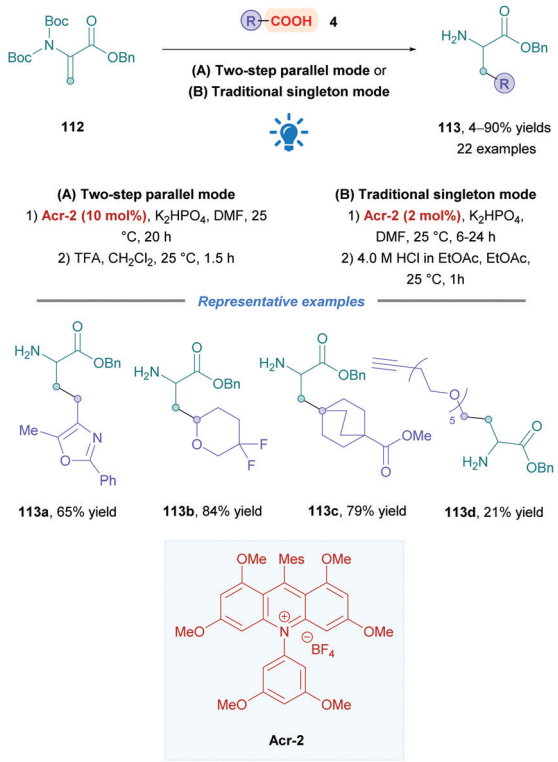

Scheme 43 Acr-Catalysed direct DGR onto dihydroalanines.

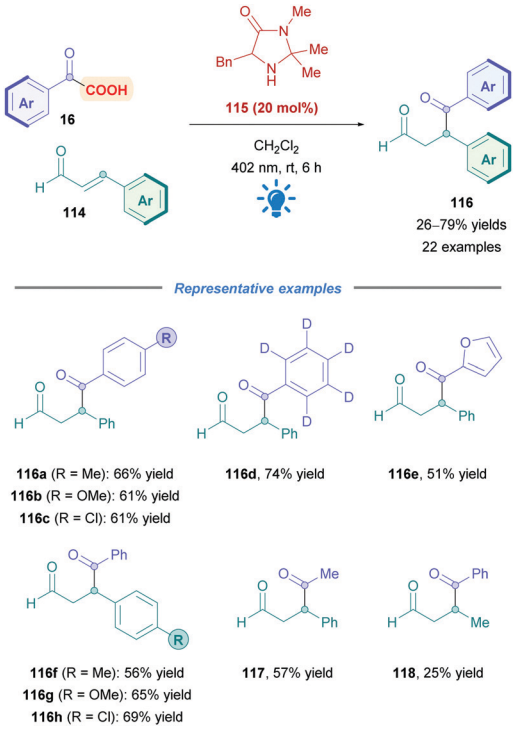

Scheme 44 Iminium-catalysed direct DGR of α-keto acids onto α,β-unsaturated aldehydes.

5-membered saturated systems. The group further demonstrated the applicability of their methodology by the synthesis of alkyne-functionalised protected amino acid **113d** of potential interest for the synthesis of linkable peptides.

2.2.8 Iminium and enamine photocatalysis. Iminium and enamine asymmetric organocatalysis continue to be thriving area of research. Recently, iminium and enamine catalysis has been combined with photocatalysis to achieve transformations that would not be otherwise easily accessible under purely thermal conditions.[107] Interestingly, excited iminium ions can act as excellent electron acceptors and, in close proximity to an electron donor, can form electron-donor–acceptor (EDA) complexes through ion-pair interactions. Gilmour and co-workers sought to use this property to react aryl α-keto acids (**16**) with α,β-unsaturated aldehydes (**114**) to access 4-keto-aldehydes (**116**) (Scheme 44).[108] Optimisation studies revealed that amine catalyst **115** was best suited to achieve low to excellent yields of **116** (26–79%). Aryl acid substrates bearing electron-donating (**116a–b**), and -withdrawing (**116c**) substituents proceeded well, and the positions of these groups had little impact on yields. Similar trends were observed when modifying the phenyl ring of the Michael acceptor (**116f–h**), though highly electron-withdrawing groups such as *para*-CF_3 and *ortho*-NO_2 gave depleted yields (45% and 26%, respectively). Other interesting substrates included acids containing a deuterated phenyl (**116d**) and furan substituents (**116e**), as well **117** and **118** bearing alkyl substituents.

The proposed mechanism is illustrated in Scheme 45. Initial reaction of the amine catalyst **115** with aldehyde **114** generates the iminium cation, which subsequently forms a close ion pair intermediate **XXXI** with the carboxylate of **16**. Photoexcitation of **XXXI** gives rise to the photoactive EDA-complex **XXXII**, which undergoes SET followed by intersystem crossing (**XXXIII**) which induces decarboxylation and radical–radical recombination (**XXXIV**) to give enamine **XXXV**. Using cinnamaldehyde derivatives as radical acceptors ensures the presence of an extended π-system, allowing favourable π,π-interactions in the EDA complex. Further evidence for the necessity of the extended π-system can be found when using crotonaldehyde as the radical acceptor, which only gave 25% of the desired product **118**. Final hydrolysis of **XXXV** completes the catalytic cycle and furnishes the desired Giese adduct **116**.

2.3 Synergistic dual photocatalysis

2.3.1 Acridinium/copper co-catalysis. Recent years have seen the emergence of methodologies that couple photoredox and TM catalysis in a synergistic fashion, otherwise known as metallaphotocatalysis. Within these dual-catalytic systems, a photocatalyst is typically used to activate the substrate, and a second non-photochemical catalytic species harnesses the reactivity of the photogenerated intermediates, thus expanding the number of chemical transformations possible. Some excellent reviews have covered this topic, which readers are encouraged to refer to if more information is desired.[109]

Due to the often highly oxidising conditions required to achieve decarboxylation, sensitive functional groups are susceptible under these reaction conditions and thus frequently require protection. This issue can be bypassed using milder

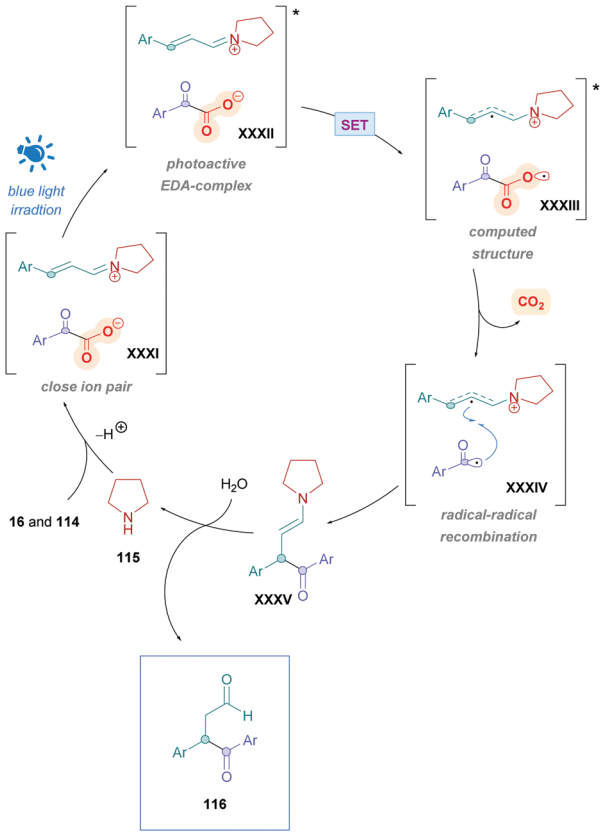

Scheme 45 Proposed mechanism for iminium-catalysed direct DGR of α-keto acids onto α,β-unsaturated aldehydes. The structure of amine catalyst **115** has been simplified for clarity.

reductive decarboxylation methodologies through the implementation of redox-active esters, avoiding the need for acid deprotonation or energetically demanding homolysis of O–H *via* a HAT process. As stated previously, however, these esters require preparation and isolation in most cases, leading to additional steps.

To address these issues, Larionov and co-workers recently devised a mild dual-catalytic system to facilitate the direct DGR of carboxylic acids without the need for pre-activation by deprotonation.[110] Employing their recently described new class of 9-arylacridine photocatalysts,[111] **Acr-3** or **Acr-4** were coupled with an efficient Cu(I)/Cu(0) catalytic cycle to access an impressive array of Giese adducts (Scheme 46A). Moderate to excellent yields were obtained for a variety of primary (**120b**, 81%), secondary (**121**, 76%) and tertiary (**120a, c–f**, and **122**, 52–83%) carboxylic acids with good functional group tolerance for halogens and (un)saturated heterocycles. Moreover, they showcased an extensive array of Michael acceptors that can undergo efficient Giese participation with moderate to excellent yields (51–91%). Less electron-poor olefins, such as acrolein derivatives (**120a–f**) and (a)cyclic α,β-unsaturated ketones (**120c and d**) were successfully converted, using piperazine as additive for the copper catalyst. However, *N*,*N*,*N*′,*N*′-tetramethyl-1,3-propylenediamine (TMPDA) was the optimal additive when investigating the scope of more electron-deficient substrates, which includes acrylonitrile, phenyl vinyl sulfones (**121**), vinyl phosphonates (**122**) and vinyl phosphine oxides. The group also showcased many examples of their protocol applied to naturally occurring and medicinally relevant compounds (**120a-b, e-f**) which possess multiple sites for potential oxidation, often significantly reducing the number of steps compared to previously reported syntheses.

Rigorous mechanistic studies unveiled the plausible presence of two competing pathways (Scheme 46B and C). Both pathways begin with hydrogen-bonded coordination of the acridine **Acr** and carboxylic acid **4** to form the activated complex **123**. Irradiation of visible light then induces decarboxylation from the singlet excited state of **123** *via* a proton-coupled electron-transfer (PCET) process to generate the alkyl radical **I** and acridinyl radical **Acr-H•**.[112] It should be noted that decarboxylation does not proceed *via* an acridinium carboxylate salt.[112] **Acr-H•** then participates in reductive SET with the Cu(I) catalyst **125** to produce Cu(0) species **126** and acridinium **Acr-H$^+$**. Meanwhile, radical **I** can follow one of two distinct routes. As depicted in Scheme 46B, **I** can participate in conjugate addition with Michael acceptor **124** to generate the radical intermediate **XXXVI**, which subsequently cross-terminates with **126** to afford Cu(I) enolate **127**. The product **128** is then furnished through protonation by acridinium **Acr-H$^+$**, which in turn regenerates the acridine catalyst **Acr** and Cu(I) catalyst **125** simultaneously, thus closing both catalytic cycles. Alternatively, radical **I** is first intercepted by Cu(0) species **126** to generate organocopper intermediate **129** (Scheme 46C). Installation of **I** onto Michael acceptor **124** can proceed to copper enolate **127′** either *via* direct Michael addition (**130a**) or *via* Cu(III) intermediate **130b**. The choice of amine additive was also paramount to the success of the reaction. Tertiary aliphatic amines were shown to perform better than secondary and primary diamines, and aromatic diamines. Evidence obtained during mechanistic studies suggests that the amine additive acts as a ligand, rather than a base, to stabilise the Cu(0) species and prevent aggregation.[113]

2.3.2 Ruthenium/amine co-catalysis. As already mentioned, performing photocatalysed direct DGRs typically suffers from the lack of precise enantiocontrol. One strategy to induce chirality is to merge photocatalysis with asymmetric organocatalysis, including enamine, iminium, Brønsted acid/base, and N-heterocyclic carbene catalyses,[114] as first demonstrated by the MacMillan group.[115] Yu and co-workers reported an elegant photoredox/amine-cocatalysed enantioselective direct DGR of α-keto acids (**116**) upon α,β-unsaturated aldehydes (**114**), accessing enantioenriched 1,4-dicarbonyl compounds (**116**) (Scheme 47).[116] Reaction optimisation revealed that using 3 equiv. of **16** with $Ru(bpz)_3(PF_6)_2$ (**[Ru-1][PF$_6$]$_2$**) and chiral amine **131** at −20 °C provided the highest yields (44–99%) and enantioselectivities (62–80% ee). Good yields were observed for aryl α-keto acids with electron-donating (**116a–b**) and -withdrawing (**116i**) groups, and the positions of the groups on the phenyl ring had little impact on yields. The same can be said with regards to the phenyl ring on the Michael acceptor (**116f–g, and j**). Primary (**132**), secondary (**133**), and tertiary (**134**) alkyl α-keto acids also proceeded smoothly, and acids bearing heteroaromatics (**116k**) were less fruitful.

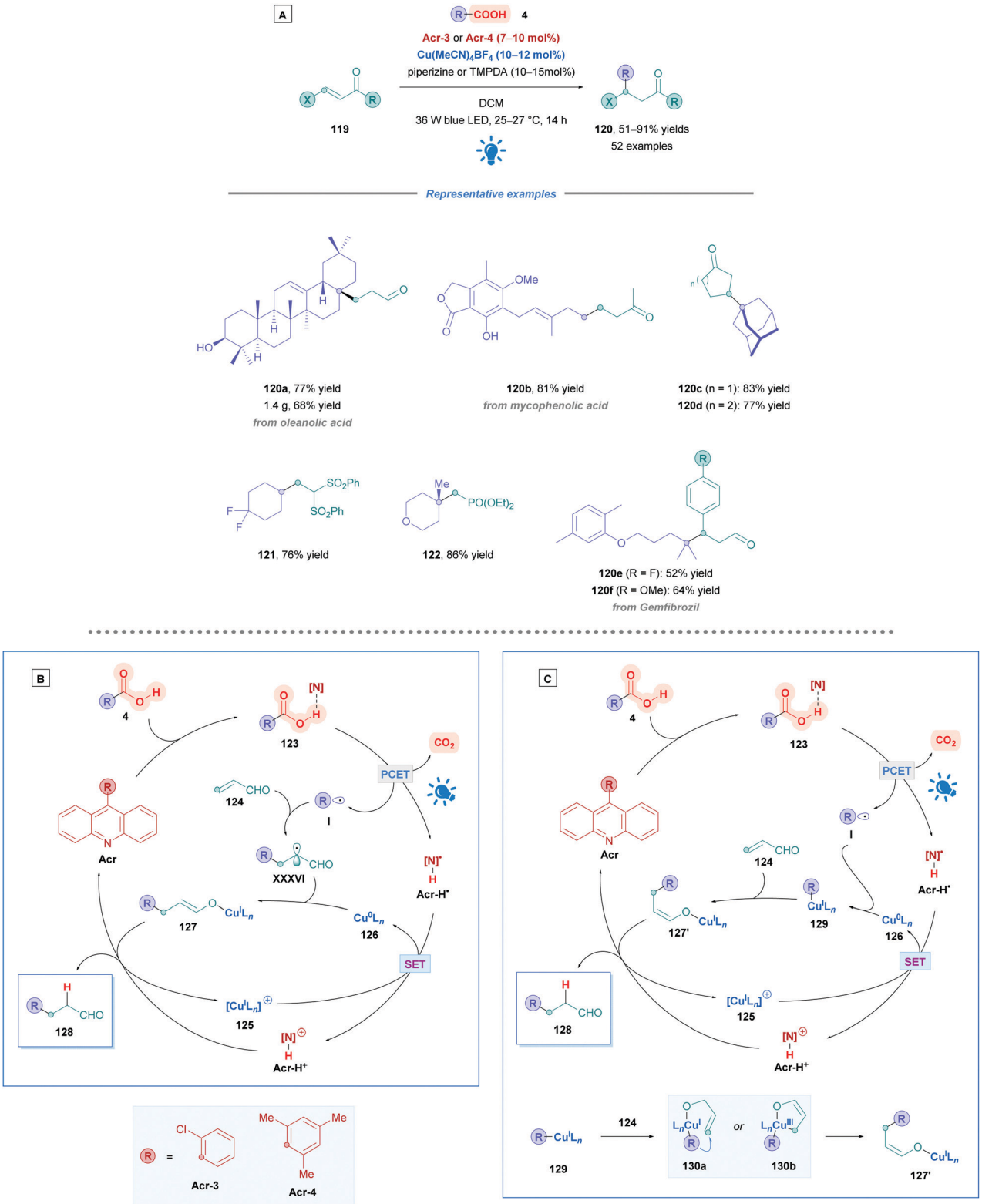

Scheme 46 Synergistic Acr/Cu-catalysed Direct DGR of carboxylic acids with proposed mechanisms. (A) Proposed mechanism *via* Giese addition of **I**. (B) Proposed mechanism *via* Cu(0) interception.

The proposed mechanism is illustrated in Scheme 48. Initial photoexcitation of **Ru(II)** to ***Ru(II)**, followed by its reductive quenching by acid **16** leads to the acyl radical **XXXVII** *via* decarboxylation. Meanwhile, chiral amine catalyst **131** reacts with aldehyde **114** to generate iminium ion **XXXVIII** *in situ*. Subsequent enantioselective conjugate addition of radical

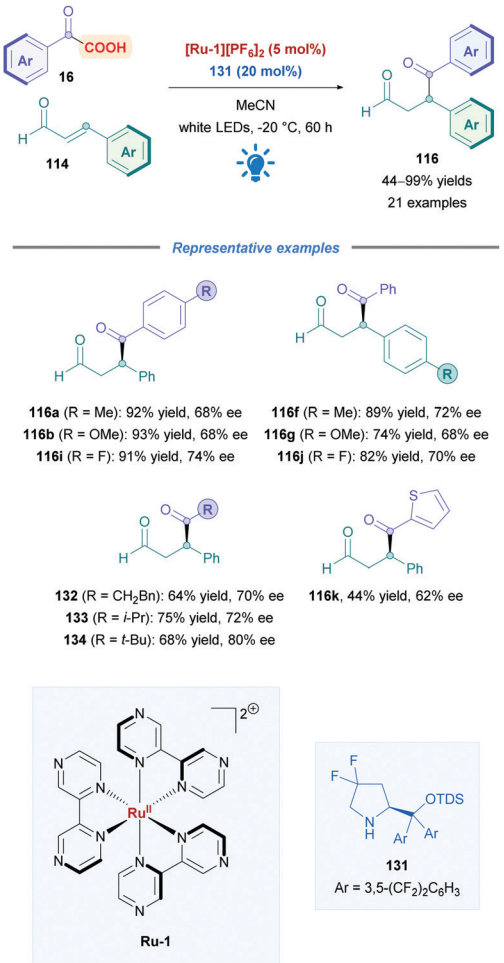

Scheme 47 Ruthenium/amine co-catalysed direct DGR of α-keto acids onto α,β-unsaturated aldehydes.

XXXVII onto **XXXVIII** gives radical **XXXIX**, which is then reduced by **Ru(I)** to close the catalytic cycle and to give enamine **XL**. Finally, hydrolysis of **XL** furnishes the final Giese adduct **116**.

2.4 Heterogeneous photocatalysis

Homogenous catalysis, as opposed to heterogeneous catalysis, is often characterised by its better tunability, higher activity and selectivity. Homogeneous catalysis has been dominating in the field of photoredox catalysis, and despite the advantages stated above, difficulties pertaining to catalyst separation, recycling, thermal stability, and cost have emerged as potential limitations for the wider application of some homogeneous PCs.[117] To overcome these limitations, there has been considerable research focussed towards the development of heterogenous catalysts, which can easily be separated and recycled.

An appealing approach to harness the advantages of homogeneous and heterogenous catalysis could consist of anchoring soluble catalysts onto insoluble supports. This approach, however, often suffers from reduction in catalytic activity and selectivity due to limited number of accessible reaction sites, leading to the heterogenised systems being unable to achieve the performance of their soluble counterparts.[117b] Alternative

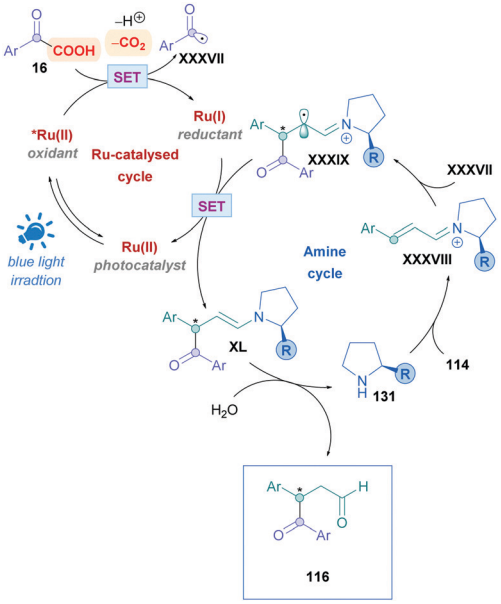

Scheme 48 Proposed mechanism of Ruthenium/amine co-catalysed direct DGR of α-keto acids onto α,β-unsaturated aldehydes. The structure of amine catalyst **131** has been simplified for clarity.

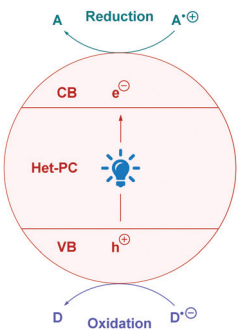

Scheme 49 General mechanism of action for semiconductor heterogenous photocatalysis.

heterogeneous systems capable of acting as PCs have instead been used, such as semiconductors, conjugates microporous polymers, covalent organic frameworks, and metal organic frameworks.[117b] A semiconductor heterogenous photocatalysts (Het-PCs) operate using the same electron and energy transfer pathways that govern homogenous photocatalytic reactions. When a Het-PC particle absorbs a photon of sufficient energy, an electron is excited from the valence band (VB) to the conducting band (CB), simultaneously establishing an oxidising and reducing species (the energy difference between the CB and VB is known as the band gap) (Scheme 49). The electrons in the CB can participate in reductive SET with electron-acceptor substrates, and the generated holes (h^+) in the VB can oxidise electron donors.

2.4.1 Titanium dioxide (TiO_2). The most frequently applied Het-PC is the naturally occurring mineral titanium dioxide, which has found use in facilitating direct DGRs. Due to the large band gap, UV(A) irradiation (>365 nm) is required to

establish the electron–hole pair and thus initiate decarboxylation. Within photocatalysis, TiO_2 (Degussa, P25) is the most widely used form of TiO_2, comprising of the polymorphs anatase and rutile in a ratio of 3 : 1.[118]

The first example of TiO_2 being used for direct DGRs was reported by Albini and co-workers in 1998.[119] They demonstrated one example by coupling 4-methoxyphenylacetic acid to maleic acid, achieving 65% yield of the Giese adduct after 60 h of UV irradiation. By 2012, Walton and co-workers had conducted a more extensive study concerning application of TiO_2 P25 for direct DGRs.[120] Under dry and anaerobic conditions in MeCN solvent, they showed that α-oxy acids could act as suitable radical precursors for addition onto maleic anhydride, maleimides, and acrylamide. Annulation was also observed when using α-phenoxy acids.

Later, the same group expanded upon their preliminary work to investigate: (1) the necessary structural features of the acids that undergo efficient Giese addition; (2) the Michael acceptor scope, paying attention towards functional group tolerance; (3) alternative catalyst forms and supports; and (4) the mechanism of the reaction (Scheme 50A).[121] Alkylations of *N*-phenylmaleimide using simple carboxylic acids that generated primary radicals gave low yields, and moderate improvements were made with acids that gave secondary and tertiary radicals. However, a significant amount of maleimide reduction to the succinimide was observed. By contrast, acids that generated primary and secondary radicals stabilised by an α-heteroatom (α-alkoxy or α-amino) gave improved yields (**14w-aa**, 29–75%), yet radicals stabilised by α-aryl moieties gave depleted yields accompanied by homocoupling (*e.g.*, **14ab**, 22%). In addition, succinimide formation was observed for all cases. The catalyst was removed by filtration, emphasising the procedural simplicity.

The group also tested the efficiencies of different forms of the TiO_2 catalyst using the reaction of phenoxyacetic acid with acrylamide. Standard TiO_2 P25 gave a yield of 47%, but employing TiO_2 PC500, which has a 6 times greater surface area compared to P25, led to a decrease in yield to 39%.[122] Even lower yields (9%) were observed when using TiO_2 Photospheres (consisting of hollow Pyrex beads with an external coating of rutile titania) due to difficulties in achieving uniform dispersion of the Photospheres throughout the reaction mixture. In contrast, the best yield (73%) was observed when the reaction was performed in Schlenk tubes coated with a fine internal layer of TiO_2 by a sol–gel process.[123] However, the authors noted that the coat could only be used three times due to the poor adherence of the catalyst on the tube surface – they therefore reasoned the conventional P25 catalyst to be the best compromise.

They next investigated the reaction of aryloxyacetic acids (*e.g.*, **135**) with *N*-substituted maleimides (*e.g.*, **136**) to give *N*-substituted-3,4-dihydrochromeno-[3,4]pyrrole-1,3-dione derivatives (*e.g.*, **137**) together with the expected Giese adduct (*e.g.*, **14ae**) (Scheme 50A). Generally, moderate to excellent yields were observed for substrates bearing electron-withdrawing or -donating substituents on the aryl ring. Selectivity for

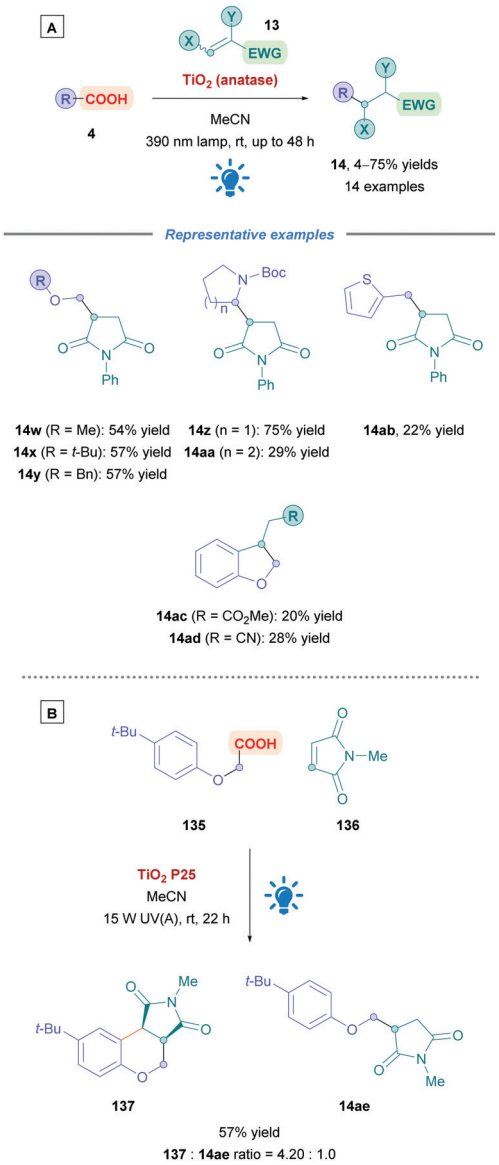

Scheme 50 TiO_2-Catalysed direct DGR of carboxylic acids onto maleimides and other Michael acceptors with (A) stabalised radical precursors and (B) *O*-aryl-α-oxy acids.

the chromenopyrrole product **137** can be increased by using combination of a denser dispersion of P25 and longer reaction times. Conversely, the standard Giese adduct **14ae** is favoured when using the sol–gel TiO_2-coated tubes, and in the presence of EWGs on the aryl moiety. The *cis* isomer of **137** was obtained in every case, as determined by ^{1}H NMR.[124]

Finally, the group demonstrated examples of intramolecular Giese reactions to give the adduct such as **14ac** and **14ad** (Scheme 50A), where low yields (20–28%) were obtained for substrates with tethered olefins bearing ester substituents. However, moderate yields (44–58%) were achieved when applying the sol–gel tube reactions.

With regards to mechanistic studies (Scheme 51A), it is proposed that initial decarboxylation of carboxylate **XLI** is induced by hole capture to give the desired radical **XLII**.

Conjugate addition of **XLII** onto the *N*-substituted maleimide **138** gives rise to the imidoalkyl radical **XLIII**. From here, SET with the CB of the TiO_2 particle is proposed to generate the corresponding enolate **XLIV** (Pathway A). Subsequent protonation[125] would afford the final Giese adduct **139**. When using aryloxyacetic acids, Pathway A becomes competitive with Pathway B, where a ring closure (6-*endo*-*trig*) of the electrophilic radical **XLIII** onto the aryl ring occurs. Increasing the electron density on the aryl ring increases its reactivity with the electrophilic radical **XLIII**, thus favouring annulation.[126] Aromatisation of the resulting cyclohexadienyl-type radical **XLV** by SET gives the final cyclised product **140**. The aromatisation process could take place through hole capture with TiO_2 to give oxonium **XLVI**, followed by proton loss. Alternatively, SET to maleimide might take place, as suggested by the work of Hoffman.[121,127] A series of protonation and electron-transfer steps of the resulting maleimide radical anions would then give the corresponding succinimides, thus explaining the significant yields of succinimides observed for these reactions. However, a high succinimide : **139** ratio was generally observed, indicating that the maleimide acceptor was also being directly reduced by TiO_2 under these conditions.

The decarboxylation process is believed to take place through specified interactions between the acid and TiO_2 surface (Scheme 51B). Initial dissociation of the acid onto the TiO_2 binds the carboxylate to the surface (**141**).[128] UV(A) irradiation then generates the electron–hole pair (**142**), which can migrate through the bulk of the semiconductor to the surface. A unique feature of the TiO_2 surface is that it is extensively hydroxylated,[129] and it is believed that the VB-holes are trapped by these moieties.[121,130] Thus, electron transfer between the 'trapped' holes and the carboxylate π-system gives the surface-bound carboxyl radical **143**. The authors then proposed a competition between decarboxylation *via* β-scission of the surface-bound radical to give the free radical species **143** and BET to **142**. The preferred step is dependent upon the stability of the free radical. For acids that generate more stabilised radicals, decarboxylation is favoured, and those less stabilised favour BET to the carboxylate. This can explain the higher yields observed for the more stabilised radicals, however other factors might be at play to decide reaction outcomes. For instance, the group were unsuccessful when trying to convert vinylacetic, ethynylacetic, and cyanoacetic acids, whilst these species should form stabilised radicals. Interestingly, when using vinylacetic acid, the corresponding allyl radical, was observed by EPR experiments.

As mentioned above, the Walton group encountered difficulties when attempting to generate the less stable aliphatic radicals, and low yields of the corresponding Giese adducts were obtained. Recently, however, Nocera and Zhu were successful in overcoming these limitations, reporting the photocatalytic hydroalkylation of electron-deficient olefins (Scheme 52).[131] Most noteworthy was their successful incorporation of primary alkyl radicals including $CH_3^{\bullet}$, achieving 22–87% for a whole range of Michael acceptors. The production of $CH_3^{\bullet}$ is known from the photooxidative degradation of acetic acid by TiO_2,[132] where it is a useful intermediate in aerobic oxidation and pollutant

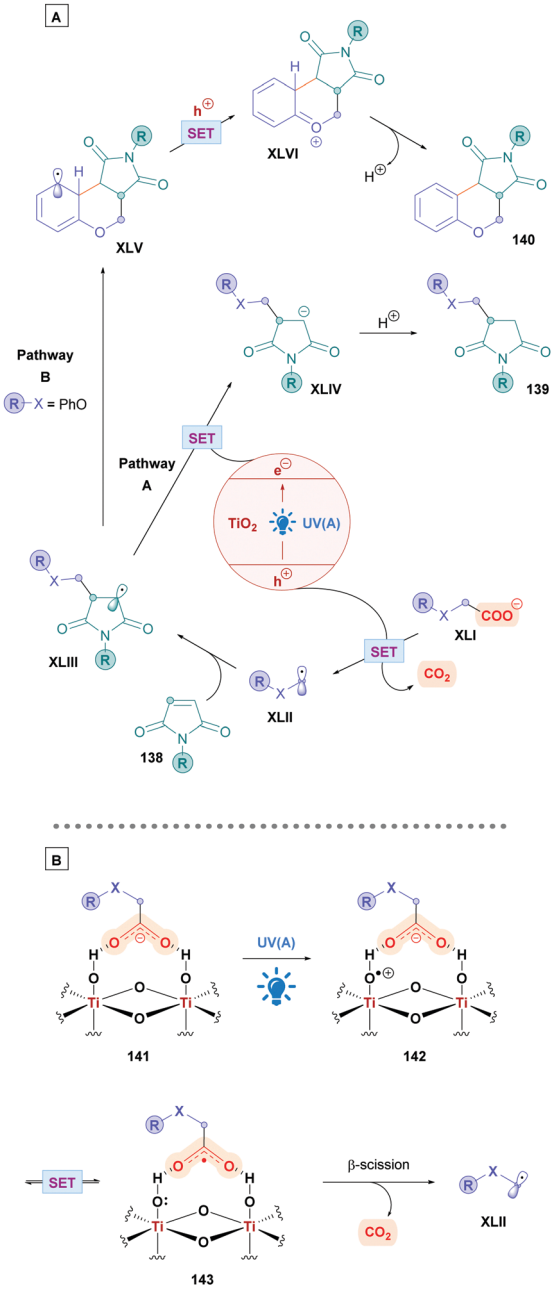

Scheme 51 (A) Proposed mechanism for TiO_2-catalysed direct DGR of carboxylic acids with maleimides. (B) Proposed mechanism for the SET oxidation between the carboxylic acid and the TiO_2 surface.

degradation conversion processes.[131,133] The authors used purely anatase titania nanoparticles instead of P25 (mixture of anatase and rutile forms). Decarboxylative Giese methylation showed broad scope for α-aryl acrylates (*e.g.*, **14ag**), with excellent functional group tolerance for electron-withdrawing and -donating groups on the aryl moiety. Aryl-substituted enones, acrylonitriles, and acrylamides also proceeded well. In addition, 2- and 4-vinylpyridines gave moderate yields (*e.g.*, **14af**). The aryl substituent was not necessary however, with Michael acceptors such as fumarate, phenyl sulfone and cyclohexanone affording their methylated products. Trisubstituted olefins were also

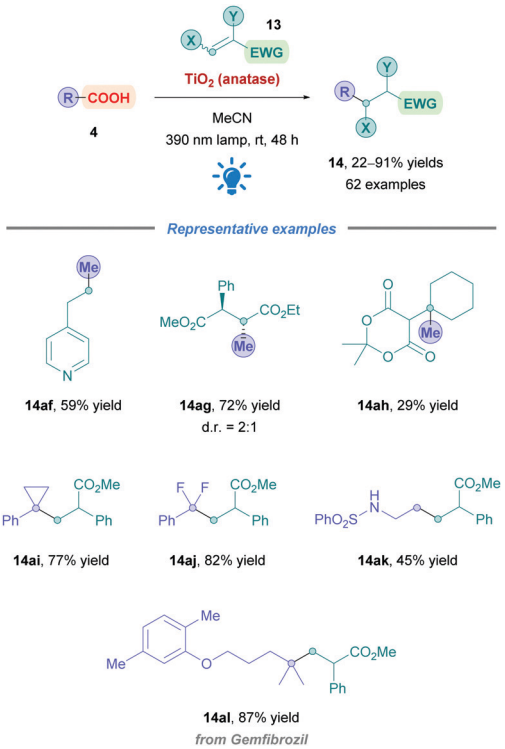

Scheme 52 TiO_2-Catalysed direct DGR of carboxylic acids for methylation and alkylation.

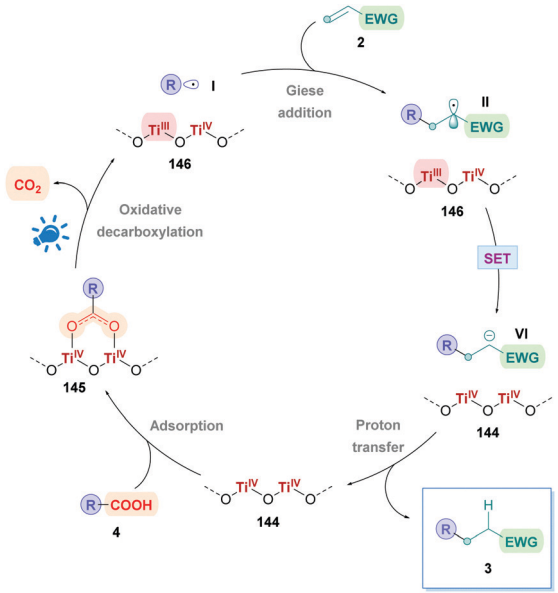

Scheme 53 Proposed mechanism for the inner-spehere, TiO_2 direct DGR of alkyl carboxylic acids.

successful (*e.g.*, **14ah**), although lower efficiency was observed for tetrasubstituted olefins.

A broad range of carboxylic acids were explored, including primary, secondary, tertiary, benzylic, and homobenzylic acids which all gave synthetically useful yields (41–91%). Furthermore, α-heteroatom carboxylic acids, *e.g.*, alkyl ether, aromatic, ether, ester, thioester, and amide, gave excellent yields overall without over-oxidation. Cyclic acids, including cyclopropane (**14ai**) and cyclobutene, were also well tolerated, in addition to primary acids bearing other functional groups in the α-position, *e.g.*, *gem*-difluoro (**14aj**), sulfonamide (**14ak**), ester, carboxylic acid, and ketone. Interestingly, no intramolecular cyclisation was observed for acids bearing alkenes and alkynes, showcasing the facile intermolecular addition of the primary radicals. α-Heterocyclic substrates and phenyl glyoxylic acid also gave their corresponding adducts. Finally, the group demonstrated the utility of their protocol through the alkylation of drug molecule Gemfibrozil (**14al**).

The mechanism (Scheme 53) is proposed to proceed through adsorption of the acid **4** onto the anatase titanium dioxide surface, with the two carboxyl oxygens coordinating to neighbouring titanium(IV) centres of **144**, generating complex **145**.[134] UV(A) irradiation leads to generation of an electron–hole pair within the anatase, allowing for oxidative cleavage of the C–C bond and inducing decarboxylation to give the alkyl radical **I**. The kinetics of the bond dissociation is facilitated through inner-sphere hole transfer from the VB to the carboxylate.[135] Evidence for the reduction of the TiO_2 catalyst (**146**) was attained using UV-vis diffusive absorbance spectroscopy of the TiO_2 catalyst, showing broad absorbance from 500 to 1100 nm (consistent with a blue coloration observed during the reaction) and reduced absorbance at the band edge (<400 nm).[136] Radical **I** then undergoes conjugate addition to the olefin **2**, generating the carbon-centred radical **II**. Reductive SET from the CB of **146** with **II** produces anion **VI**, followed by proton transfer from the acetic acid (confirmed by deuterium labelling experiments) to close the catalytic cycle and furnish the desired Giese adduct **3**. The formation of **VI** to **3** could alternatively proceed through a concerted proton-coupled electron transfer. The proximity of the photogenerated hole in VB and an electron in CB prevents dimerization of the **I** and redox side reactions.

Another key feature of this reaction is the inner-sphere direct electron transfer mediated oxidation of the carboxylic acid, without the need for an ancillary base, which is often required for a majority of homogenous photocatalytic systems involving outer-sphere oxidation of carboxylates. The absence of base also permits the application of this transformation to carboxylic acids bearing alkyl halide moieties, with excellent yields achieved and without loss of halide functionality.

The drawback of using TiO_2 catalysts is the requirement of higher energy UV light in order to achieve photocatalytic activity, which ultimately limits the substrate scope. Extension into the visible-light region can be achieved by doping TiO_2 with metal cations (Cd, Ce, Mn, Bi *etc.*) and non-metallic anions.[137] However, in addition to these additives often being expensive and toxic, the thermal stability of these catalysts is reduced and create undesired electron traps.[137b] Furthermore, while heterogenous systems benefit from higher stability and easier separation, homogenous systems are more attractive due to better fine-tuning capacities, enhanced activity and

selectivity, as well as convenient solution-phase reaction monitoring and mechanistic studies.[138] Recently, McIntosh and co-workers synthesised bimetallic Ti–O–Ti bridged amine bis(phenolate) complexes that displayed homogeneous photocatalytic activity for the generation of $^1O_2$ when irradiated with blue light (420 nm).[138] Further investigation into the tunability and utility of TiO_2-derived catalysts would be beneficial for direct DGRs, as well as other organic transformations.

Since the submission of this manuscript, Inoue and co-workers published a photocatalytic direct DGR involving Pt-doped TiO_2 to couple densely oxygenated structures to Michael acceptors.[139]

3. Silver catalysis (Kochi conditions)

In the 1970s, Kochi pioneered oxidative decarboxylation using readily available persulfate salts.[140] The presence of strong acids and catalytic Ag accelerates the rate-limiting decomposition of the persulfate ion to generate a highly oxidising persulfate radical ($E^{red}_{1/2}$ = +2.5 to +3.1 V *vs.* the normal hydrogen electrode (NHE)).[141] Minisci and co-workers famously utilised Kochi's conditions to enable decarboxylative radical addition onto heteroaromatics.[142]

It is only in recent years that researchers have begun to use Ag(I)-catalysed Kochi conditions to facilitate decarboxylative radical addition onto electron-deficient olefins to generate cyclic[143] and fluorinated[144] products. The only known example to date of Kochi-type conditions being applied to direct DGR transformations was demonstrated by the Baran group during their total synthesis of (−)-maximiscin (**150**, Scheme 54).[145] The group desired to perform a key C–C bond formation step through decarboxylation of lactone intermediate **147** to synthesise **149** using phenyl vinyl sulfone (**148**) as the chosen Michael acceptor. Initially, they attempted to use a reductive manifold, employing their Ni-catalysed decarboxylative Giese protocol[15e] which was shown to be unsuccessful due to competing HAT processes. Further extensive screening of a variety of redox strategies, including photocatalysis and C–H activation, surprisingly led them to Kochi-type conditions as a simple solution that could both form the desired C–C bond and aldehyde moiety of **149** in one-pot, with $Fe_2(SO_4)_2$ serving as a unique co-catalyst. Mechanistically, it is believed that initial saponification of lactone **147** gives rise to the carboxylate **XLVII**, rendering it compatible for Ag-catalysed decarboxylation followed by addition of resulting radical **XLVIII** onto **148**. Radical intermediate **XLIX** then undergoes a 1,5-HAT process to generate α-oxy radical **L**. The $Fe_2(SO_4)_2$ additive is believed to then facilitate Fe-catalysed oxidation of **L**, furnishing the desired product **149**.[146] Moreover, the reaction was surprisingly clean with no further purification required before the next step, and suffered little detriment in yields when applied on a gram scale (91%) with excellent diastereoselectivity (>20 : 1 d.r.).

It should be noted that while Baran's example shown in Scheme 54 is, to our knowledge, the only example of a true direct DGR using Kochi conditions, there are a few examples of

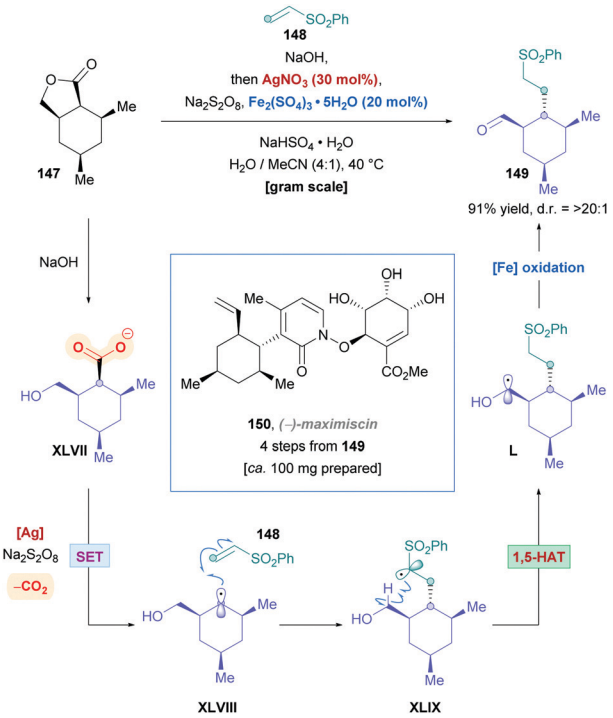

Scheme 54 Direct DGR using oxidative silver catalysis (Kochi conditions) for the total synthesis of (−)-maximiscin.

interrupted Giese reactions, in which the radical conjugate addition intermediate is trapped by an arene,[143a–g] alkyne,[143h] or nitrile[143i] to form a new cyclic system (*e.g.*, Scheme 55). These examples typically use either Ag-mediated Kochi conditions, or related metal-free conditions. In addition, Ag-catalysed decarboxylative allylations have also been reported.[147]

4. Organo-electrochemistry

Recently, organo-electrochemistry has been re-established as an intense area of research.[148] Electrochemistry provides organic chemists access to highly selective reactions under relatively mild and tunable conditions.[148a] In addition, the use of an electric current negates the need for stoichiometric oxidants and reductants.[148a] As far as we are aware, however, electrochemical oxidative decarboxylation[149] has yet to be used for direct DGRs, though generating carbon-centred radicals using decarboxylative Kolbe[10] electrolysis for trifluoro-

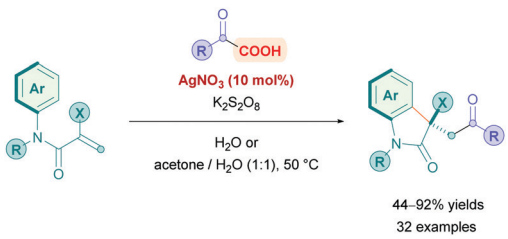

Scheme 55 Kochi conditions used for an interrupted Giese where the conjugate addition intermediate is trapped by an arene for cyclisation.

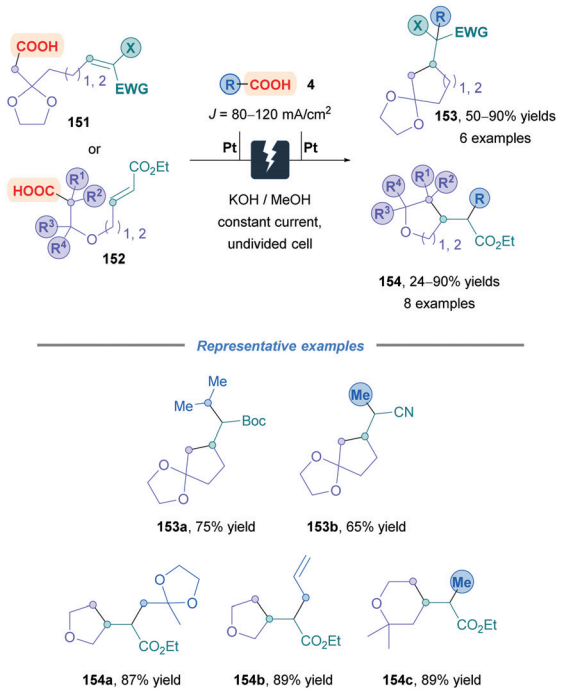

Scheme 56 Marko's organo-electrochemistry method for Kolbe decarboxylation followed by radical cyclisation.

methylations[150] and tandem annulations[151] are known. Wang and co-workers have recently reported using electrochemistry for the indirect DGR of NHPI esters, which proceeds through a reductive decarboxylation mechanism.[152]

The closest reaction to a direct DGR was reported by Markó in 2008 (Scheme 56),[151b] building on work by Schäfer and co-workers.[151a] A Kolbe decarboxylation of **141** or **142** followed by a Giese-type radical conjugate addition forms a radical intermediate. However, instead of HAT to form the Giese adduct, here the radical intermediate is trapped by an alkyl radical formed from another acid RCO_2H (**4**). A variety of 5- and 6-membered rings (**143** or **144**) were formed in this way (Scheme 56).

5. Conclusions

In this review, we have summarised the latest developments on Giese reactions that proceed *via* direct decarboxylation of carboxylic acids. Different methodologies to facilitate decarboxylation including photocatalysis involving transition metal- and organo-based systems, heterogenous photocatalysis, dual catalysis as well as silver catalysis were discussed. The mild conditions associated with these methodologies grant organic chemists access to a diverse range of novel C–C coupled products which are often not otherwise attainable by conventional nucleophilic protocols. While most of the progress made in the past decade has been related to photocatalysis, Baran's synthesis of (−)-maximiscin[145] demonstrates that non-photocatalytic methods can offer additional and complementary protocols. As to future development of the field, we envisage that research towards developing direct DGRs using organo-electrochemistry would further advance the field.

Additional improvements could also be made to direct DGRs, such as further development of enantioselective DGRs, improved chemoselective protocols for enhanced functional group tolerance (*i.e.* for oxidation-prone and base-labile substrates), and the use of more sustainable reaction conditions. Indeed, base-free Giese methods using cheap and available titanium oxide photocatalysts currently have the drawback of requiring UV irradiation rather than visible light irradiation, and enantioselective protocols are currently still rather limited in substrate scope.

The direct DGR has so far been exploited in a plethora of applications, emphasising their utility in organic synthesis. Applications include chemoselective bioconjugation of peptides,[85] synthesis of unnatural amino acids,[49,80,102,106] polymerisation,[72g] macrocyclisations[38,72a,72b,72j] and natural product/drug molecule synthesis,[26,43,50,79,145] though there is no doubt that further applications will be forthcoming as the field progresses.

Conflicts of interest

There are no conflicts to declare.

Acknowledgements

We would like to thank the Engineering and Physical Sciences Research Council and GSK for financial support [industrial CASE PhD studentship to DMK; grant code: EP/V519522/1].

Notes and references

1 For recent reviews on radical chemistry, see: (*a*) M. Yan, J. C. Lo, J. T. Edwards and P. S. Baran, *J. Am. Chem. Soc.*, 2016, **138**, 12692–12714; (*b*) J. M. Smith, S. J. Harwood and P. S. Baran, *Acc. Chem. Res.*, 2018, **51**, 1807–1817; (*c*) S. Ni, N. M. Padial, C. Kingston, J. C. Vantourout, D. C. Schmitt, J. T. Edwards, M. M. Kruszyk, R. R. Merchant, P. K. Mykhailiuk, B. B. Sanchez, S. Yang, M. A. Perry, G. M. Gallego, J. J. Mousseau, M. R. Collins, R. J. Cherney, P. S. Lebed, J. S. Chen, T. Qin and P. S. Baran, *J. Am. Chem. Soc.*, 2019, **141**, 6726–6739.

2 For selected reviews on two-electron conjugate additions, see: (*a*) B. E. Rossiter and N. M. Swingle, *Chem. Rev.*, 1992, **92**, 771–806; (*b*) J. Leonard, E. Díez-Barra and S. Merino, *Eur. J. Org. Chem.*, 1998, 2051–2061; (*c*) M. P. Sibi and S. Manyem, *Tetrahedron*, 2000, **56**, 8033–8061; (*d*) J. L. Vicario, D. Badía and L. Carrillo, *Synthesis*, 2007, 2065–2092; (*e*) A. Alexakis, J. E. Bäckvall, N. Krause, O. PàMies and M. DiéGuez, *Chem. Rev.*, 2008, **108**, 2796–2823; (*f*) S. R. Harutyunyan, T. Den Hartog, K. Geurts, A. J. Minnaard and B. L. Feringa, *Chem. Rev.*, 2008, **108**, 2824–2852; (*g*) A. G. Csákÿ, G. D. L. Herrán and M. C. Murcia, *Chem. Soc. Rev.*, 2010, **39**, 4080–4102;

(*h*) K. Zheng, X. Liu and X. Feng, *Chem. Rev.*, 2018, **118**, 7586–7656; (*i*) D. Pichon, J. Morvan, C. Crévisy and M. Mauduit, *Beilstein J. Org. Chem.*, 2020, **16**, 212–232.

3 (*a*) B. Giese and S. Lachhein, *Angew. Chem., Int. Ed. Engl.*, 1981, **20**, 967; (*b*) B. Giese, *Angew. Chem., Int. Ed. Engl.*, 1983, **22**, 753–764; (*c*) B. Giese and J. Dupuis, *Angew. Chem., Int. Ed. Engl.*, 1983, **22**, 622–623; (*d*) B. Giese, J. A. González-Gómez and T. Witzel, *Angew. Chem., Int. Ed. Engl.*, 1984, **23**, 69–70.

4 For selected examples showcasing decarboxylative Giese-type reactions to form carbon-heteroatom bonds, see: (*a*) S. B. Lang, K. C. Cartwright, R. S. Welter, T. M. Locascio and J. A. Tunge, *Eur. J. Org. Chem.*, 2016, 3331–3334; (*b*) J. Davies, N. S. Sheikh and D. Leonori, *Angew. Chem., Int. Ed.*, 2017, **56**, 13361–13365; (*c*) H. Jiang and A. Studer, *Angew. Chem., Int. Ed.*, 2017, **56**, 12273–12276; (*d*) V. R. Yatham, P. Bellotti and B. König, *Chem. Commun.*, 2019, **55**, 3489–3492; (*e*) N. X. Xu, B. X. Li, C. Wang and M. Uchiyama, *Angew. Chem., Int. Ed.*, 2020, **59**, 10639–10644.

5 B. Giese, *Angew. Chem., Int. Ed. Engl.*, 1983, **95**, 771–782.

6 (*a*) K. U. Ingold and J. K. Kochi, *Free Radicals*, Wiley, New York, 1973; (*b*) H. Knoll, *Z. Chem.*, 1982, **22**, 245–252.

7 A. L. Gant Kanegusuku and J. L. Roizen, *Angew. Chem., Int. Ed.*, 2021, **60**, 21116–21149.

8 For selected examples on interrupted direct DGRs, see: (*a*) X.-F. Xia, S.-L. Zhu, C. Chen, H. Wang and Y.-M. Liang, *J. Org. Chem.*, 2016, **81**, 1277–1284; (*b*) Q.-F. Bai, C. Jin, J.-Y. He and G. Feng, *Org. Lett.*, 2018, **20**, 2172–2175; (*c*) Y. Shi, H. Xiao, X.-H. Xu and Y. Huang, *Org. Biomol. Chem.*, 2018, **16**, 8472–8476; (*d*) C. Shu, R. S. Mega, B. J. Andreassen, A. Noble and V. K. Aggarwal, *Angew. Chem., Int. Ed.*, 2018, **57**, 15430–15434; (*e*) Y. Yu, W. Yuan, H. Huang, Z. Cai, P. Liu and P. Sun, *J. Org. Chem.*, 2018, **83**, 1654–1660; (*f*) G. Chen, C. Li, J. Peng, Z. Yuan, P. Liu and X. Liu, *Org. Biomol. Chem.*, 2019, **17**, 8527–8532; (*g*) H. Yang, G. Wei and Z. Jiang, *ACS Catal.*, 2019, **9**, 9599–9605; (*h*) R. S. Mega, V. K. Duong, A. Noble and V. K. Aggarwal, *Angew. Chem.*, 2020, **132**, 4405–4409; (*i*) Y. Su, R. Zhang, W. Xue, X. Liu, Y. Zhao, K.-H. Wang, D. Huang, C. Huo and Y. Hu, *Org. Biomol. Chem.*, 2020, **18**, 1940–1948; (*j*) H. Zhao, N. Ni, X. Li, D. Cheng and X. Xu, *Polyhedron*, 2021, **206**, 115337; (*k*) Y. Y. Cheng, J. X. Yu, T. Lei, H. Y. Hou, B. Chen, C. H. Tung and L. Z. Wu, *Angew. Chem., Int. Ed.*, 2021, **60**, 26822–26828; (*l*) L.-L. Liao, G.-M. Cao, Y.-X. Jiang, X.-H. Jin, X.-L. Hu, J. J. Chruma, G.-Q. Sun, Y.-Y. Gui and D.-G. Yu, *J. Am. Chem. Soc.*, 2021, **143**, 2812–2821.

9 (*a*) J. Schwarz and B. König, *Green Chem.*, 2016, **18**, 4743–4749; (*b*) J. Schwarz and B. König, *Green Chem.*, 2018, **20**, 323–361.

10 (*a*) H. Kolbe, *Liebigs Ann. Chem.*, 1848, **64**, 339–341; (*b*) H. Kolbe, *Liebigs Ann. Chem.*, 1849, **69**, 257–294.

11 H. Hunsdiecker and C. Hunsdiecker, *Chem. Ber.*, 1942, **75**, 291–297.

12 (*a*) D. H. R. Barton, D. Crich and W. B. Motherwell, *J. Chem. Soc., Chem. Commun.*, 1983, 939–941; (*b*) D. H. R. Barton, Y. Hervé, P. Potier and J. Thierry, *J. Chem. Soc., Chem. Commun.*, 1984, 1298–1299; (*c*) D. H. R. Barton, D. Bridon, I. Fernandaz-Picot and S. Z. Zard, *Tetrahedron*, 1987, **43**, 2733–2740.

13 (*a*) D. H. R. Barton, D. Crich and G. Kretzschmar, *Tetrahedron Lett.*, 1984, **25**, 1055–1058; (*b*) D. H. R. Barton, C. Ching-Yuh and J. C. Jaszberenyi, *Tetrahedron Lett.*, 1992, **33**, 5013–5016.

14 (*a*) K. Okada, K. Okamoto, N. Morita, K. Okubo and M. Oda, *J. Am. Chem. Soc.*, 1991, **113**, 9401–9402; (*b*) S. Murarka, *Adv. Synth. Catal.*, 2018, **360**, 1735–1753; (*c*) S. K. Parida, T. Mandal, S. Das, S. K. Hota, S. De Sarkar and S. Murarka, *ACS Catal.*, 2021, **11**, 1640–1683.

15 For selected examples involving NHPI esters, see: (*a*) M. J. Schnermann and L. E. Overman, *Angew. Chem., Int. Ed.*, 2012, **51**, 9576–9580; (*b*) G. L. Lackner, K. W. Quasdorf and L. E. Overman, *J. Am. Chem. Soc.*, 2013, **135**, 15342–15345; (*c*) C. R. Jamison and L. E. Overman, *Acc. Chem. Res.*, 2016, **49**, 1578–1586; (*d*) Y. Slutskyy and L. E. Overman, *Org. Lett.*, 2016, **18**, 2564–2567; (*e*) T. Qin, L. R. Malins, J. T. Edwards, R. R. Merchant, A. J. E. Novak, J. Z. Zhong, R. B. Mills, M. Yan, C. Yuan, M. D. Eastgate and P. S. Baran, *Angew. Chem., Int. Ed.*, 2017, **56**, 260–265; (*f*) L. Z. Gao, G. Q. Wang, J. Cao, D. D. Yuan, C. Xu, X. W. Guo and S. H. Li, *Chem. Commun.*, 2018, **54**, 11534–11537; (*g*) C. Zheng, G. Z. Wang and R. Shang, *Adv. Synth. Catal.*, 2019, **361**, 4500–4505.

16 Y.-R. Luo, *Comprehensive Handbook of Chemical Bond Energies*, 1st edn, CRC Press, Boca Raton, FL, 2007.

17 J. D. Griffin, M. A. Zeller and D. A. Nicewicz, *J. Am. Chem. Soc.*, 2015, **137**, 11340–11348.

18 (*a*) W. Zhang, *Tetrahedron*, 2001, **57**, 7237–7262; (*b*) G. S. C. Srikanth and S. L. Castle, *Tetrahedron*, 2005, **61**, 10377–10441.

19 (*a*) P. Perlmutter, *Conjugate Addition Reactions in Organic Synthesis*, 1st edn, Pergamon, Oxford, 1992; (*b*) P. Renaud and M. Gerster, *Angew. Chem., Int. Ed.*, 1998, **37**, 2562–2579; (*c*) M. P. Sibi and N. A. Porter, *Acc. Chem. Res.*, 1999, **32**, 163–171; (*d*) M. P. Sibi, S. Manyem and J. Zimmerman, *Chem. Rev.*, 2003, **103**, 3263–3296.

20 For selected reviews on photoredox catalysis, see: (*a*) J. W. Tucker and C. R. J. Stephenson, *J. Org. Chem.*, 2012, **77**, 1617–1622; (*b*) J.-P. Goddard, C. Ollivier and L. Fensterbank, *Acc. Chem. Res.*, 2016, **49**, 1924–1936; (*c*) D. Ravelli, S. Protti and M. Fagnoni, *Chem. Rev.*, 2016, **116**, 9850–9913; (*d*) M. H. Shaw, J. Twilton and D. W. C. Macmillan, *J. Org. Chem.*, 2016, **81**, 6898–6926; (*e*) J. K. Matsui, S. B. Lang, D. R. Heitz and G. A. Molander, *ACS Catal.*, 2017, **7**, 2563–2575; (*f*) S. Roslin and L. R. Odell, *Eur. J. Org. Chem.*, 2017, 1993–2007; (*g*) H. Yi, G. Zhang, H. Wang, Z. Huang, J. Wang, A. K. Singh and A. Lei, *Chem. Rev.*, 2017, **117**, 9016–9085; (*h*) L. Marzo, S. K. Pagire, O. Reiser and B. König, *Angew. Chem., Int. Ed.*, 2018, **57**, 10034–10072; (*i*) C.-S. Wang, P. H. Dixneuf and J.-F. Soulé, *Chem. Rev.*, 2018, **118**, 7532–7585.

21 L. Capaldo, L. Buzzetti, D. Merli, M. Fagnoni and D. Ravelli, *J. Org. Chem.*, 2016, **81**, 7102–7109.

22 (*a*) C. K. Prier, D. A. Rankic and D. W. C. MacMillan, *Chem. Rev.*, 2013, **113**, 5322–5363; (*b*) T. Koike and M. Akita, *Inorg. Chem. Front.*, 2014, **1**, 562–576; (*c*) K. Teegardin, J. I. Day, J. Chan and J. Weaver, *Org. Process Res. Dev.*, 2016, **20**, 1156–1163.
23 Y. Miyake, K. Nakajima and Y. Nishibayashi, *Chem. Commun.*, 2013, **49**, 7854–7856.
24 G. D'Aprano, E. Proynov, M. Lebœuf, M. Leclerc and D. R. Salahub, *J. Am. Chem. Soc.*, 1996, **118**, 9736–9742.
25 (*a*) D. A. Smith and S. Vijayakumar, *Tetrahedron Lett.*, 1991, **32**, 3617–3620; (*b*) X. Li, Y.-D. Wu and D. Yang, *Acc. Chem. Res.*, 2008, **41**, 1428–1438; (*c*) X.-J. Liao, W. Guo and S.-H. Xu, *Acta Crystallogr., Sect. E*, 2011, **67**, o1732; (*d*) R. K. Castellano, Y. Li, E. A. Homan, A. J. Lampkins, I. V. Marín and K. A. Abboud, *Eur. J. Org. Chem.*, 2012, 4483–4492.
26 L. Chu, C. Ohta, Z. Zuo and D. W. C. MacMillan, *J. Am. Chem. Soc.*, 2014, **136**, 10886–10889.
27 G.-Z. Wang, R. Shang, W.-M. Cheng and Y. Fu, *Org. Lett.*, 2015, **17**, 4830–4833.
28 C. Walling and E. R. Briggs, *J. Am. Chem. Soc.*, 1946, **68**, 1141–1145.
29 (*a*) L. J. Gooßen, B. Zimmermann and T. Knauber, *Angew. Chem., Int. Ed.*, 2008, **47**, 7103–7106; (*b*) R. Shang and L. Liu, *Sci. China: Chem.*, 2011, **54**, 1670–1687; (*c*) T. Patra and D. Maiti, *Chem. – Eur. J.*, 2017, **23**, 7382–7401.
30 J.-Q. Chen, R. Chang, Y.-L. Wei, J.-N. Mo, Z.-Y. Wang and P.-F. Xu, *J. Org. Chem.*, 2018, **83**, 253–259.
31 C. C. Nawrat, C. R. Jamison, Y. Slutskyy, D. W. C. Macmillan and L. E. Overman, *J. Am. Chem. Soc.*, 2015, **137**, 11270–11273.
32 S. Y. Abbas, P. Zhao and L. E. Overman, *Org. Lett.*, 2018, **20**, 868–871.
33 Y. Slutskyy, C. R. Jamison, G. L. Lackner, D. S. Müller, A. P. Dieskau, N. L. Untiedt and L. E. Overman, *J. Org. Chem.*, 2016, **81**, 7029–7035.
34 A. Millet, Q. Lefebvre and M. Rueping, *Chem. – Eur. J.*, 2016, **22**, 13464–13468.
35 M. S. Lowry, J. I. Goldsmith, J. D. Slinker, R. Rohl, R. A. Pascal, G. G. Malliaras and S. Bernhard, *Chem. Mater.*, 2005, **17**, 5712–5719.
36 F. Monti, A. Baschieri, I. Gualandi, J. J. Serrano-Pérez, J. M. Junquera-Hernández, D. Tonelli, A. Mazzanti, S. Muzzioli, S. Stagni, C. Roldan-Carmona, A. Pertegás, H. J. Bolink, E. Ortí, L. Sambri and N. Armaroli, *Inorg. Chem.*, 2014, **53**, 7709–7721.
37 A. Gualandi, E. Matteucci, F. Monti, A. Baschieri, N. Armaroli, L. Sambri and P. G. Cozzi, *Chem. Sci.*, 2017, **8**, 1613–1620.
38 S. J. McCarver, J. X. Qiao, J. Carpenter, R. M. Borzilleri, M. A. Poss, M. D. Eastgate, M. M. Miller and D. W. C. Macmillan, *Angew. Chem., Int. Ed.*, 2017, **56**, 728–732.
39 P. Fernandez-Rodriguez, F. Legros, T. Maier, A. Weber, M. Méndez, V. Derdau, G. Hessler, M. Kurz, A. Villar-Garea and S. Ruf, *Eur. J. Org. Chem.*, 2021, 782–787.
40 S. Zhang, Z. M. Tan, H. N. Zhang, J. L. Liu, W. T. Xu and K. Xu, *Chem. Commun.*, 2017, **53**, 11642–11645.
41 C. Cai, S. Yu, B. Cao and X. Zhang, *Chem. – Eur. J.*, 2012, **18**, 9992–9998.
42 L. Gingipalli, J. Boerth, D. Emmons, T. Grebe, H. Hatoum-Mokdad, B. Peng, L. Sha, S. Tentarelli, H. Wang, Y. Wu, X. Zheng, S. Edmondson and A. Gopalsamy, *Org. Lett.*, 2020, **22**, 3418–3422.
43 S. Inuki, K. Sato, T. Fukuyama, I. Ryu and Y. Fujimoto, *J. Org. Chem.*, 2017, **82**, 1248–1253.
44 T. Guo, L. Zhang, Y. Fang, X. Jin, Y. Li, R. Li, X. Li, W. Cen, X. Liu and Z. Tian, *Adv. Synth. Catal.*, 2018, **360**, 1352–1357.
45 (*a*) K. Schlüter, R. D. Walter, B. Bergmann and T. Kurz, *Eur. J. Med. Chem.*, 2006, **41**, 1385–1397; (*b*) C. T. Behrendt, A. Kunfermann, V. Illarionova, A. Matheeussen, T. Gräwert, M. Groll, F. Rohdich, A. Bacher, W. Eisenreich, M. Fischer, L. Maes and T. Kurz, *ChemMedChem*, 2010, **5**, 1673–1676.
46 A. Noble, R. S. Mega, D. Pflästerer, E. L. Myers and V. K. Aggarwal, *Angew. Chem., Int. Ed.*, 2018, **57**, 2155–2159.
47 (*a*) D. J. Craik, D. P. Fairlie, S. Liras and D. Price, *Chem. Biol. Drug Des.*, 2013, **81**, 136–147; (*b*) A. Henninot, J. C. Collins and J. M. Nuss, *J. Med. Chem.*, 2018, **61**, 1382–1414.
48 M. Zhang, P. He and Y. Li, *Chem. Res. Chinese Univ.*, 2021, **37**, 1044–1054.
49 K. Merkens, F. J. Aguilar Troyano, J. Djossou and A. Gómez-Suárez, *Adv. Synth. Catal.*, 2020, **362**, 2354–2359.
50 J. C. Deforest, R. A. Samame, G. Suryn, A. Burtea and S. D. Rychnovsky, *J. Org. Chem.*, 2018, **83**, 8914–8925.
51 C. R. J. Stephenson, T. P. Yoon and D. W. C. MacMillan, *Visible Light Photocatalysis in Organic Chemistry*, 1st edn, Wiley-VCH, Weinheim, 2018.
52 C. B. Larsen and O. S. Wenger, *Chem. – Eur. J.*, 2018, **24**, 2039–2058.
53 K. S. Kjær, N. Kaul, O. Prakash, P. Chábera, N. W. Rosemann, A. Honarfar, O. Gordivska, L. A. Fredin, K.-E. Bergquist, L. Häggström, T. Ericsson, L. Lindh, A. Yartsev, S. Styring, P. Huang, J. Uhlig, J. Bendix, D. Strand, V. Sundström, P. Persson, R. Lomoth and K. Wärnmark, *Science*, 2019, **363**, 249–253.
54 (*a*) C. A. Parker and E. J. Bowen, *Proc. R. Soc. Lond. A*, 1953, **220**, 104–116; (*b*) C. G. Hatchard and C. A. Parker, *Proc. R. Soc. Lond. A*, 1956, **235**, 518–536.
55 (*a*) C. Weller, S. Horn and H. Herrmann, *J. Photochem. Photobiol., A*, 2013, **268**, 24–36; (*b*) D. M. Mangiante, R. D. Schaller, P. Zarzycki, J. F. Banfield and B. Gilbert, *ACS Earth Space Chem.*, 2017, **1**, 270–276; (*c*) G. C. O'Neil, L. Miaja-Avila, Y. I. Joe, B. K. Alpert, M. Balasubramanian, D. M. Sagar, W. Doriese, J. W. Fowler, W. K. Fullagar, N. Chen, G. C. Hilton, R. Jimenez, B. Ravel, C. D. Reintsema, D. R. Schmidt, K. L. Silverman, D. S. Swetz, J. Uhlig and J. N. Ullom, *J. Phys. Chem. Lett.*, 2017, **8**, 1099–1104; (*d*) J. E. Vernia, M. R. Warmin, J. A. Krause, D. L. Tierney and M. J. Baldwin, *Inorg. Chem.*, 2017, **56**, 13029–13034; (*e*) S. Straub, P. Brünker, J. Lindner and P. Vöhringer, *Angew. Chem., Int. Ed.*, 2018, **57**, 5000–5005.
56 Y. Abderrazak, A. Bhattacharyya and O. Reiser, *Angew. Chem., Int. Ed.*, 2021, **60**, 21100–21115.

57 G. Feng, X. Wang and J. Jin, *Eur. J. Org. Chem.*, 2019, 6728–6732.
58 For selected reviews on TBADT, see: (*a*) C. Tanielian, *Coord. Chem. Rev.*, 1998, **178–180**, 1165–1181; (*b*) M. D. Tzirakis, I. N. Lykakis and M. Orfanopoulos, *Chem. Soc. Rev.*, 2009, **38**, 2609; (*c*) D. Ravelli, S. Protti and M. Fagnoni, *Acc. Chem. Res.*, 2016, **49**, 2232–2242.
59 For selected reviews on POMs, see: (*a*) T. Yamase and T. Usami, *J. Chem. Soc., Dalton Trans.*, 1988, 183–190; (*b*) S. Protti, D. Ravelli, M. Fagnoni and A. Albini, *Chem. Commun.*, 2009, 7351–7353; (*c*) T. Basile, L. Capaldo, D. Ravelli and P. Quadrelli, *Eur. J. Org. Chem.*, 2020, 1443–1447.
60 (*a*) M. T. Pope and A. Müller, *Angew. Chem., Int. Ed. Engl.*, 1991, **30**, 34–48; (*b*) J. J. Borrás-Almenar, E. Coronado and A. Mueller, *Polyoxometalate Molecular Science*, Kluwer Academic Publisher, Dordrecht, The Netherlands, 2003; (*c*) D.-L. Long, E. Burkholder and L. Cronin, *Chem. Soc. Rev.*, 2007, **36**, 105–121; (*d*) N. Dupré, P. Rémy, K. Micoine, C. Boglio, S. Thorimbert, E. Lacôte, B. Hasenknopf and M. Malacria, *Chem. – Eur. J.*, 2010, **16**, 7256–7264; (*e*) S.-S. Wang and G.-Y. Yang, *Chem. Rev.*, 2015, **115**, 4893–4962.
61 D. C. Duncan, T. L. Netzel and C. L. Hill, *Inorg. Chem.*, 1995, **34**, 4640–4646.
62 D. Ravelli, M. Fagnoni, T. Fukuyama, T. Nishikawa and I. Ryu, *ACS Catal.*, 2018, **8**, 701–713.
63 (*a*) I. Texier, J. A. Delaire and C. Giannotti, *Phys. Chem. Chem. Phys.*, 2000, **2**, 1205–1212; (*b*) S. Montanaro, D. Ravelli, D. Merli, M. Fagnoni and A. Albini, *Org. Lett.*, 2012, **14**, 4218–4221.
64 V. D. Waele, O. Poizat, M. Fagnoni, A. Bagno and D. Ravelli, *ACS Catal.*, 2016, **6**, 7174–7182.
65 D. W. Manley and J. C. Walton, *Org. Lett.*, 2014, **16**, 5394–5397.
66 (*a*) T. Yamase, N. Takabayashi and M. Kaji, *J. Chem. Soc., Dalton Trans.*, 1984, 793–799; (*b*) R. F. Renneke, M. Pasquali and C. L. Hill, *J. Am. Chem. Soc.*, 1990, **112**, 6585–6594.
67 M. A. Fox, *Photoinduced Electron Transfer: Part B. Experimental Techniques and Medium Effects*, Elsevier, Amsterdam and New York, 1988.
68 C. Hansch, A. Leo and R. W. Taft, *Chem. Rev.*, 1991, **91**, 165–195.
69 D. Ravelli, A. Albini and M. Fagnoni, *Chem. – Eur. J.*, 2011, **17**, 572–579.
70 G. Guirado, C. N. Fleming, T. G. Lingenfelter, M. L. Williams, H. Zuilhof and J. P. Dinnocenzo, *J. Am. Chem. Soc.*, 2004, **126**, 14086–14094.
71 For selected reviews on organophotocatalysis, see: (*a*) N. A. Romero and D. A. Nicewicz, *Chem. Rev.*, 2016, **116**, 10075–10166; (*b*) E. Speckmeier, T. G. Fischer and K. Zeitler, *J. Am. Chem. Soc.*, 2018, **140**, 15353–15365; (*c*) A. Vega-Peñaloza, J. Mateos, X. Companyó, M. Escudero-Casao and L. Dell'Amico, *Angew. Chem., Int. Ed.*, 2021, **60**, 1082–1097.
72 (*a*) Y. Yoshimi, M. Masuda, T. Mizunashi, K. Nishikawa, K. Maeda, N. Koshida, T. Itou, T. Morita and M. Hatanaka, *Org. Lett.*, 2009, **11**, 4652–4655; (*b*) K. Nishikawa, Y. Yoshimi, K. Maeda, T. Morita, I. Takahashi, T. Itou, S. Inagaki and M. Hatanaka, *J. Org. Chem.*, 2013, **78**, 582–589; (*c*) Y. Yoshimi, S. Hayashi, K. Nishikawa, Y. Okita, K. Maeda, T. Morita and T. Itou, *Res. Chem. Intermed.*, 2013, **39**, 397–402; (*d*) Y. Yoshimi, S. Washida, Y. Okita, K. Nishikawa, K. Maeda, S. Hayashi and T. Morita, *Tetrahedron Lett.*, 2013, **54**, 4324–4326; (*e*) K. Maeda, H. Saito, K. Osaka, K. Nishikawa, M. Sugie, T. Morita, I. Takahashi and Y. Yoshimi, *Tetrahedron*, 2015, **71**, 1117–1123; (*f*) K. Osaka, M. Sugie, M. Yamawaki, T. Morita and Y. Yoshimi, J, *Photochem. Photobiol., A*, 2016, **317**, 50–55; (*g*) M. Yamawaki, A. Ukai, Y. Kamiya, S. Sugihara, M. Sakai and Y. Yoshimi, *ACS Macro Lett.*, 2017, **6**, 381–385; (*h*) Y. Yoshimi, *J. Photochem. Photobiol., A*, 2017, **342**, 116–130; (*i*) T. Yamamoto, T. Iwasaki, T. Morita and Y. Yoshimi, *J. Org. Chem.*, 2018, **83**, 3702–3709; (*j*) T. Iwasaki, Y. Tajimi, K. Kameda, C. Kingwell, W. Wcislo, K. Osaka, M. Yamawaki, T. Morita and Y. Yoshimi, *J. Org. Chem.*, 2019, **84**, 8019–8026; (*k*) K. Osaka, A. Usami, T. Iwasaki, M. Yamawaki, T. Morita and Y. Yoshimi, *J. Org. Chem.*, 2019, **84**, 9480–9488; (*l*) S. Kubosaki, H. Takeuchi, Y. Iwata, Y. Tanaka, K. Osaka, M. Yamawaki, T. Morita and Y. Yoshimi, *J. Org. Chem.*, 2020, **85**, 5362–5369.
73 R. M. Borg, D. R. Arnold and T. S. Cameron, *Can. J. Chem.*, 1984, **62**, 1785–1802.
74 (*a*) H. E. Zimmerman and P. A. Wang, *J. Am. Chem. Soc.*, 1990, **112**, 1280–1281; (*b*) H. E. Zimmerman and P. A. Wang, *J. Am. Chem. Soc.*, 1993, **115**, 2205–2216.
75 Z. Zuo, H. Cong, W. Li, J. Choi, G. C. Fu and D. W. C. Macmillan, *J. Am. Chem. Soc.*, 2016, **138**, 1832–1835.
76 For selected examples using the MOC strategy, see: (*a*) T. Kawabata, K. Yahiro and K. Fuji, *J. Am. Chem. Soc.*, 1991, **113**, 9694–9696; (*b*) K. Fuji and T. Kawabata, *Chem. – Eur. J.*, 1998, **4**, 373–376; (*c*) H. Zhao, D. C. Hsu and P. R. Carlier, *Synthesis*, 2005, 1–16.
77 Y. Ozaki, T. Yamada, T. Mizuno, K. Osaka, M. Yamawaki, H. Maeda, T. Morita and Y. Yoshimi, *Tetrahedron*, 2019, **75**, 130493.
78 T. Yamada, Y. Ozaki, M. Yamawaki, Y. Sugiura, K. Nishino, T. Morita and Y. Yoshimi, *Tetrahedron Lett.*, 2017, **58**, 835–838.
79 K. Minagawa, D. Kamakura, K. Hagiwara and M. Inoue, *Tetrahedron*, 2020, **76**, 131385.
80 O. Zhang and J. W. Schubert, *J. Org. Chem.*, 2020, **85**, 6225–6232.
81 F. Bureš, *RSC Adv.*, 2014, **4**, 58826–58851.
82 Y. Yin, Y. Dai, H. Jia, J. Li, L. Bu, B. Qiao, X. Zhao and Z. Jiang, *J. Am. Chem. Soc.*, 2018, **140**, 6083–6087.
83 L. Lin, X. Bai, X. Ye, X. Zhao, C.-H. Tan and Z. Jiang, *Angew. Chem., Int. Ed.*, 2017, **56**, 13842–13846.
84 V. Srivastava, P. K. Singh, A. Srivastava and P. P. Singh, *RSC Adv.*, 2021, **11**, 14251–14259.
85 S. Bloom, C. Liu, D. K. Kölmel, J. X. Qiao, Y. Zhang, M. A. Poss, W. R. Ewing and D. W. C. Macmillan, *Nat. Chem.*, 2018, **10**, 205–211.

86 Z. Zuo and D. W. C. Macmillan, *J. Am. Chem. Soc.*, 2014, **136**, 5257–5260.
87 M. Galicia and F. J. González, *J. Electrochem. Soc.*, 2002, **149**, D46–D50.
88 M. Novak, A. Miller, T. C. Bruice and G. Tollin, *J. Am. Chem. Soc.*, 1980, **102**, 1465–1467.
89 V. I. Timofeev, R. N. Chuprov-Netochin, V. R. Samigina, V. V. Bezuglov, K. A. Miroshnikov and I. P. Kuranova, *Acta Crystallogr., Sect. F: Struct. Biol. Commun.*, 2010, **66**, 259–263.
90 I. Carmichael, W. P. Helman and G. L. Hug, *J. Phys. Chem. Ref. Data*, 1987, **16**, 239–260.
91 N. F. Nikitas, P. L. Gkizis and C. G. Kokotos, *Org. Biomol. Chem.*, 2021, **19**, 5237–5253.
92 (*a*) K. Iijima, I. Oonishi, S. Fujisawa and S. Shibata, *Bull. Chem. Soc. Jpn.*, 1987, **60**, 3887–3890; (*b*) L. T. Okano, T. C. Barros, D. T. H. Chou, A. J. Bennet and C. Bohne, *J. Phys. Chem. B*, 2001, **105**, 2122–2128; (*c*) Ò. Rubio-Pons, L. Serrano-Andrés, D. Burget and P. Jacques, *J. Photochem. Photobiol., A*, 2006, **179**, 298–304.
93 D.-L. Zhu, Q. Wu, D. J. Young, H. Wang, Z.-G. Ren and H.-X. Li, *Org. Lett.*, 2020, **22**, 6832–6837.
94 D.-L. Zhu, R. Xu, Q. Wu, H.-Y. Li, J.-P. Lang and H.-X. Li, *J. Org. Chem.*, 2020, **85**, 9201–9212.
95 (*a*) Y. Maki, I. Oyabu, S. Ohara, M. Sako, Y. Kitade and K. Hirota, *Chem. Pharm. Bull.*, 1989, **37**, 3239–3242; (*b*) R. Hauptmann, A. Petrosyan, F. Fennel, M. A. Argüello Cordero, A. E. Surkus and J. Pospech, *Chem. – Eur. J.*, 2019, **25**, 4325–4329.
96 F. El-Hage, C. Schöll and J. Pospech, *J. Org. Chem.*, 2020, **85**, 13853–13867.
97 S. P. Pitre, C. D. McTiernan and J. C. Scaiano, *ACS Omega*, 2016, **1**, 66–76.
98 S. Fukuzumi, H. Kotani, K. Ohkubo, S. Ogo, N. V. Tkachenko and H. Lemmetyinen, *J. Am. Chem. Soc.*, 2004, **126**, 1600–1601.
99 S. Fukuzumi, K. Ohkubo, T. Suenobu, K. Kato, M. Fujitsuka and O. Ito, *J. Am. Chem. Soc.*, 2001, **123**, 8459–8467.
100 T. Chinzei, K. Miyazawa, Y. Yasu, T. Koike and M. Akita, *RSC Adv.*, 2015, **5**, 21297–21300.
101 N. P. Ramirez and J. C. Gonzalez-Gomez, *Eur. J. Org. Chem.*, 2017, 2154–2163.
102 P. Ji, Y. Zhang, Y. Dong, H. Huang, Y. Wei and W. Wang, *Org. Lett.*, 2020, **22**, 1557–1562.
103 J. E. Rose, P. D. Leeson and D. Gani, *J. Chem. Soc., Chem. Commun.*, 1992, 1784–1786.
104 (*a*) T. Furuta, H. Takahashi and Y. Kasuya, *J. Am. Chem. Soc.*, 1990, **112**, 3633–3636; (*b*) J. E. Baldwin, R. M. Adlington, D. G. Marquess, A. R. Pitt, M. J. Porter and A. T. Russell, *Tetrahedron*, 1996, **52**, 2515–2536.
105 L.-Y. Lian and D. A. Middleton, *Prog. Nucl. Magn. Reson. Spectrosc.*, 2001, **39**, 171–190.
106 A. A. Shah, M. J. Kelly and J. J. Perkins, *Org. Lett.*, 2020, **22**, 2196–2200.
107 Y.-Q. Zou, F. M. Hörmann and T. Bach, *Chem. Soc. Rev.*, 2018, **47**, 278–290.
108 T. Morack, C. Mück-Lichtenfeld and R. Gilmour, *Angew. Chem., Int. Ed.*, 2019, **58**, 1208–1212.
109 (*a*) K. L. Skubi, T. R. Blum and T. P. Yoon, *Chem. Rev.*, 2016, **116**, 10035–10074; (*b*) J. C. Tellis, C. B. Kelly, D. N. Primer, M. Jouffroy, N. R. Patel and G. A. Molander, *Acc. Chem. Res.*, 2016, **49**, 1429–1439; (*c*) C. B. Kelly, N. R. Patel, D. N. Primer, M. Jouffroy, J. C. Tellis and G. A. Molander, *Nat. Protoc.*, 2017, **12**, 472–492; (*d*) J. Twilton, C. Le, P. Zhang, M. H. Shaw, R. W. Evans and D. W. C. Macmillan, *Nat. Rev. Chem.*, 2017, **1**, 0052; (*e*) E. B. McLean and A.-L. Lee, *Tetrahedron*, 2018, **74**, 4881–4902; (*f*) W.-J. Zhou, Y.-H. Zhang, Y.-Y. Gui, L. Sun and D.-G. Yu, *Synthesis*, 2018, 3359–3378.
110 H. T. Dang, G. C. Haug, V. T. Nguyen, N. T. H. Vuong, V. D. Nguyen, H. D. Arman and O. V. Larionov, *ACS Catal.*, 2020, **10**, 11448–11457.
111 V. T. Nguyen, V. D. Nguyen, G. C. Haug, N. T. H. Vuong, H. T. Dang, H. D. Arman and O. V. Larionov, *Angew. Chem., Int. Ed.*, 2020, **59**, 7921–7927.
112 V. T. Nguyen, V. D. Nguyen, G. C. Haug, H. T. Dang, S. Jin, Z. Li, C. Flores-Hansen, B. S. Benavides, H. D. Arman and O. V. Larionov, *ACS Catal.*, 2019, **9**, 9485–9498.
113 N. T. S. Phan, M. Van Der Sluys and C. W. Jones, *Adv. Synth. Catal.*, 2006, **348**, 609–679.
114 W. Yao, E. A. Bazan-Bergamin and M. Y. Ngai, *ChemCatChem*, 2021, e202101292.
115 D. A. Nicewicz and D. W. C. MacMillan, *Science*, 2008, **322**, 77–80.
116 J.-J. Zhao, H.-H. Zhang, X. Shen and S. Yu, *Org. Lett.*, 2019, **21**, 913–916.
117 (*a*) D. J. Cole-Hamilton, *Science*, 2003, **299**, 1702–1706; (*b*) S. Gisbertz and B. Pieber, *ChemPhotoChem*, 2020, **4**, 456–475; (*c*) Y. Okada, *Chem. Rec.*, 2021, **21**, 1–17.
118 T. Ohno, K. Sarukawa, K. Tokieda and M. Matsumura, *J. Catal.*, 2001, **203**, 82–86.
119 L. Cermenati, M. Mella and A. Albini, *Tetrahedron*, 1998, **54**, 2575–2582.
120 D. W. Manley, R. T. McBurney, P. Miller, R. F. Howe, S. Rhydderch and J. C. Walton, *J. Am. Chem. Soc.*, 2012, **134**, 13580–13583.
121 D. W. Manley, R. T. McBurney, P. Miller, J. C. Walton, A. Mills and C. O'Rourke, *J. Org. Chem.*, 2014, **79**, 1386–1398.
122 M. Noorjahan, M. Pratap Reddy, V. Durga Kumari, B. Lavédrine, P. Boule and M. Subrahmanyam, *J. Photochem. Photobiol., A*, 2003, **156**, 179–187.
123 A. Mills, N. Elliott, G. Hill, D. Fallis, J. R. Durrant and R. L. Willis, *Photochem. Photobiol. Sci.*, 2003, **2**, 591–596.
124 R. B. Roy and G. A. Swan, *J. Chem. Soc. C*, 1969, 1886–1891.
125 B. Kraeutler and A. J. Bard, *J. Am. Chem. Soc.*, 1978, **100**, 5985–5992.
126 (*a*) E.-A. I. Heiba, R. M. Dessau and W. J. Koehl, *J. Am. Chem. Soc.*, 1968, **90**, 1082–1084; (*b*) E.-A. I. Heiba, R. M. Dessau and W. J. Koehl, *J. Am. Chem. Soc.*, 1969, **91**, 138–145; (*c*) M. E. Kurz, V. Baru and P. N. Nguyen, *J. Org. Chem.*, 1984, **49**, 1603–1607; (*d*) A. Citterio,

R. Sebastiano, A. Maronati, R. Santi and F. Bergamini, *J. Chem. Soc., Chem. Commun.*, 1994, 1517–1518.

127 (*a*) S. Marinković and N. Hoffmann, *Int. J. Photoenergy*, 2003, **5**, 175–182; (*b*) S. Marinković and N. Hoffmann, *Eur. J. Org. Chem.*, 2004, 3102–3107.

128 M. A. Henderson, *Surf. Sci. Rep.*, 2011, **66**, 185–297.

129 (*a*) C. Deiana, E. Fois, S. Coluccia and G. Martra, *J. Phys. Chem. C*, 2010, **114**, 21531–21538; (*b*) C. Salazar and M. A. Nanny, *J. Catal.*, 2010, **269**, 404–410.

130 S. H. Szczepankiewicz, A. J. Colussi and M. R. Hoffmann, *J. Phys. Chem. B*, 2000, **104**, 9842–9850.

131 Q. Zhu and D. G. Nocera, *J. Am. Chem. Soc.*, 2020, **142**, 17913–17918.

132 E. L. Quah, J. N. Wilson and H. Idriss, *Langmuir*, 2010, **26**, 6411–6417.

133 (*a*) D. S. Muggli, S. A. Keyser and J. L. Falconer, *Catal. Lett.*, 1998, **55**, 129–132; (*b*) Q. Chen, J. M. Song, F. Pan, F. L. Xia and J. Y. Yuan, *Environ. Technol.*, 2009, **30**, 1103–1109.

134 D. C. Grinter, M. Nicotra and G. Thornton, *J. Phys. Chem. C*, 2012, **116**, 11643–11651.

135 (*a*) J. M. Saveant, *J. Am. Chem. Soc.*, 1992, **114**, 10595–10602; (*b*) A. Houmam, *Chem. Rev.*, 2008, **108**, 2180–2237.

136 J. N. Schrauben, R. Hayoun, C. N. Valdez, M. Braten, L. Fridley and J. M. Mayer, *Science*, 2012, **336**, 1298–1301.

137 (*a*) R. Chauhan, A. Kumar and R. P. Chaudhary, *Spectrochim. Acta, Part A*, 2012, **98**, 256–264; (*b*) R. Daghrir, P. Drogui and D. Robert, *Ind. Eng. Chem. Res.*, 2013, **52**, 3581–3599; (*c*) M. Pawar, S. Topcu Sendoğdular and P. Gouma, *J. Nanomater.*, 2018, 1–13.

138 K. Behm, E. Fazekas, M. J. Paterson, F. Vilela and R. D. McIntosh, *Chem. – Eur. J.*, 2020, **26**, 9486–9494.

139 D. Kuwana, Y. Komori, M. Nagatomo and M. Inoue, *J. Org. Chem.*, 2022, **87**, 730–736.

140 (*a*) J. M. Anderson and J. K. Kochi, *J. Am. Chem. Soc.*, 1970, **92**, 1651–1659; (*b*) J. M. Anderson and J. K. Kochi, *J. Org. Chem.*, 1970, **35**, 986–989.

141 P. Neta, R. E. Huie and A. B. Ross, *J. Phys. Chem. Ref. Data*, 1988, **17**, 1027–1284.

142 (*a*) F. Fontana, F. Minisci, M. C. Nogueira Barbosa and E. Vismara, *J. Org. Chem.*, 1991, **56**, 2866–2869; (*b*) F. Minisci, R. Bernardi, F. Bertini, R. Galli and M. Perchinummo, *Tetrahedron*, 1971, **27**, 3575–3579.

143 (*a*) H. Wang, L.-N. Guo and X.-H. Duan, *Adv. Synth. Catal.*, 2013, **355**, 2222–2226; (*b*) W.-P. Mai, G.-C. Sun, J.-T. Wang, G. Song, P. Mao, L.-R. Yang, J.-W. Yuan, Y.-M. Xiao and L.-B. Qu, *J. Org. Chem.*, 2014, **79**, 8094–8102; (*c*) H. Yang, L.-N. Guo and X.-H. Duan, *RSC Adv.*, 2014, **4**, 52986–52990; (*d*) K. Sun, S.-J. Li, X.-L. Chen, Y. Liu, X.-Q. Huang, D.-H. Wei, L.-B. Qu, Y.-F. Zhao and B. Yu, *Chem. Commun.*, 2019, **55**, 2861–2864; (*e*) G. Feng, C. Jin, J.-Y. He and Q.-F. Bai, *Synlett*, 2020, 1517–1522; (*f*) Z. Zhang, C. Jia, X. Kong, M. Hussain, Z. Liu, W. Liang, L. Jiang, H. Jiang and J. Ma, *ACS Sustainable Chem. Eng.*, 2020, **8**, 16463–16468; (*g*) Q. Liu, L. Wang, J. Liu, S. Ruan and P. Li, *Org. Biomol. Chem.*, 2021, **19**, 3489–3496; (*h*) J. Li, W.-J. Hao, P. Zhou, Y.-L. Zhu, S.-L. Wang, S.-J. Tu and B. Jiang, *RSC Adv.*, 2017, **7**, 9693–9703; (*i*) S.-S. Wang, H. Fu, Y. Shen, M. Sun and Y.-M. Li, *J. Org. Chem.*, 2016, **81**, 2920–2929; (*j*) K. Yan, D. Yang, W. Wei, F. Wang, Y. Shuai, Q. Li and H. Wang, *J. Org. Chem.*, 2015, **80**, 1550–1556.

144 C.-G. Li, Q. Xie, X.-L. Xu, F. Wang, B. Huang, Y.-F. Liang and H.-J. Xu, *Org. Lett.*, 2019, **21**, 8496–8500.

145 K. S. McClymont, F.-Y. Wang, A. Minakar and P. S. Baran, *J. Am. Chem. Soc.*, 2020, **142**, 8608–8613.

146 C. Walling, *Acc. Chem. Res.*, 1975, **8**, 125–131.

147 (*a*) L. Cui, H. Chen, C. Liu and C. Li, *Org. Lett.*, 2016, **18**, 2188–2191; (*b*) X. Li, R. Zhang, X. Zhang, P. Zhu and T. Yao, *Chem. – Asian J.*, 2020, **15**, 1175–1179.

148 For recent reviews on organo-electrochemistry, see: (*a*) E. J. Horn, B. R. Rosen and P. S. Baran, *ACS Cent. Sci.*, 2016, **2**, 302–308; (*b*) M. Yan, Y. Kawamata and P. S. Baran, *Chem. Rev.*, 2017, **117**, 13230–13319; (*c*) S. Möhle, M. Zirbes, E. Rodrigo, T. Gieshoff, A. Wiebe and S. R. Waldvogel, *Angew. Chem., Int. Ed.*, 2018, **57**, 6018–6041; (*d*) A. Wiebe, T. Gieshoff, S. Möhle, E. Rodrigo, M. Zirbes and S. R. Waldvogel, *Angew. Chem., Int. Ed.*, 2018, **57**, 5594–5619; (*e*) D. Pollok and S. R. Waldvogel, *Chem. Sci.*, 2020, **11**, 12386–12400; (*f*) C. Kingston, M. D. Palkowitz, Y. Takahira, J. C. Vantourout, B. K. Peters, Y. Kawamata and P. S. Baran, *Acc. Chem. Res.*, 2020, **53**, 72–83; (*g*) C. Zhu, N. W. J. Ang, T. H. Meyer, Y. Qiu and L. Ackermann, *ACS Cent. Sci.*, 2021, **7**, 415–431; (*h*) N. Chen, Z. Ye and F. Zhang, *Org. Biomol. Chem.*, 2021, **19**, 5501–5520.

149 K. D. Moeller, *Tetrahedron*, 2000, **56**, 9527–9554.

150 (*a*) R. N. Renaud and P. J. Champagne, *Can. J. Chem.*, 1975, **53**, 529–534; (*b*) K. Uneyama and H. Nanbu, *J. Org. Chem.*, 1988, **53**, 4598–4599; (*c*) V. N. Andreev, V. A. Grinberg, A. G. Dedov, A. S. Loktev, N. A. Mayorova, I. I. Moiseev and A. A. Stepanov, *Russ. J. Electrochem.*, 2013, **49**, 996–1000; (*d*) K. Arai, K. Watts and T. Wirth, *ChemistryOpen*, 2014, **3**, 23–28.

151 (*a*) A. Matzeit, H. J. Schäfer and C. Amatore, *Synthesis*, 1995, 1432–1444; (*b*) F. Lebreux, F. Buzzo and I. E. Markó, *Synlett*, 2008, 2815–2820.

152 X. Chen, X. Luo, X. Peng, J. Guo, J. Zai and P. Wang, *Chem. – Eur. J.*, 2020, **26**, 3226–3230.